Archives of Pharmacal Research (2023) 46:207–272
https://doi.org/10.1007/s12272-023-01443-4

Online ISSN 1976-3786
Print ISSN 0253-6269

Archives of Pharmacal Research
www.springer.com/12272

REVIEW

Phytochemistry and pharmacology of natural prenylated flavonoids

Hua-Wei Lv[1] · Qiao-Liang Wang[1] · Meng Luo[1] · Meng-Di Zhu[2] · Hui-Min Liang[1] · Wen-Jing Li[1] · Hai Cai[1] · Zhong-Bo Zhou[3] · Hong Wang[1] · Sheng-Qiang Tong[1] · Xing-Nuo Li[1]

Received: 10 August 2022 / Accepted: 7 March 2023 / Published online: 14 April 2023

Abstract

Prenylated flavonoids are a special kind of flavonoid derivative possessing one or more prenyl groups in the parent nucleus of the flavonoid. The presence of the prenyl side chain enriched the structural diversity of flavonoids and increased their bioactivity and bioavailability. Prenylated flavonoids show a wide range of biological activities, such as anti-cancer, anti-inflammatory, neuroprotective, anti-diabetic, anti-obesity, cardioprotective effects, and anti-osteoclastogenic activities. In recent years, many compounds with significant activity have been discovered with the continuous excavation of the medicinal value of prenylated flavonoids, and have attracted the extensive attention of pharmacologists. This review summarizes recent progress on research into natural active prenylated flavonoids to promote new discoveries of their medicinal value.

Keywords Phytochemistry · Prenylated flavonoid · Pharmacological activity · Anti-cancer · Anti-inflammatory

Introduction

Prenylated flavonoids are a special type of flavonoid derivative that is characteristic of modified by prenylation of the skeleton. Prenylation refers to alkyl-substituent groups, such as prenyl, geranyl, lavandulyl, and farnesyl groups, which have more potential for further modification, such as oxidation, cyclization, and hydroxylation, and enrich the structural and biological diversity of prenylated flavonoids (Shi et al. 2021). According to reported studies over the past decade, more than 1000 prenylated flavonoids have been discovered from natural sources.

✉ Sheng-Qiang Tong
sqtong@126.com

✉ Xing-Nuo Li
li_xingnuo@163.com

[1] College of Pharmaceutical Science & Zhejiang Provincial Key Laboratory of TCM for Innovative R&D and Digital Intelligent Manufacturing of TCM Great Health Products & Key Laboratory of Marine Fishery Resources Exploitment & Utilization of Zhejiang Province, Zhejiang University of Technology, 310014 Hang zhou, P. R. China

[2] Research Center of Analysis and Measurement, Zhejiang University of Technology University, 310014 Hang Zhou, P. R. China

[3] School of Pharmacy, Youjiang Medical University for Nationalities, 533000 Baise, P. R. China

Prenylated flavonoids are the main active ingredient in many traditional Chinese medicines and functional food resources, such as *Morus alba*, *Glycyrrhiza uralensis, Humulus lupulus*, *Artocarpus heterophyllus*, *Glycine max*, and *Ficus carica* fruits, and are promising lead compounds or nutraceuticals due to their diverse health benefits in oncotherapy (Wen et al. 2021), glycolipid metabolism balance (Jo et al. 2021), and the cardiovascular system (Song et al. 2011). Compared with nonprenylated flavonoids, prenylated flavonoids possess higher lipid solubility, an affinity for the cell membrane, and gastrointestinal absorption capacity due to the presence of prenyl groups (Hošek et al. 2011; Jakimiuk et al. 2021). Therefore, prenylated flavonoids show more potential to interact with diverse cellular targets. In recent years, the biological activity of prenylated flavonoids has attracted great attention from many research teams due to their promising pharmacological properties.

In the present review, a total of 1036 prenylated flavonoids obtained from 127 species belonging to 62 genera of 26 families (Tables 1, 2 and 3, Fig. 1) during the past decade were systematically summarized. The prenylated flavonoids were classified into 6 categories (Fig. 2), prenylated flavones (**1-261**), prenylated flavanones (**262–567**), prenylated chalcones (**568–689**), prenylated isoflavones (**690–908**), prenylated flavans (**909–943**) and isoflavans (**944–1005**), and prenylated flavonostilbenes and

Table 1 Species from Fabaceaeand Euphorbiaceae

Fabaceae						Euphorbiaceae	
Genus	Species	Genus	Species	Genus	Species	Genus	Species
Adenocarpus	*A. cincinnatus*		*E. excelsa*	*Maackia*	*M. amurensis*	*Euphorbia*	*E. hirta*
Cajanus	*C. cajan*		*E. latissima*	*Millettia*	*M. extensa*		*E. humifusa*
Deguelia	*D. costata*		*E. melanacantha*		*M. oblata*	*Macaranga*	*M. adenantha*
	D. duckeana		*E. mildbraedii*		*M. pachycarpa*		*M. balansae*
Derris	*D. ferruginea*		*E. poeppigiana*		*M. pachyloba*		*M. barteri*
	D. trifoliate		*E. sacleuxii*	*Platycelphium*	*P. voënse*		*M. denticulata*
Desmodium	*D. caudatum*		*E. schliebenii*	*Pongamia*	*P. pinnata*		*M. gigantifolia*
	D. congestum		*E. sigmoidea*	*Pseudarthria*	*P. hookeri*		*M. indica*
	D. podocarpum	*Eysehardtia*	*E. platycarpa*	*Psoralea*	*P. corylifolia*		*M. kurzii*
	D. renifolium	*Flemingia*	*F. latifolia*	*Shuteria*	*S. sinensis*		*M. tanarius*
Erinacea	*E. Anthyllis*		*F. macrophylla*	*Sophora*	*S. flavescens*		*M. trichocarpa*
Eriosema	*E. chinense*		*F. philippinensis*		*S. interrupta*		*M. triloba*
	E. laurentii	*Glycyrrhiza*	*G. iconica*		*S. pachycarpa*		
	E. montanum		*G. uralensis*		*S. tonkinensis*		
Erythrina	*E. addisoniae*	*Hedysarum*	*H. gmelinii*	*Trifolium*	*T. resupinatum*		
	E. caffra	*Indigofera*	*I. spicata*				

Table 2 Species from Moraceae,Berberidaceae, and Papilionaceae

Moraceae				Berberidaceae		Papilionaceae	
Genus	Species	Genus	Species	Genus	Species	Genus	Species
Artocarpus	*A. communis*	*Cudrania*	*C. cochinchinensis*	*Berberis*	*B. thunbergii*	*Dalea*	*D. elegans*
	A. altilis		*C. tricuspidat*	*Dysosma*	*D. versipellis*		*D. frutescens*
	A. anisophyllus		*C. tricuspidata*	*Epimedium*	*E. brevicornu*		*D. searlsiae*
	A. champeden	*Ficus*	*F. altissima*		*E. grandiflorum*	*Tephrosia*	*T. apollinea*
	A. elasticus		*F. carica*		*E. koreanum*		*T. rhodesica*
	A. heterophyllus		*F. hirta*	*Sinopodophyllum*	*S. emodi*		*T. subtriflora*
	A. integer		*F. thonningii*		*S. hexandrum*		
	A. integer var. silvestris	*Maclura*	*M. cochinchinensis*				
	A. lakoocha		*M. pomifera*				
	A. lowii		*M. tinctoria*				
	A. nigrifolius	*Morus*	*M. alba*				
	A. rigida		*M. nigra*				
Brosimum	*B. acutifolium*		*M. yunnanensis*				
Broussonetia	*B. kazinoki*	*Dorstenia*	*D. barteri*				
Chlorophora	*C. regia*						

biflavonoids (**1006–1036**) according to their structural features (Fig. 3). Fabaceae, Moraceae, and Euphorbiaceae are the three leading families with abundant prenylflavonoids. The biosynthesis of prenylated flavonoids, preliminary active screening results, structure-activity relationships (SARs), and mechanism of active prenylated flavonoids were also summarized, aiming to provide an overview of natural, active prenylated flavonoids and their pharmacological properties.

Biosynthesis of prenylated flavonoids

In general, prenylated flavonoid biosynthesis in plant can conveniently be divided into three stages: (a) formation of the C_6–C_3–C_6 skeleton (Fig. 4a). L-phenylalanine or L-tyrosine was used to produce 4-coumaroyl-CoA, which can be combined with three molecules of malonyl-CoA to yield the chalcone backbone. (b) biosynthesis of the different classes of flavonoids (Fig. 4b). Chalcones are

Table 3 Species from otherfamilies

Family	Genus	Species	Family	Genus	Species
Rutaceae	*Amyris*	*A. madrensis*	Ophioglossaceae	*Helminthostachys*	*H. zeylanica*
		A. pinnata	Cannabaceae	*Humulus*	*H. lupulus*
	Melicope	*M. triphylla*	Hypericaceae	*Hypericum*	*H. calycinum*
		M. lunu-ankenda	Poaceae	*Imperata*	*I. cylindrica*
Rubiaceae	*Arcytophyllum*	*A. thymifolium*	Anacardiaceae	*Lannea*	*L. alata*
	Tarenna	*T. grandiflora*	Plumbaginaceae	*Limonium*	*L. leptophyllum*
Platanaceae	*Platanus*	*P. acerifolia*	Lamiaceae	*Orthosiphon*	*O. stamineus*
		P. orientalis	Scrophulariaceae	*Paulownia*	*P. tomentosa*
Thymelaeaceae	*Daphne*	*D. giraldii*	Cupressaceae	*Platycladus*	*P. orientalis*
Burseraceae	*Commiphora*	*C. opobalsamum*	Orchidaceae	*Pleione*	*P. bulbocodioides*
Najadaceae	*Cymodocea*	*C. nodosa*	Polygonaceae	*Polygonum*	*P. limbatum*
Cyperaceae	*Eleocharis*	*E. tuberosa*	Celastraceae	*Tripterygium*	*T. wilfordii*
Clusiaceae	*Garcinia*	*G. dulcis*	Asteraceae	*Helichrysum*	*H. teretifolium*

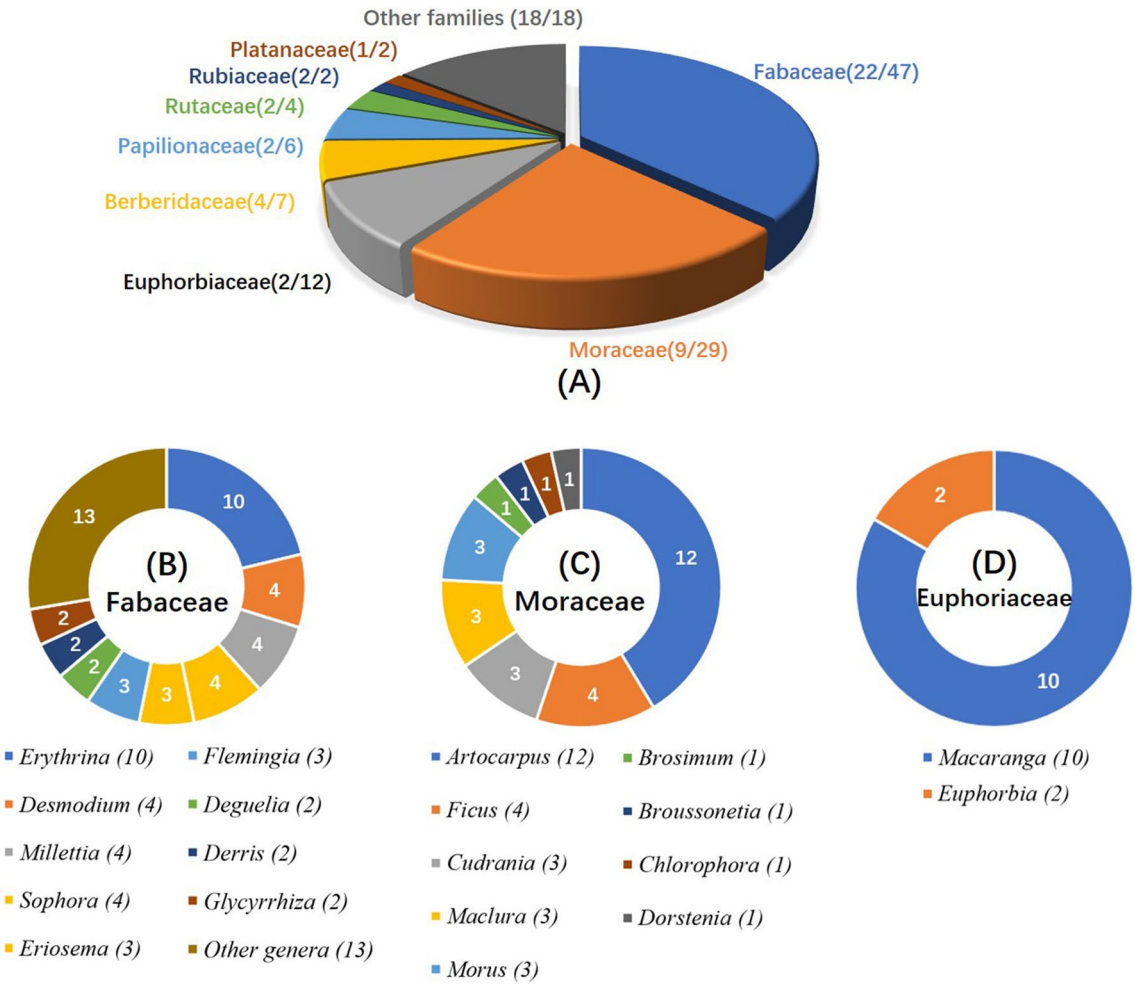

Fig. 1 Statistics for the families (**A**); numbers in parentheses are the statistics for the genus/species. Statistics for genera from Fabaceae (**B**), Moraceae (**C**), and Euphoriaceae (**D**); numbers in parentheses are the statistics for species

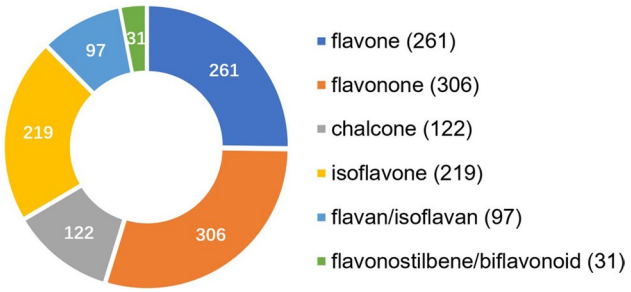

Fig. 2 Statistics for the number of prenylated flavonoids

proved to be the precursors to other subclasses of flavonoids and can be catalyzed by chalcone flavanone isomerase to obtain the basic skeleton of flavonoid which continues through a series of enzymatic modifications to yield flavones, flavans, isoflavones, and so on. (c) biosynthesis of the prenylated flavonoids (Figs. 5 and 6). Prenyltransferases are the key catalytic enzyme for prenylated modification of the flavonoids and have been attracting increasing attention due to greatly contributing to the structural diversity of flavonoids. The reaction catalyzed by prenyltransferases represents a Friedel–Crafts alkylation of the flavonoid skeleton in the biosynthesis of natural prenylflavonoids. Most of the prenyltransferases exhibit strict substrate specificity and low catalytic efficiency. Metal ion, especially Mg^{2+}, is required for the catalytic activity. Up to now, only a few flavonoid prenyltransferases have been identified. The general characteristic of flavonoid prenyltransferases discovered from natural sources was summarized in Table 4..

Natural prenylated flavonoids

Prenylated flavonoids with cytotoxicity

Prenylated flavonoids were found to possess more potential cytotoxicity against various cancer cells due to the introduction of the prenyl side chain on the flavonoid skeleton which enhances the binding affinity of flavonoids toward P-glycoprotein. 2-(4-hydroxy-phenyl)-8-(3-methyl-but-2-enyl)-chroman-4-one (**1**) (Fig. 7) isolated from *Artocarpus heterophyllus* and displaying strong cytotoxic effect against MCF-7, A-549, SW480, and HL-60 cells, with IC_{50} values ranging from 1.03 to 5.28 μM (Liu et al. 2020). Licoflavone C (**3**), also called 4′,5,7-trihydroxy-8-prenylflavone (Ye et al. 2021), was identified in *Ficus hirta*, *Retama raetam*, and *Morus alba*. It exhibited cytotoxicity against HL-60, HepG2, A549, and NCI-H292 cells with IC_{50} values ranging from 7.0 to 13.85 μM (Qin et al. 2015a; Li et al. 2018). Three prenylated flavonols (**5**, **139**, and **164**) were isolated from leaves of *Macaranga barteri* and showed antiproliferative activity against four human cancer cell lines, MCF-7, A549, PC-3, and HeLa cells. Broussoflavonol F (**164**) displayed the highest cytotoxicity against these four human cancer cell lines with IC_{50} value of 3.83–4.13 μM. While 8-prenylkaempferol (**5**) lacks the C-3′ prenyl side chain on the B ring had a slight lower cytotoxicity (IC_{50} value of 6.22–6.88 μM) than **164**. Isomacarangin (**139**) bearing a geranyl group in position C-8 also led to a slight reduction in antiproliferative activity (IC_{50} value of 8.43–8.72 μM) (Segun et al. 2019).

Nine prenylated flavonoids, isolated from the fruits of *Sinopodophyllum hexandrum*, were tested for their cytotoxicity against human breast-cancer T47D cells in vitro. Sinopodophylline B (**10**), 6-prenylquercetin 3-methyl ether (**71**), topazolin (**72**), and 5, 7, 4′-trihydroxy-3′-(3-methylbut-2-enyl)-3-methoxy flavone (**104**) showed cytotoxicity against

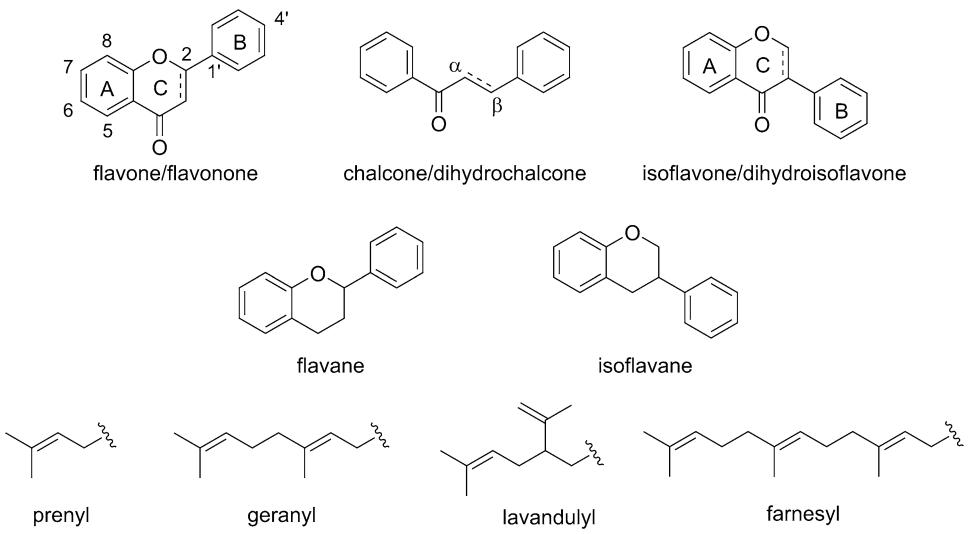

Fig. 3 Basic skeleton of flavonoids and prenyl groups

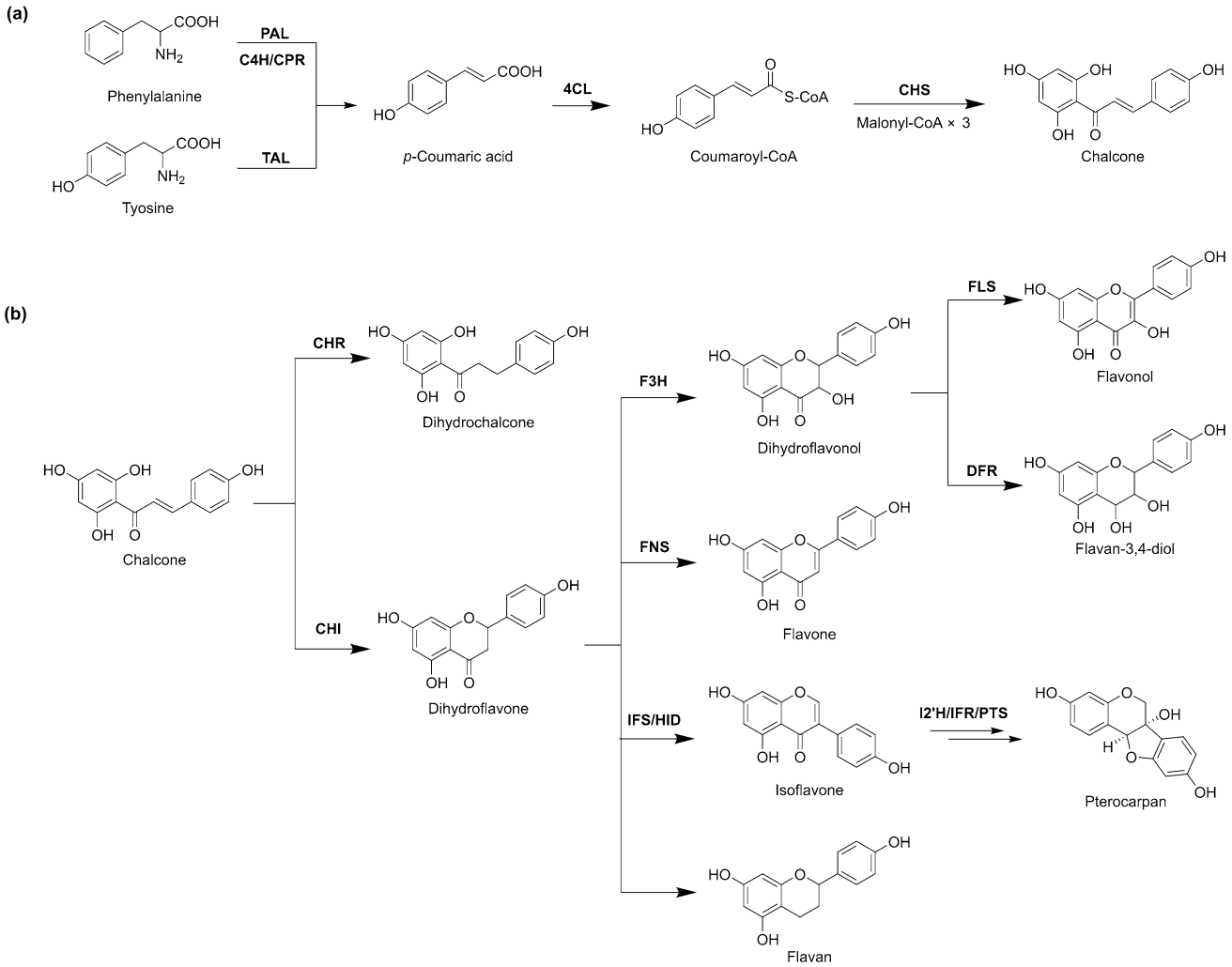

Fig. 4 Biosynthesis of the chalcone skeleton and the different classes of flavonoids. Enzyme names are abbreviated as follows: *PAL* phenylalanine ammonia lyase; *C4H* cinnamate 4-hydroxylase; *CPR* cytochrome P450 reductase; *TAL* tyrosine ammonia lyase; *4CL* 4-coumarate-CoA ligase; *CHS* chalcone synthase; *CHR* chalcone reductase; *CHI* chalcone isomerase; *F3H* flavanone 3-hydroxylase; *FNS* flavone synthas; *IFS* isoflavone synthase; *HID* 2-hydroxyisoflavanone dehydratase; *FLS* flavonol synthase; *DFR* dihydroflavonol 4-reductase; *I2′H* isoflavone hydroxylase; *IFR* isoflavone reductase; *PTS* pterocarpan synthase.

T47D cells with IC_{50} values of 1.5, 6.3, 11.9, and 2.0 μM, respectively, whereas sinopodophyllines C (**197**) and D (**219**) exhibited weak cytotoxicity against T47D cells with IC_{50} values of 46.0 and 36.8 μM. It suggested that 3′-hydroxyl group on the B ring and unmodified monoprenyl side chain promote the cytotoxicity, and the cyclization of the prenyl side chain would decrease the cytotoxicity (Wang et al. 2017c)0.5,7,3′,5′-Tetramethoxy-6-*C*-prenylflavone (**61**), 6-(3-methyl-(*E*)-1-butenyl) chrysin (**79**), bracteflavone B (**80**), and dinklagin C (**81**), from *Artocarpus heterophyllus* displayed strong cytotoxic effects against MCF-7, A-549, SMMC-7721, SW480, and HL-60 cells with IC_{50} values ranging from 1.46 to 16.26 μM (Liu et al. 2020).

72 and licoflavonol (**73**), isolated from *Glycyrrhiza uralensis*, exhibited cytotoxicities against SW480 cells with IC_{50} values of 14.53 and 8.23 μM, respectively (Tang et al. 2016). Most prenylflavonoids isolated from the twigs of *Artocarpus nigrifolius* exhibited cytotoxicity against SiHa and SGC-7901 cells. 6-Prenyl-4′,5,7-trihydroxyflavone (**64**) showed inhibitory activity against SiHa (IC_{50} value of 13.3) and SGC-7901(IC_{50} value of 9.6). Comparing the structures of **64** and artocarpesin (**65**), it suggested that the hydroxyl group of C-2′ on the B ring would dramatically decrease cytotoxicity. Eleocharin A (**84**) showed strong cytotoxicity against SiHa and SGC-7901 cells with IC_{50} values of 0.7 and 8.3 μM, respectively. The inhibitory activities of two structurally similar analogues, 5,4′-dihydroxy-3′-methoxy-(6:7)-2,2-dimethylpyrano-flavone (**85**) and carpachromenol (**86**), declined sharply against both two cell lines, which revealed the 3′-methoxyl group was

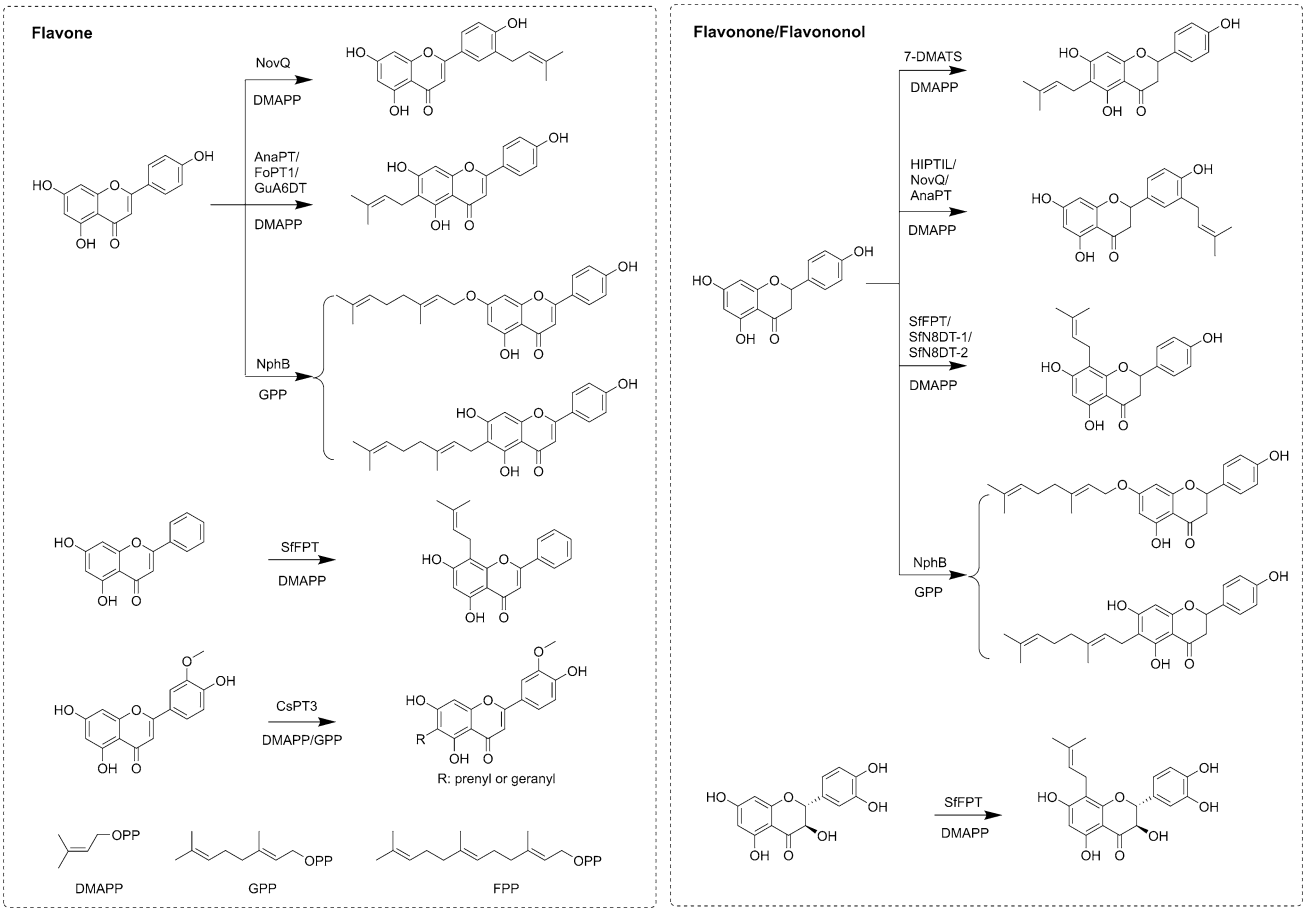

Fig. 5 Biosynthesis of the prenylated flavonoids (I)

unfavorable, but the 3′-hydroxyl maybe was crucial for the antiproliferative activity (Liu et al. 2018b).

Sinoflavonoid U (**91**) is from *Sinopodophyllum hexandrum* and exhibited cytotoxicity against MCF-7 and HepG2 cells with IC_{50} values of 6.25 and 3.83 μM, respectively. However, Sinoflavonoid T (**90**) possessing the same B and C rings from flavone skeleton as **91** displayed no cytotoxicity against MCF-7 and HepG2 cell lines, which suggested 2-(1-hydroxy-1-methylethyl)dihydrofurano group on ring A is structurally required for the cytotoxity against the MCF-7 and HepG2 cells lines (Sun et al. 2019). The cytotoxicity of prenylated flavonoids from the fruits of *Sinopodophyllum emodi* was evaluated against MCF-7 and HepG2 cells. Podoverine A (**106**) exhibited cytotoxicity against MCF-7 and HepG2 cells with IC_{50} values of 9.50 and 2.46 μM, respectively. However, oxidation or hydroxylation of prenyl group dramatically decrease cytotoxicity against MCF-7 and HepG2. Additionally, quercetin-3-methyl ether, a non-prenylation flavone, show more potent cytotoxicity than quercetin, suggesting methoxy at C-3 may contribute to its cytotoxicity against MCF-7 and HepG2 (Sun et al. 2015).

6,8-Diprenylkaempferol (**154**) displayed a strong cytotoxic effect against the H460 cell line with an IC_{50} value of 4.67 μM (Long et al. 2022). 6,8-Diprenyleriodictyol (**155**), isolated from *Derris ferruginea*, showed cytotoxicity against MRC-5 and KB cells with IC_{50} values of 8.0 and 8.5 μM, respectively (Morel et al. 2013).

Seven prenylated flavonoids (**6**, **15**, **92**, **99**, **162**, **191**, and **192**) from the leaves of *Epimedium Koreanum* were evaluated for cytotoxic activities against lung cancer A549 and NCI-H292 cells. Baohuoside I (**15**), epimedokoreanin D (**99**), epimedokoreanin B (**162**), epicornuin F (**191**), and epicornuin B (**192**) of which inhibited the proliferation of A549 and NCI-292 cells with IC_{50} values of 5.7–23.5 μM. Compound **162** showed cytotoxicity against A549 and NCI-H292 cells with IC_{50} values of 7.90 and 5.69 μM, respectively and **191** exhibited cytotoxicity against NCI-H292 cells with an IC_{50} value of 6.44 μM. Compounds **191** and **192** were structurally similar to **162**, only one hydroxyl substitution in one prenyl decreased the cytotoxicity. Compared to the structures of these compounds, it suggested that glycosylation of the flavonoid and hydroxylation of the prenyl group

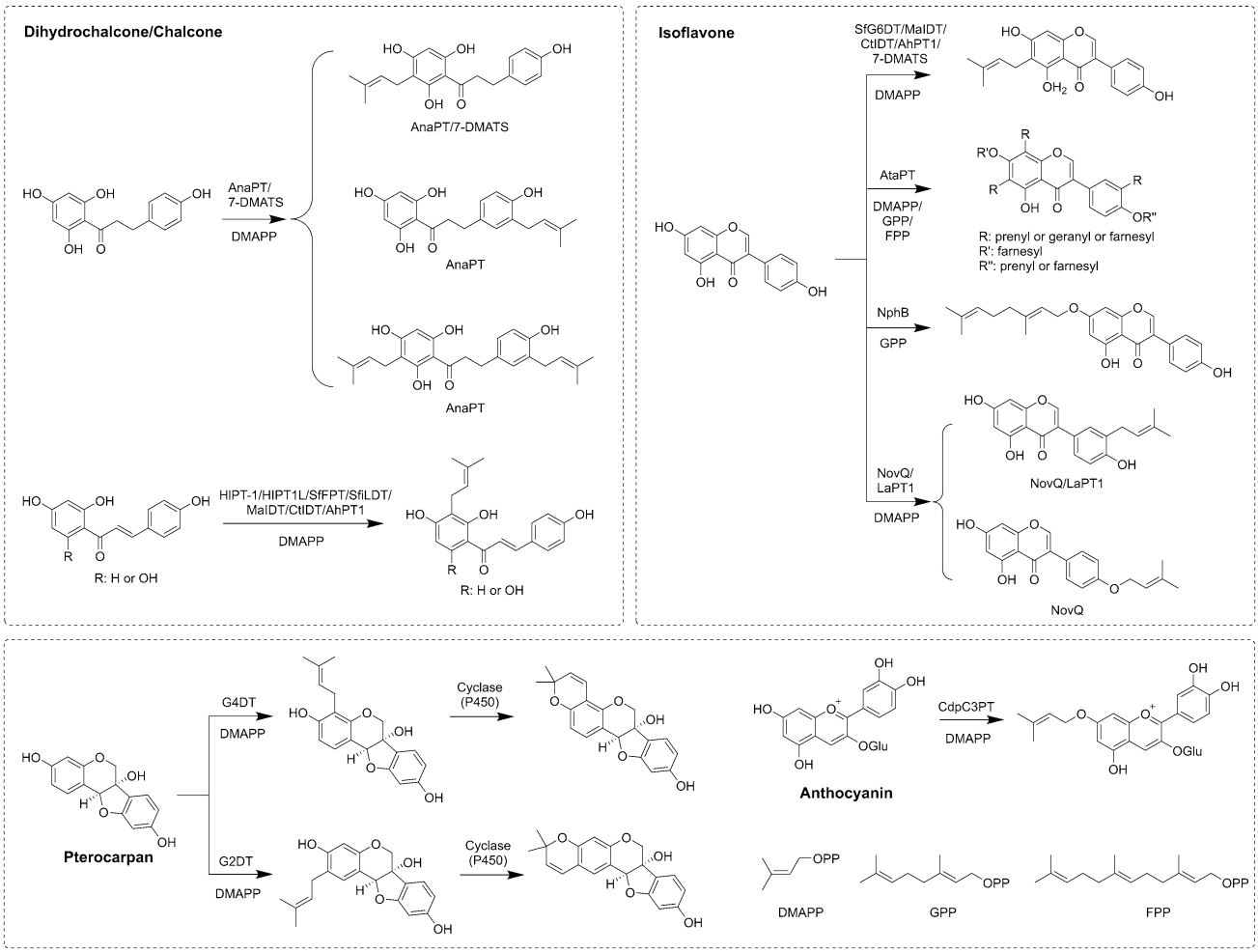

Fig. 6 Biosynthesis of the prenylated flavonoids (II).

decreased the cytotoxicity of the compounds (Zhang et al. 2020).

A diprenylated flavonol (**164**) exhibited significant cytotoxicity against MCF-7, A549, PC-3, and HeLa cells with IC_{50} values ranging from 5.40 to 5.82 μM (Segun et al. 2019). Daphnegiravone D (**165**), a 3-methoxy derivative of **164**, showed cytotoxic activity against human hepatocellular carcinoma cells (HepG2 and Hep3B cells) with IC_{50} values of 9.89 and 1.63 μM, respectively (Wang et al. 2017a).

Several prenylated flavonoids with pyran ring at A or B ring show potential cytotoxicity against different cancer cells. Kuwanon C (**166**) and morusinol (**207**) are from *Morus alba* root bark and showed cytotoxicity against THP-1 human monocytic leukemic cells with IC_{50} values of 1.7 and 4.3 μM, respectively (Zelová et al. 2014). Three flavonols, macarindicin E (**199**), macadenathin B (**200**), and macarindicin F (**227**), each bearing a pyran ring showed stronger cytotoxic activity than macarindicin D (**63**) and glyasperin A (**168**) as well as the non-prenylated flavonoids, kaempferol, quercetin, and quercitrin (Huonga et al. 2019). Artonin E (**202**) is from the bark of *Artocarpus elasticus* and possessed cytotoxicities against MCF-7 and MDA-MB-231 cells with IC_{50} values of 2.6 and 13.5 μg/mL, respectively (Ramli et al. 2016). The diprenylated flavones (**204**, **207**, and **229**) exhibited cytotoxicity against A549, NCI-H292, HepG2, and Hep3B cells with IC_{50} values ranging from 8.91 to 29.2 μM. Morusin (**204**) possessing an intact prenyl side chain exhibit more potent cytotoxicity than **207** bearing a hydroxylated prenyl side chain at C-3, suggesting hydroxylation of the prenyl side chain at C-3 decreased the cytotoxicity (Li et al. 2018; Wang et al. 2017a).

Paulownia tomentosa fruits are rich in geranylated flavonoids (**368–371**, **373**, **382**, **385**, **412**, and **420**) (Fig. 8) which exhibited potent antiproliferative activities against THP-1 ($IC_{50} < 10$ μM). However, the non-geranylated flavonoids, 3′,4′,5′-trimethoxyflavanone, eriodictyol, and naringenin, were inactive in comparison to flavonoids with geranyl side chains. The cytotoxic effect of geranylated flavonoids is possibly related to their lipophilicity and to their greater ability to penetrate the membranes of

Table 4 Flavonoid prenyltransferase genes characterized from natural sources

Source	gene	Structure	Specificity	Substrate/ Prenyl donor/ Cofactor	References
Artocarpus heterophyllus	AhPT1	402 amino acids, 7–8 putative transmembrane domains	Flavones and flavanones with 6-hydroxyl at A ring, chalcones with 2′,4′-dihydroxyl at A ring, isoflavones with 5-hydroxyl at A ring and alkenyl between C-2 and C-3 at C ring	2′,4′-dihydroxychalcone, 2′,4,4′-trihydroxychalcone, 6-hydroxyflavone, 2′,6-dihydroxyflavone, 3′,6-dihydroxyflavone, 4′,6-dihydroxyflavone, 6-hydroxyflavanone, genistein/ DMAPP/Mg^{2+}, Mn^{2+}	Yang et al. 2020
Cannabis sativa	CsPT3	/	/	Chrysoeriol, apigenin/ DMAPP, GPP/Mg^{2+}	Rea et al. 2019
Cudrania tricuspidata	CtIDT	398 amino acids, 7 putative transmembrane regions	Preferred isoflavone, hydroxyl group at the C-2 of chalcones decreased the activity, hydroxyl group at the C-2′ of isoflavone increased the activity	isoliquiritigenin, 2′,4′-dihydroxychalcone, 2,4,2′,4′-tetrahydroxychalcone, butein, genistein, 2′-hydroxygenistein/DMAPP, GPP /Mg^{2+}, Mn^{2+}, Ca^{2+}, Fe^{2+}, Ba^{2+}	Wang et al. 2014
Glycine max	G2DT-2 (GmPT01)	394 amino acids 9 putative transmembrane regions	Prenylated (-)-glycinol at C-2	Glycinol/DMAPP/Mg^{2+}	Sukumaran et al. 2018
	IDT3 (GmPT10d)	403 amino acids 8 putative transmembrane regions	Preferred isoflavone	Daidzein, genistein/DMAPP/ Mg^{2+}	
G. max	C4DT	412 amino acids 9 transmembrane regions	Preferred coumestrol	Coumestrol/DMAPP/Mg^{2+}	Yoneyama et al. 2016
	G2DT	408 amino acids, 9 transmembrane regions	Preferred (-)-glycinol	(-)-Glycinol/DMAPP/Mg^{2+}	
	IDT1	402 amino acids 9 transmembrane regions	Preferred isoflavone,	Daidzein, genistein/DMAPP/ Mg^{2+}	
	IDT2	410 amino acids 9 transmembrane regions	Preferred isoflavone,	Daidzein, genistein/DMAPP/ Mg^{2+}	
G. max	G4DT	409 amino acids, 9 transmembrane domains	Pterocapan-specific Prenylated glycinol at C-4	(-)-glycinol/DMAPP/Mg^{2+}	Akashi et al. 2009
Glycyrrhiza uralensis	GuA6DT	412 amino acids 9 transmembrane α-helices	Prenylated 5,7-dihydroxyflavone at C-6	Apigenin, chrysin, diosmtin, luteolin, norartocarpetin, chrysoeroil/GPP/Mg^{2+}, Mn^{2+}, Zn^{2+}, Fe^{2+}, Co^{2+}, Ca^{2+}, Ba^{2+}	Li et al. 2014
Humulus lupulus	HlPT-1	/	/	Naringenin chalcone/DMAPP/ Mg^{2+}	Tsurumaru et al. 2012
Lithospermum erythrorhizon	LePGT1	9 transmembrane α-helices	*p*-hydroxybenzoic acid, GPP-specific	*p*-hydroxybenzoic acid/GPP/ Mg^{2+}	Ohara et al. 2009

Table 4 (continued)

Source	gene	Structure	Specificity	Substrate/ Prenyl donor/ Cofactor	References
Lupinus albus	LaPT1	408 amino acids, 9 transmembrane regions	Isoflavonoid-specific, prenylated genistein at C-3′ on B-ring	Genistein, 2′-hydroxygenistein/ DMAPP/ Mg^{2+}, Mn^{2+}, Ni^{2+}, Co^{2+}, Zn^{2+}, Ca^{2+}	Shen et al. 2012
Morus alba	MaIDT	402 amino acids, 7 transmembrane regions	Preferred 2′,4′-dihydroxychalcones	Isoliquiritigenin, 2′,4′-dihydroxychalcone, 2,4,2′,4′-tetrahydroxychalcone, apigenin, 2′-hydroxygenistein, butein, genistein, /DMAPP, GPP/Mg^{2+}, Ba^{2+}, Ca^{2+}, Mn^{2+}, Fe^{2+}, Ni^{2+}	Wang et al. 2014
Sophora flavescens	SfN8DT-1	410 amino acids, 9 transmembrane α-helices	Flavanones-specific, prenylated naringenin at C-8	Naringenin, liguiritigenin, hesperetin/DMAPP/ Mg^{2+}	Sasaki et al. 2008, Yang et al. 2015
	SfN8DT-2	407 amino acids, 9 transmenbrane α-helices	Flavanones-specific, prenylated naringenin at C-8	Naringenin, liguiritigenin, hesperetin/DMAPP/ Mg^{2+}	
S. flavescens	SfN8DT-3	410 amino acids, 9 transmenbrane α-helices	/	Naringenin, liquiritigenin/ DMAPP/Mg^{2+}	Sasaki et al. 2011
	SfG6DT	407 amino acids, 7–9 transmembrane α-helices	Isoflavone-specific, prenylated genistein at C-6	Genistein, biochanin A/DMAPP, GPP, FPP/ Mg^{2+}, Ni^{2+}, Mn^{2+}, Ca^{2+}	
	SfiLDT	/	Chalcone-specific	Isoliquiritigenin/ DMAPP/ Mg^{2+}	
S. flavescens	SfFPT	407 amino acids, 8 transmembrane α-helices	A few select flavanones at the C-8 position, stereospecificity: preferred levorotatory flavanones to produce (2S)-prenylflavanones	Pinocembrin, naringenin, chrysin, taxifolin, liquiritigenin, steppogenin, eriodictyol, hesperetin, sakuranetin, isosakuranetin, tsugafolin, phloretin/ DMAPP, GPP/ Mg^{2+}, Ba^{2+}, Ca^{2+}, Fe^{2+}, Co^{2+}, Cu^{2+}, Zn^{2+}, Mn^{2+}	Chen et al. 2013
Aspergillus fumigatus	7-DMATS	/	Preferred prenylation position at C-6, between the two hydroxyl groups.	Naringenin, 7-hydroxyflavanone, eriodictyol, hesperetin, silibinin, phloretin, apigenin, genistein, biochanin A / DMAPP/Ca^{2+}	Yu et al. 2011, Zhou et al. 2015
Aspergillus terreus	AtaPT	424 amino acids	Possessed the ability to form mono-, di- and/or triprenylated products with C–C and/or C–O bonds	Genistein/DMAPP, GPP, FPP, GGPP, PPP	Chen et al. 2016
Neosartorya fischeri	AnaPT	/	Flavanones and isoflavones at C-6 of the A ring or C-3′ of the B ring	Naringenin, 7-hydroxyflavanone, eriodictyol, hesperetin, silibinin, phloretin, apigenin, genistein, biochanin A / DMAPP, GPP/Ca^{2+}	Zhou et al. 2015

Table 4 (continued)

Source	gene	Structure	Specificity	Substrate/ Prenyl donor/ Cofactor	References
Neosartorya fischer	CdpC3PT		Regiospecific 7-O-prenylation of anthocyanins	Cyanidin-3-O-glucoside, cyanidin-3-O-galactoside, petunidin-3-O-galactoside, cyanidin-3-O-arabinoside, peonidin-3-O-galactoside, malvidin-3-O-galactoside, malvidin-3-O-arabinoside/ DMAPP/Ca^{2+}	Bao et al. 2021
Fusarium oxysporum	FoPT1	427 amino acids	Favonoids with 5,7-dihydroxyl and 4-carbonyl groups, 2,3-alkenyl in flavonoid skeleton was beneficial for catalysis	Apigenin, kaempferol, luteolin, naringenin, genistein, dihydrogenistein, hesperetin/ DMAPP/Ca^{2+}, Mg^{2+}, Mn^{2+}, Ni^{2+}, Co^{2+}, Fe^{2+}	Yang et al. 2016
Stigmatella aurantiaca	AuaA	/	/	Naringenin, phloretin/FPP/Mg^{2+}	Stec et al. 2012
Streptomyces niveus	NovQ	323 amino acids	/	Naringenin, apigenin, daizein, genistein/ DMAPP/Mg^{2+}	Ozaki et al. 2009
Streptomyces sp. strain CL190	NphB	/	Catalyzed C-geranylation and O-geranylation	Naringenin, apigenin, genistein, daidzein, chrysin/GPP/Mg^{2+}	Kumano et al. 2008, Shindo et al. 2011
Streptomyces coelicolor A3(2)	SCO7190	/	Catalyzed C-prenylation	Naringenin/DMAPP/	Kumano et al. 2008

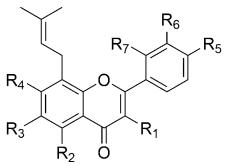

	R_1	R_2	R_3	R_4	R_5	R_6	R_7
1	H	H	H	H	OH	H	H
2	H	OH	H	OMe	OH	H	OH
3	H	OH	H	OH	OH	H	H
4	H	OMe	OMe	OMe	OH	OMe	H
5	OH	OH	H	OH	OH	H	H
6	OH	OH	H	OH	OMe	H	H
7	OH	OH	H	OH	OH	OH	H
8	OH	OMe	H	OH	OH	H	H
9	OMe	OH	H	OH	OH	H	H
10	OMe	OH	H	OH	OH	OH	H

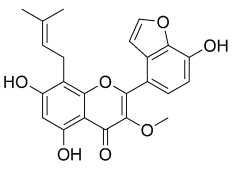

11

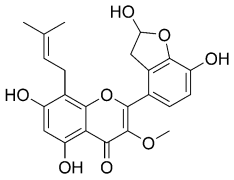

12

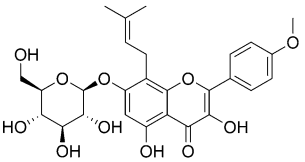

13

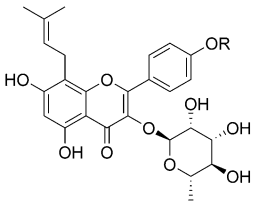

14 R=H
15 R=CH_3

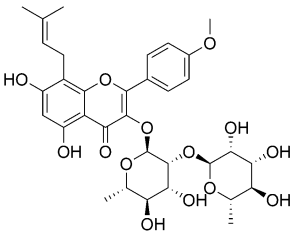

16

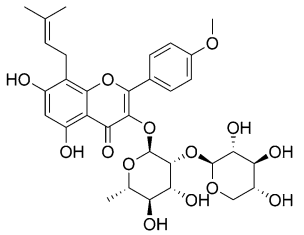

17

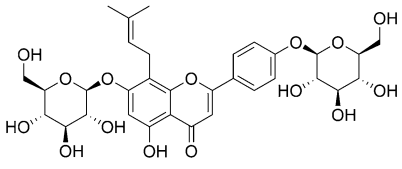

18

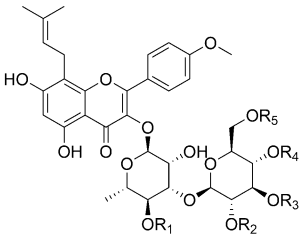

	R_1	R_2	R_3	R_4	R_5
19	Ac	H	H	H	Ac
20	Ac	H	H	H	H
21	Ac	H	H	Ac	Ac
22	Ac	Ac	H	H	Ac
23	Ac	H	Ac	H	Ac
24	Ac	H	H	H	Ac
25	H	H	H	H	H

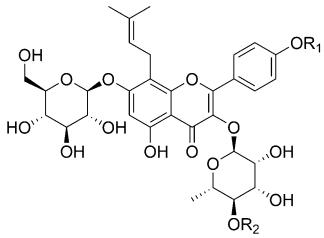

	R_1	R_2
26	Me	H
27	H	H
28	Me	Ac

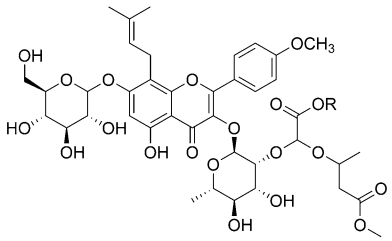

29 R=H
30 R=-$(CH_2)_3CH_3$
31 R=Me

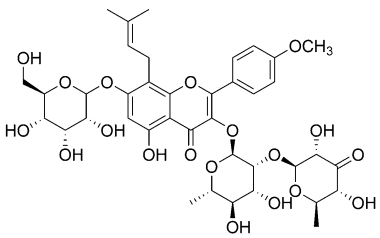

32

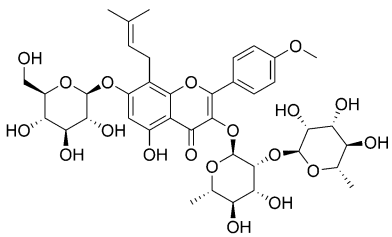

33

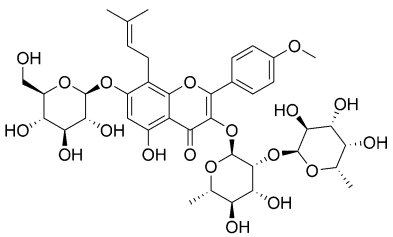

34

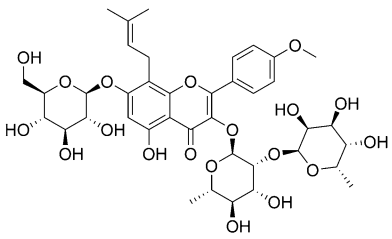

35

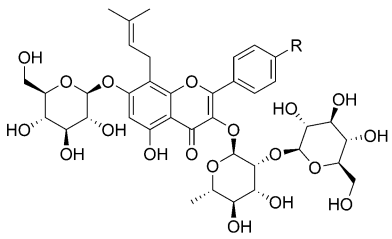

36 R=OMe
37 R=OH

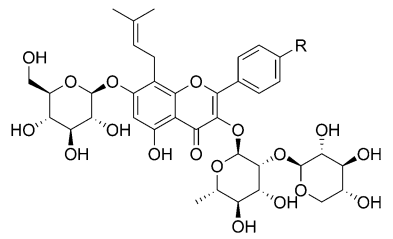

38 R=OMe
39 R=OH

Fig. 7 Chemical structures of prenylated flavones (**1–261**)

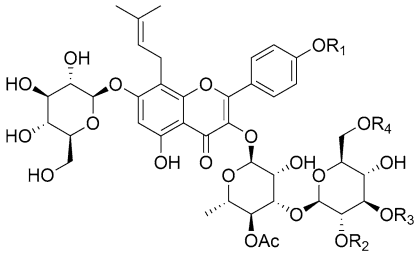

	R_1	R_2	R_3	R_4
40	Me	H	H	H
41	Me	Ac	H	Ac
42	Me	H	Ac	Ac
43	H	H	Ac	Ac

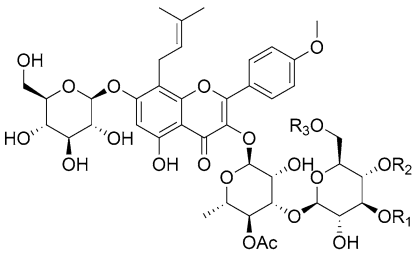

	R_1	R_2	R_3
44	H	H	Ac
45	Ac	H	H
46	H	Ac	Ac

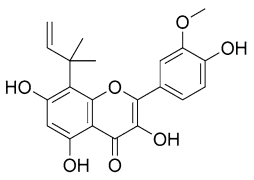

47

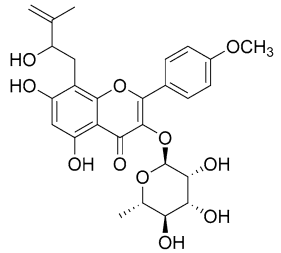

48

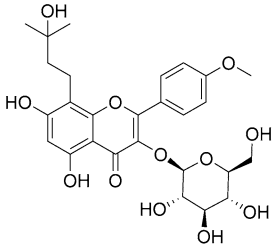

49

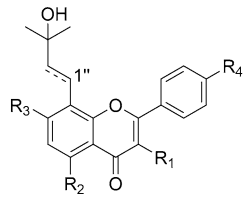

	R_1	R_2	R_3	R_4
50	OH	OH	OH	OMe
51	H	H	OMe	H

$\Delta^{1''}$

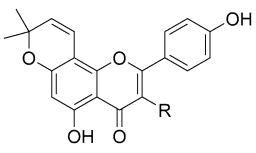

52 R=H
53 R=OH

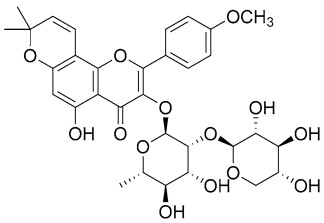

54

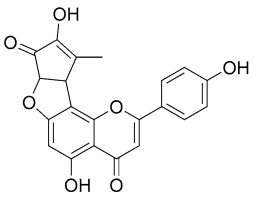

55

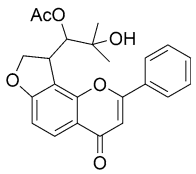

56

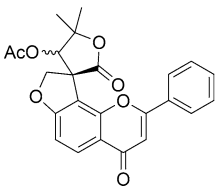

57 α–OAc
58 β–OAc

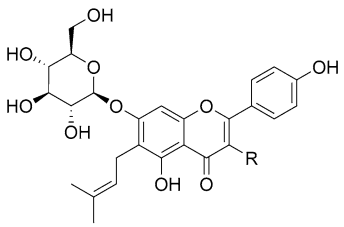

59 R=OMe
60 R=OH

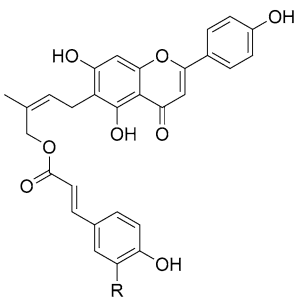

75 R=H
76 R=OMe

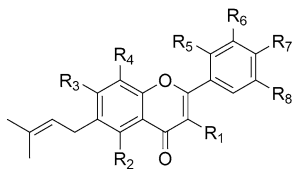

	R_1	R_2	R_3	R_4	R_5	R_6	R_7	R_8
61	H	OMe	OMe	H	H	OMe	H	OMe
62	H	OH	OH	H	H	OH	OH	H
63	OH	OH	OH	H	H	H	OH	CHO
64	H	OH	OH	H	H	H	OH	H
65	H	OH	OH	H	OH	H	OH	H
66	H	H	OH	H	H	H	OH	H
67	OH	OH	OH	H	H	OH	OMe	OH
68	OH	OH	OH	OMe	H	OH	OMe	H
69	OH	OH	OH	H	OMe	H	OH	H
70	OH	OH	OH	H	H	OH	OH	H
71	OMe	OH	OH	H	H	OH	OH	H
72	OMe	OH	OH	H	H	H	OH	H
73	OH	OH	OH	H	H	H	OH	H

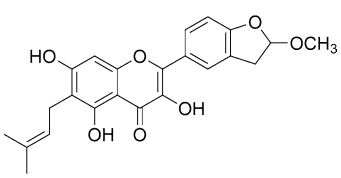

74

Fig. 7 (continued)

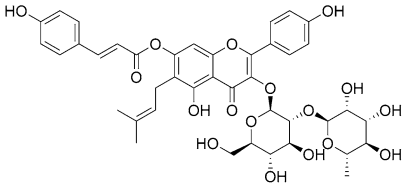

77

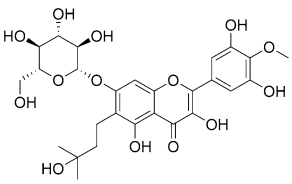

78

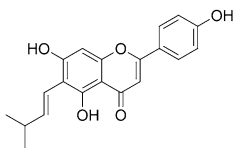

79

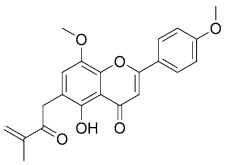

80

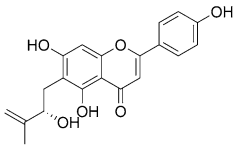

81

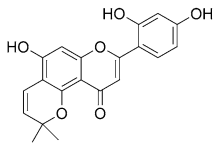

89

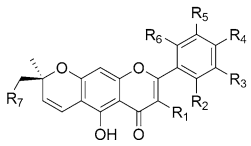

	R_1	R_2	R_3	R_4	R_5	R_6	R_7
82	H	OH	H	OH	H	H	H
83	OH	H	H	OH	H	OMe	H
84	H	H	H	OH	OH	H	H
85	H	H	H	OH	OMe	H	H
86	H	H	H	OH	H	H	OH
87	OH	H	OH	OMe	OH	H	H
88	OH	H	OH	OH	H	H	H

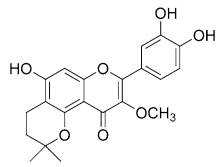

90

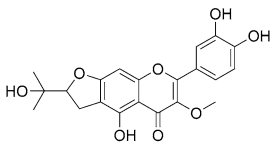

91

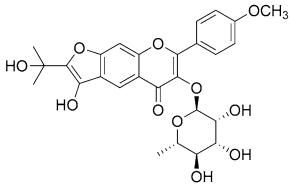

92

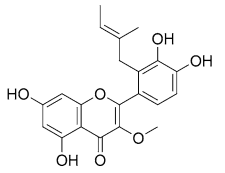

93

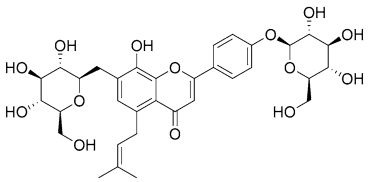

94

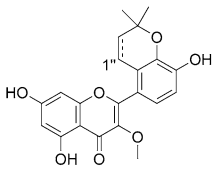

95 $\Delta^{1''}$
96

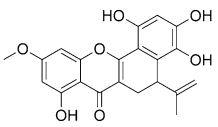

97

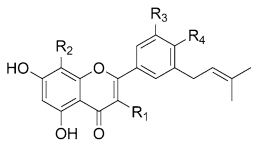

	R_1	R_2	R_3	R_4
98	H	H	OH	OMe
99	H	H	OH	OH
100	H	Me	OH	OH
101	OH	H	H	OH
102	OH	H	OH	OH
103	H	H	H	OH
104	OMe	H	H	OH

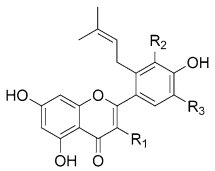

	R_1	R_2	R_3
105	OH	H	OMe
106	OMe	OH	H
107	OH	H	OH
108	OH	OMe	H

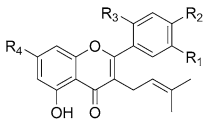

	R_1	R_2	R_3	R_4
109	OH	OMe	OH	OMe
110	H	OH	OMe	OH
111	H	OH	H	OH

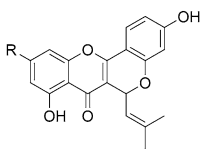

112 R=OH
113 R=OMe

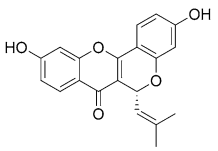

114

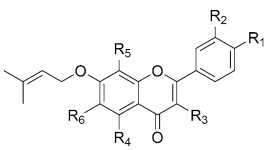

	R_1	R_2	R_3	R_4	R_5	R_6
115	OH	H	β-OH	OH	H	H
116	OMe	OMe	OH	H	H	H
117	OMe	OH	OH	OH	OMe	H
118	OMe	OMe	OMe	OMe	H	H
119	OMe	OMe	OMe	OMe	OMe	OMe
120	OMe	H	OMe	OH	H	OMe
121	OH	OMe	OH	OH	OMe	H
122	-OCH$_2$O-		OMe	OMe	H	H

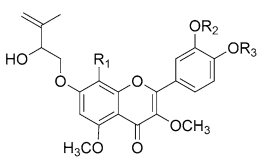

	R_1	R_2	R_3
123	H	Me	Me
124	OMe	Me	Me
125	H	-CH$_2$-	
126	OMe	-CH$_2$-	

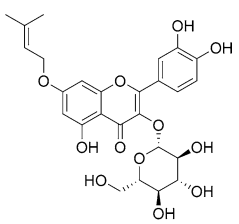

127

Fig. 7 (continued)

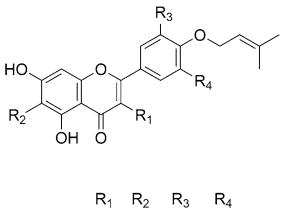

	R_1	R_2	R_3	R_4
128	H	OMe	H	H
129	H	OMe	H	OMe

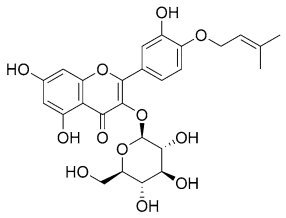

130

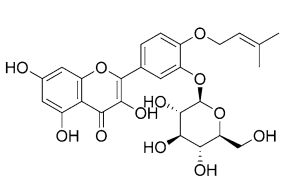

131

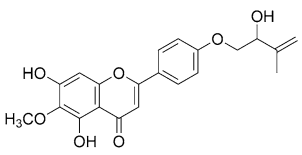

132

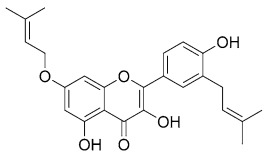

133

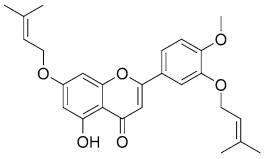

134

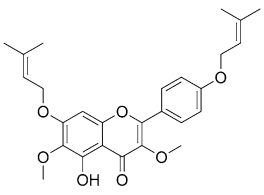

135

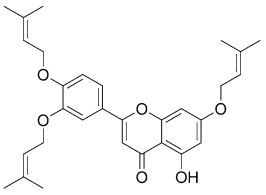

136

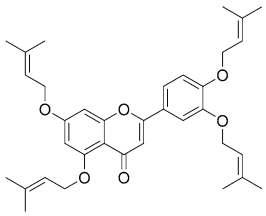

137

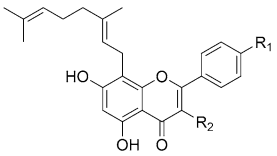

	R_1	R_2
138	OH	H
139	OH	OH
140	OGlu	H

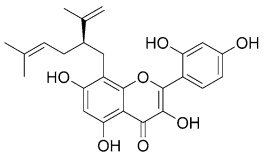

141

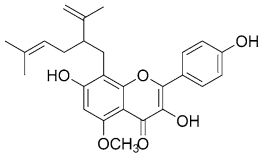

142

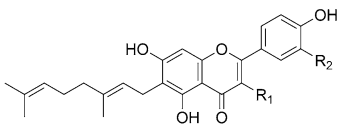

	R_1	R_2
143	OH	H
144	OH	OH
145	OMe	OH
146	H	H

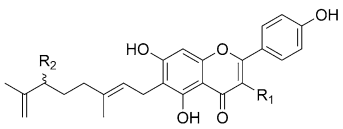

	R_1	R_2
147	H	α-OH
148	OH	OH

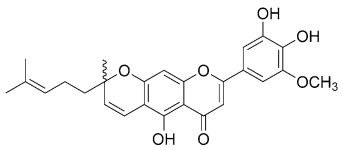

149

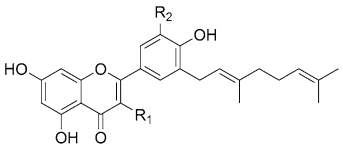

	R_1	R_2
150	OH	OH
151	H	H

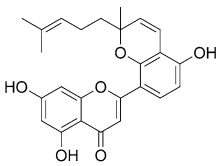

152

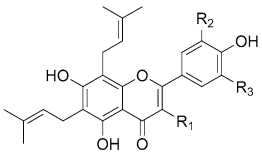

	R_1	R_2	R_3
153	OH	H	OMe
154	OH	H	H
155	H	OH	H
156	OMe	OH	H

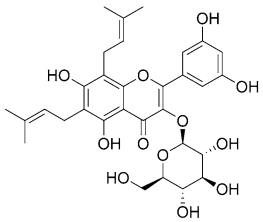

157

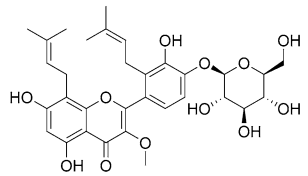

158

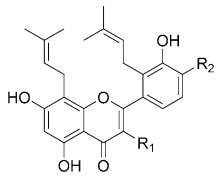

	R_1	R_2
159	OH	OH
160	OMe	OH

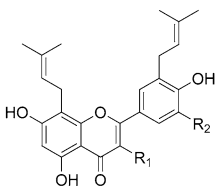

	R_1	R_2
161	H	H
162	H	OH
163	OH	OH
164	OH	H
165	OMe	H

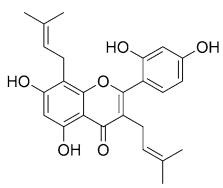

166

Fig. 7 (continued)

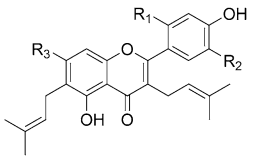

	R_1	R_2	R_3
167	OH	H	OH
168	H	OH	OH
169	OH	H	OMe

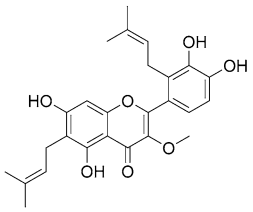

170

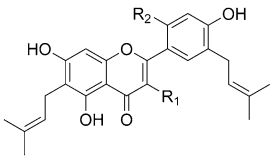

	R_1	R_2
171	OH	H
172	H	OH

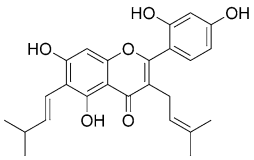

173

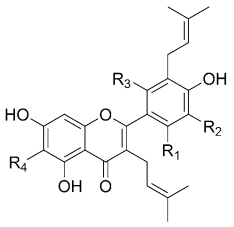

	R_1	R_2	R_3	R_4
174	H	OH	OMe	OH
175	OH	H	H	H
176	H	H	OH	H

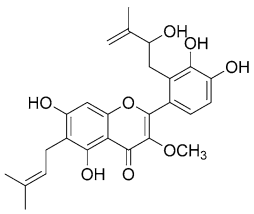

177

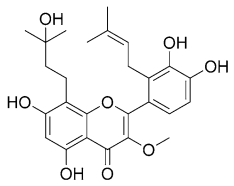

178

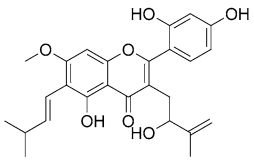

179

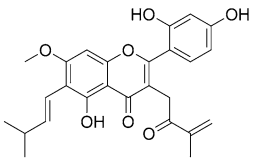

180

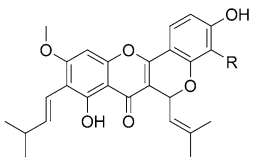

181 R=H
182 R=OH

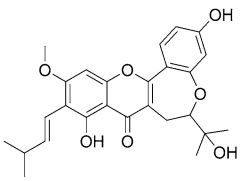

183

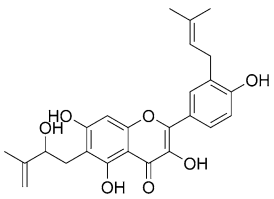

184

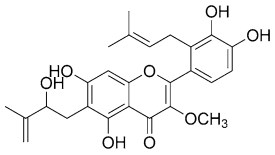

185

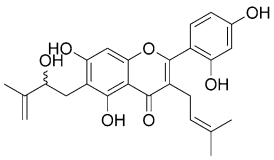

186

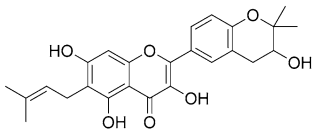

187

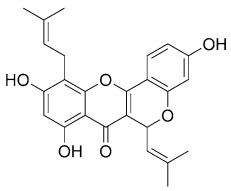

188

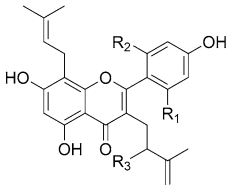

	R_1	R_2	R_3
189	OH	H	OH
190	H	OH	=O

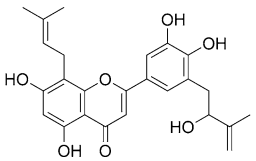

191

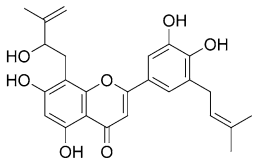

192

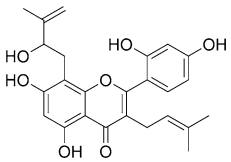

193

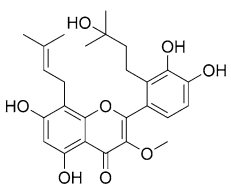

194

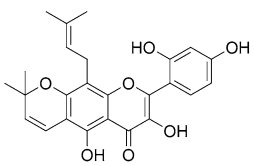

195

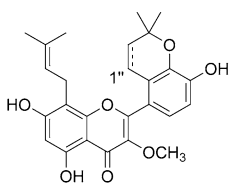

196
197 $\Delta^{1''}$

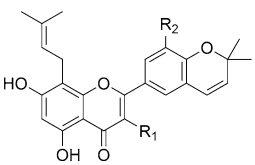

	R_1	R_2
198	OMe	OH
199	OH	H

Fig. 7 (continued)

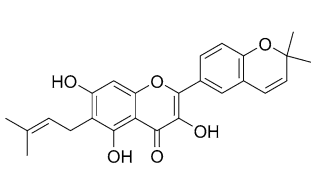

200

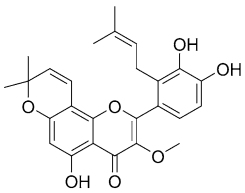

201

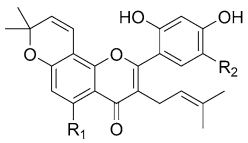

	R1	R2
202	OH	OH
203	OMe	OH
204	OH	H

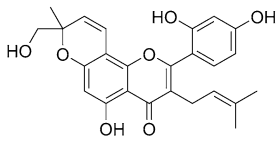

205

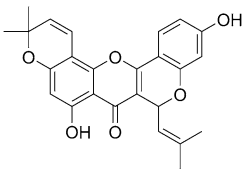

206

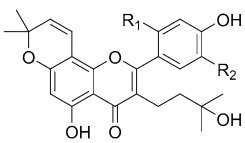

	R1	R2
207	OH	H
208	OMe	OH

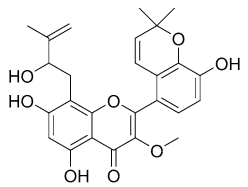

209

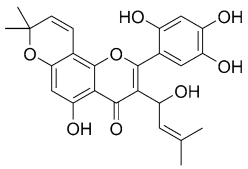

210

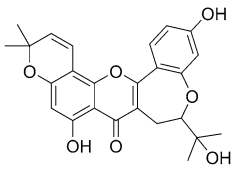

211

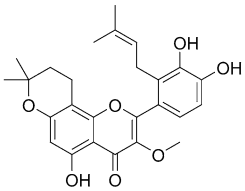

212

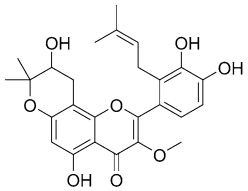

213

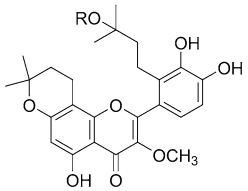

214 R=H

215 R=Me

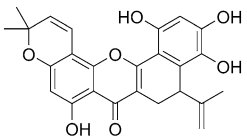

216

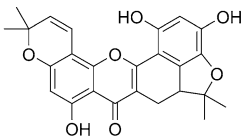

217

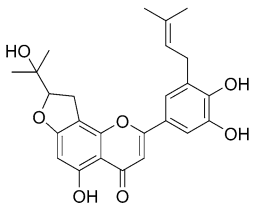

218

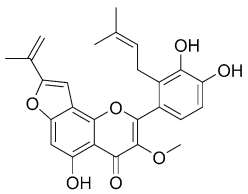

219

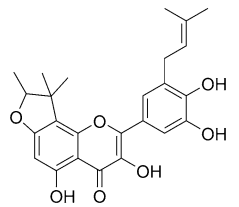

220

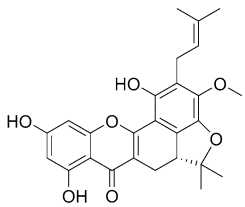

221

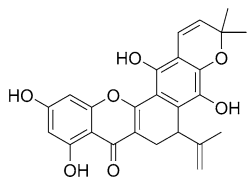

222

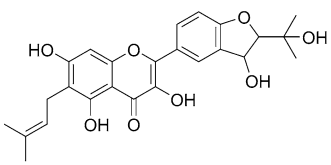

223

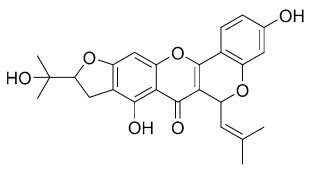

224

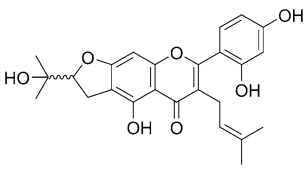

225

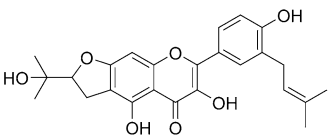

226

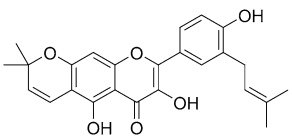

227

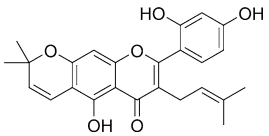

228

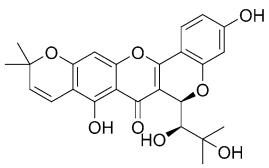

229

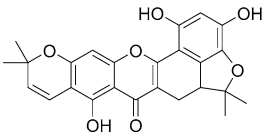

230

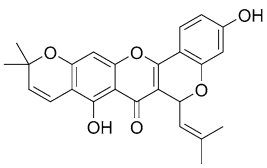

231

Fig. 7 (continued)

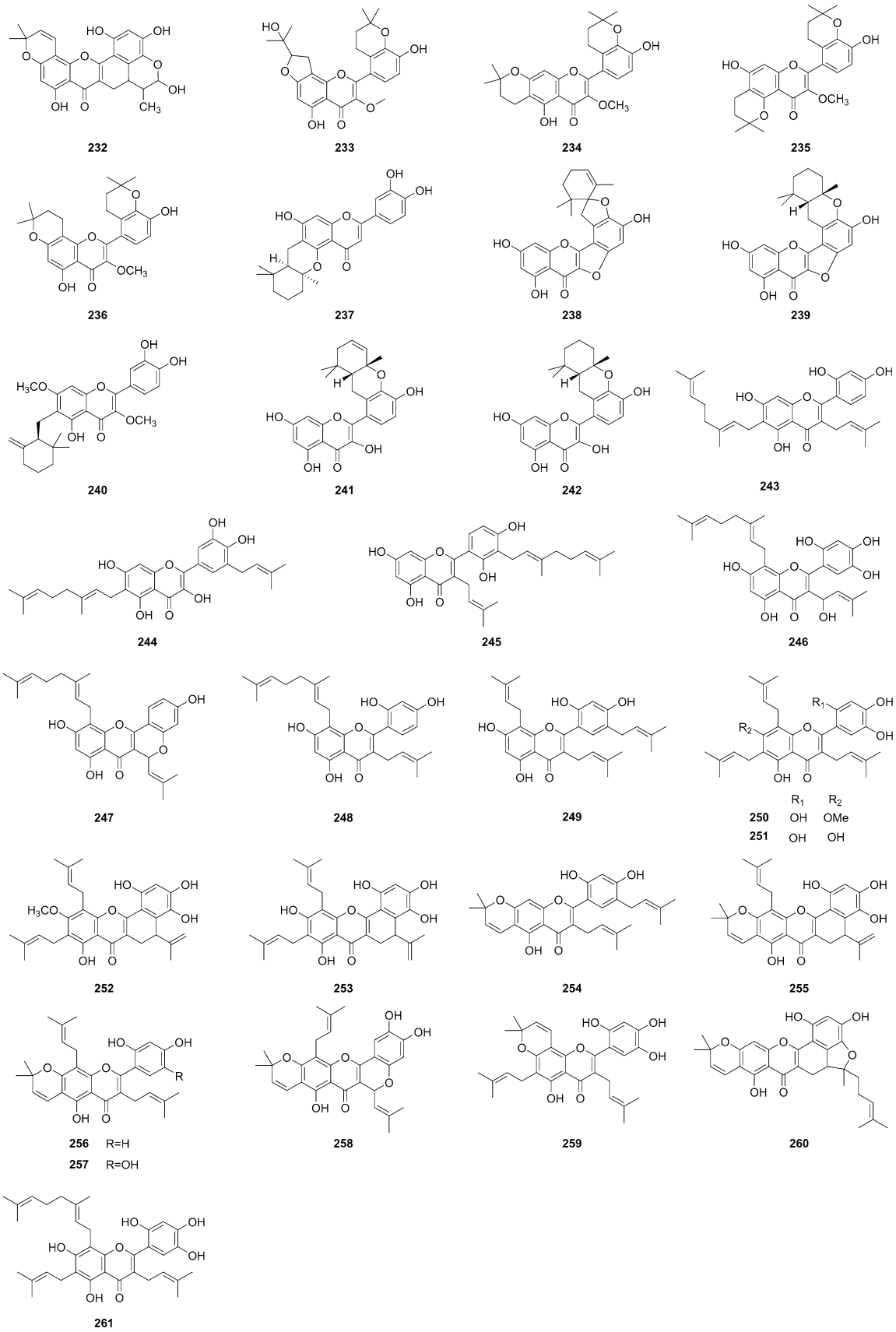

Fig. 7 (continued)

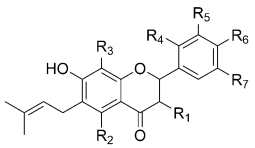

	R_1	R_2	R_3	R_4	R_5	R_6	R_7
262	H	H	H	H	H	OH	H
263	H	OH	H	H	OH	OMe	OH
264	H	OH	H	H	OMe	OH	H
265	H	OH	Me	H	OH	OH	H
266	H	OH	H	H	OH	OH	H
267	H	OH	H	H	H	OH	H
268	OH	OH	H	H	H	OH	H
269	H	H	H	OH	H	OH	OMe
270	OH	OH	H	H	OH	OMe	OH

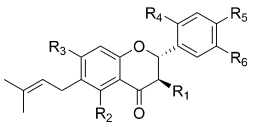

	R_1	R_2	R_3	R_4	R_5	R_6
271	H	OH	OH	H	OH	OMe
272	H	OH	OMe	H	OH	H
273	H	H	OH	H	OH	H
274	OH	OH	OH	OH	OH	H
275	H	OH	OH	OH	OH	H
276	H	OH	OH	H	H	H
277	H	H	OMe	H	OH	H
278	OH	OH	OMe	H	OH	H

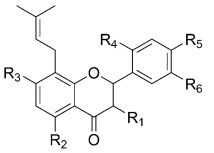

	R_1	R_2	R_3	R_4	R_5	R_6
279	H	H	OH	OH	OH	H
280	H	OH	OH	H	OH	H
281	H	OMe	OH	H	OH	H
282	H	OH	OH	OH	H	H
283	H	OH	OH	H	OH	OMe
284	H	OH	OH	H	H	H
285	H	H	OMe	H	OH	H
286	OH	OMe	OH	H	OH	H
287	OH	OH	OH	H	OH	H
288	H	OH	OH	OH	OH	OMe
289	H	H	OH	H	OH	H

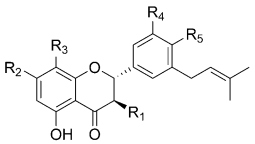

	R_1	R_2	R_3	R_4	R_5
290	H	OH	H	OH	OMe
291	H	OH	H	OMe	OH
292	H	OH	H	OH	OH
293	H	OMe	H	H	OMe
294	H	OH	Me	OH	OH
295	H	OH	H	H	OH
296	H	OH	H	H	OMe
297	H	OH	H	CHO	OMe
298	OH	OH	H	OH	OH

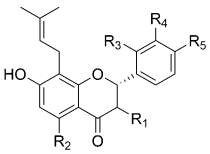

	R_1	R_2	R_3	R_4	R_5
299	β–OH	OH	H	OH	OMe
300	α–OH	OMe	H	H	OH
301	β–OH	OH	H	H	H
302	β–OH	H	H	H	OH
303	β–OH	OH	OH	H	OH
304	β–OH	OH	H	H	OH
305	β–OH	OH	H	OMe	OH
306	H	OH	H	H	OMe

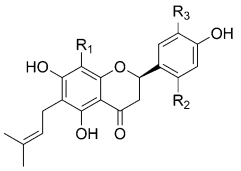

	R_1	R_2	R_3
307	H	OMe	H
308	Me	H	OH

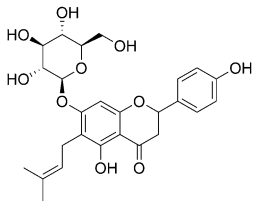

309

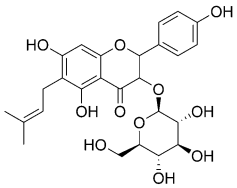

311

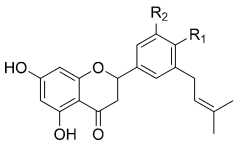

	R_1	R_2
311	OMe	OH
312	OH	OH
313	OH	H

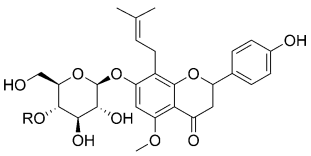

314 R=Me
315 R=H

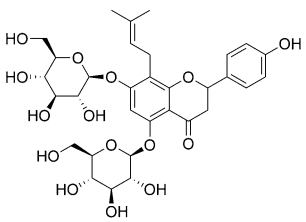

316

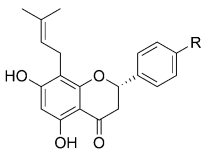

317 R=OH
318 R=H

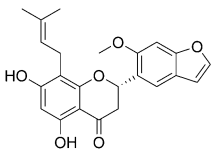

319

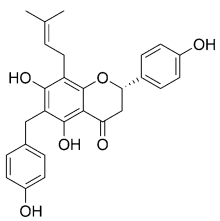

320

Fig. 8 Chemical structures of prenylated flavonones (**262–567**)

cells. The presence of a β-carbon (proximal) OH group on a geranyl chain (**385**, $IC_{50} = 6.5\ \mu M$) did not affect the cytotoxicity, but an OH group on the distal end of the side-chain (**399**, $IC_{50} > 20\ \mu M$) caused a loss of cytotoxic effect. The substituents on ring B of the flavonoid structure seemed to have minor effects on the cytotoxic potential of the geranylated flavonoids (Hanáková et al. 2015). Another phytochemical study of the fruit of *Paulownia*

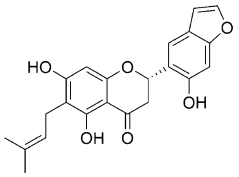

321

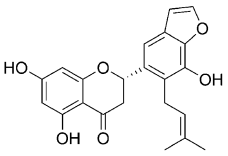

322

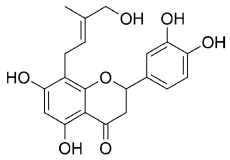

323

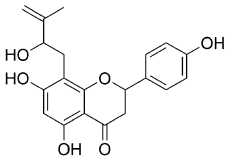

324

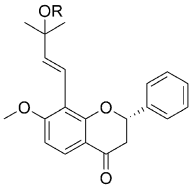

325 R=H
326 R=CH_3

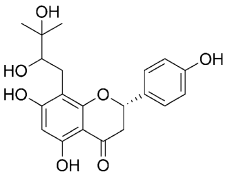

327

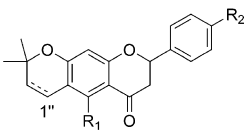

	R_1	R_2
328	OH	H
329	H	OH

$\Delta^{1''}$

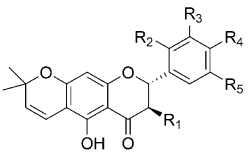

	R_1	R_2	R_3	R_4	R_5
330	OH	OH	H	OH	H
331	OH	OH	H	OMe	H
332	H	H	OH	OH	H
333	OH	H	OH	OMe	OH

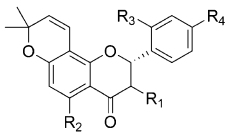

	R_1	R_2	R_3	R_4
334	H	H	H	OH
335	OH	OH	H	OH
336	β–OH	OH	OH	OH
337	β–OH	OH	OH	OMe

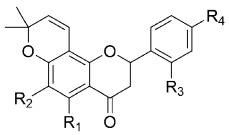

	R_1	R_2	R_3	R_4
338	OH	Me	OMe	OH
339	H	H	H	OMe
340	OH	H	H	OH

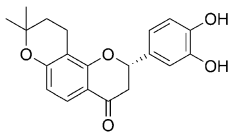

341

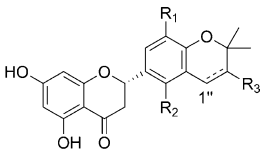

	R_1	R_2	R_3	
342	H	H	H	$\Delta^{1''}$
343	OMe	H	H	$\Delta^{1''}$
344	H	OH	H	$\Delta^{1''}$
345	OH	H	H	$\Delta^{1''}$
346	OH	H	OH	
347	OH	H	H	

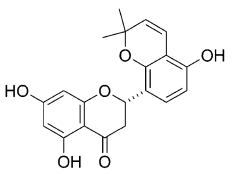

348

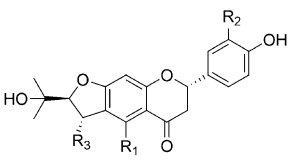

	R_1	R_2	R_3
349	H	OMe	OH
350	H	H	H

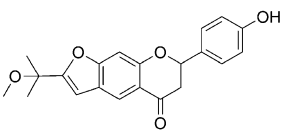

351

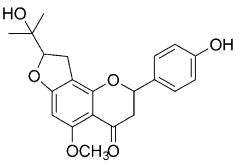

352 R=OMe
353 R=H

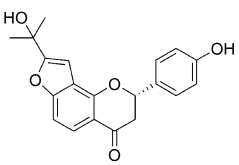

354

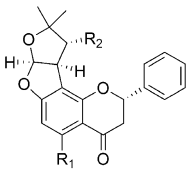

	R_1	R_2
355	H	OH
356	OMe	OAc
357	H	OAc

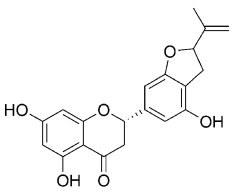

358

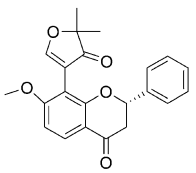

359

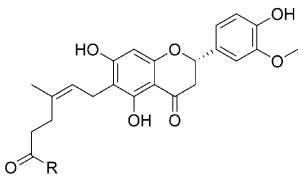

360 R=OMe
361 R=H

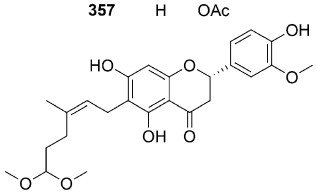

362

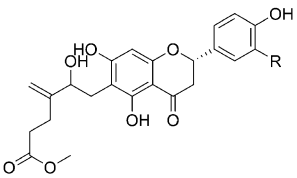

363 R=OMe
364 R=H

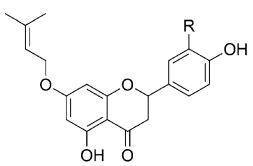

365 R=H
366 R=OH

Fig. 8 (continued)

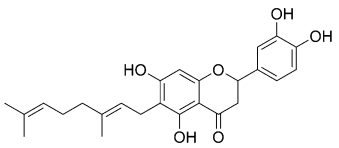

367

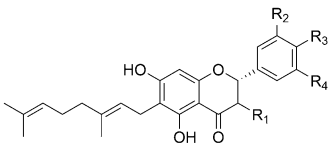

	R_1	R_2	R_3	R_4
368	H	H	OMe	OMe
369	H	H	OH	H
370	H	OH	OMe	OMe
371	β–OH	OMe	OH	OMe
372	OH	H	OH	OMe
373	H	H	OH	OMe
374	H	H	OH	OH
375	H	OH	OH	OMe
376	H	OMe	OH	OMe
377	β-OH	OH	OH	H
378	β-OH	H	OH	H
379	H	OH	OMe	OH
380	β-OH	H	OMe	OH

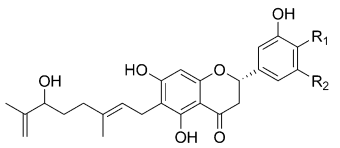

	R_1	R_2
381	OMe	OH
382	OH	H

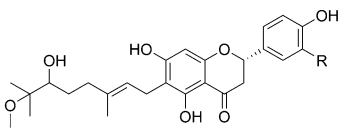

383 R=H
384 R=OMe

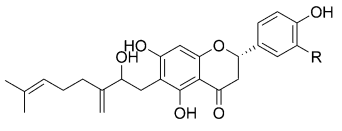

385 R=OMe
386 R=OH
387 R=H

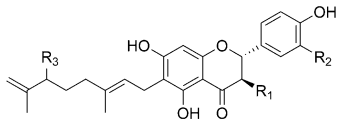

	R_1	R_2	R_3
388	OH	H	OH
389	H	H	OH
390	H	OMe	=O

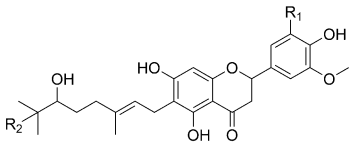

	R_1	R_2
391	OMe	OMe
392	OMe	OH

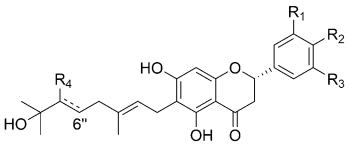

	R_1	R_2	R_3	R_4	
393	H	OH	H	OH	
394	H	OH	H	H	
395	OH	OH	H	H	
396	OH	OMe	H	H	
397	OMe	OH	OMe	H	
398	OMe	OH	OH	H	
399	H	OH	OMe	H	$\Delta^{6''}$

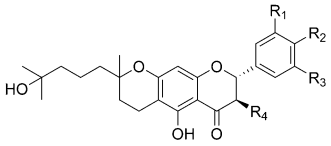

	R_1	R_2	R_3	R_4
400	OH	OH	H	H
401	OH	OMe	H	H
402	OMe	OH	OMe	H
403	OMe	OH	H	OH
404	OH	OH	H	OH
405	OMe	OH	OH	H
406	H	OH	H	H

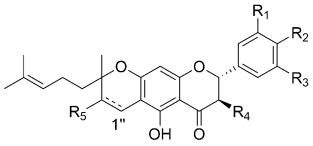

	R_1	R_2	R_3	R_4	R_5	
407	H	OH	OMe	OH	H	$\Delta^{1''}$
408	OH	H	OH	H	H	$\Delta^{1''}$
409	OH	OH	OMe	H	H	$\Delta^{1''}$
410	H	OH	OH	H	H	$\Delta^{1''}$
411	H	OH	OMe	H	H	$\Delta^{1''}$
412	H	OH	OMe	H	OH	

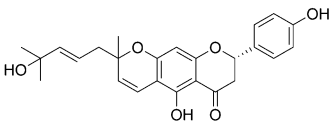

413

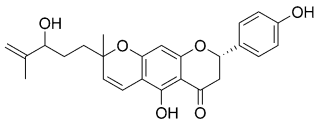

414

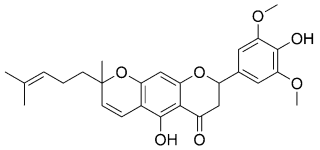

415

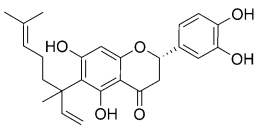

416

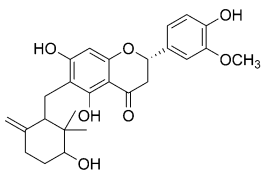

417

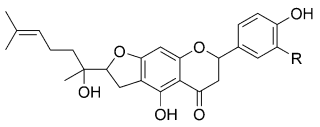

418 R=OH
419 R=H

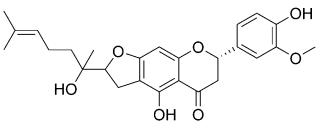

420

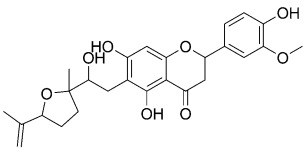

421

Fig. 8 (continued)

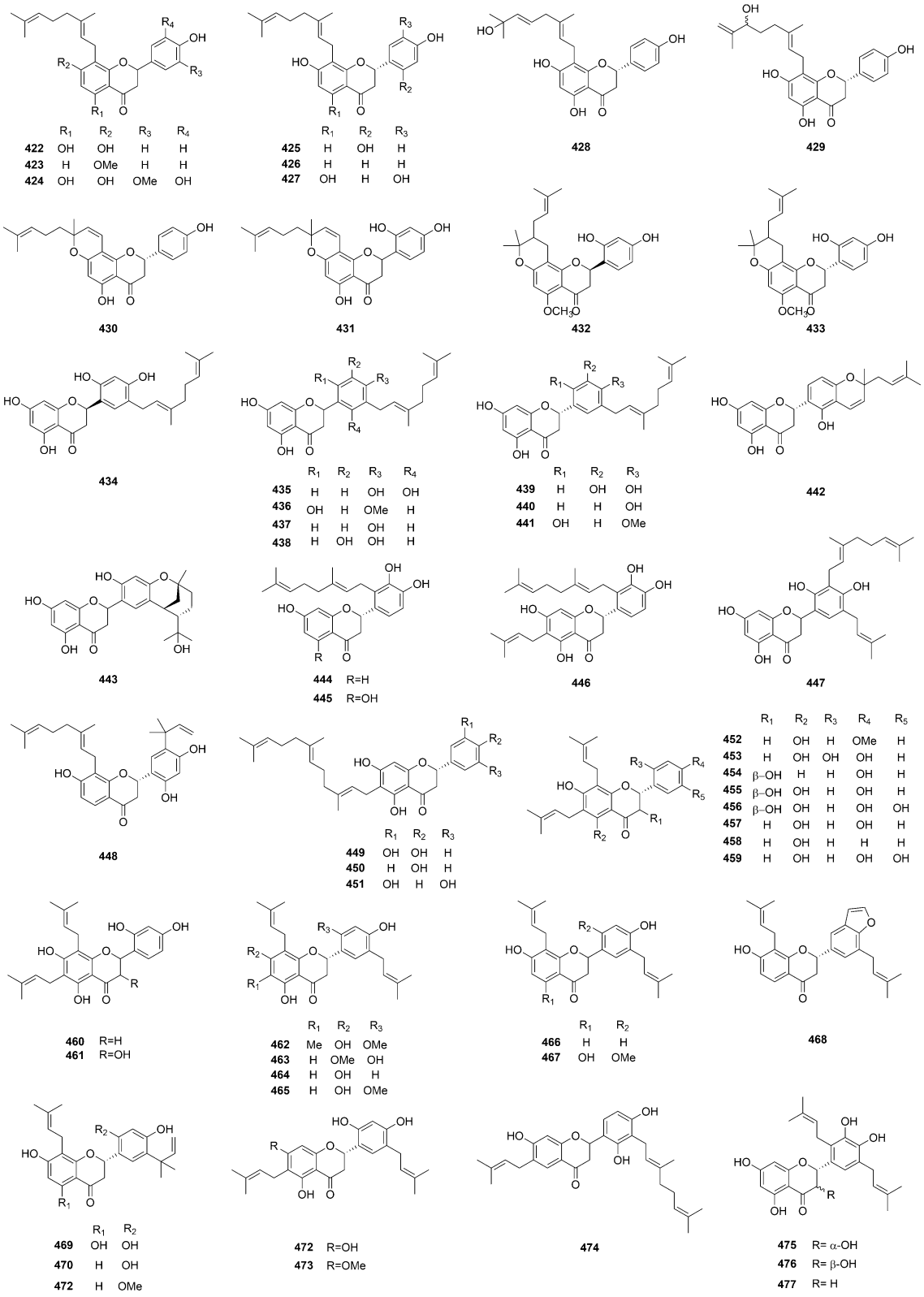

Fig. 8 (continued)

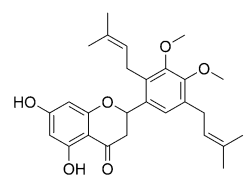

478

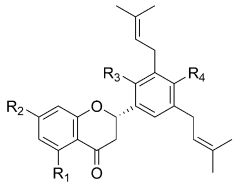

	R_1	R_2	R_3	R_4
479	OH	OH	H	OH
480	OH	OH	OH	OH
481	OH	OH	H	OMe
482	OH	OMe	H	OH
483	H	OH	H	OH

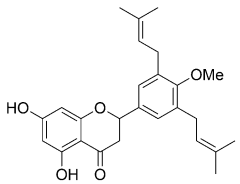

484

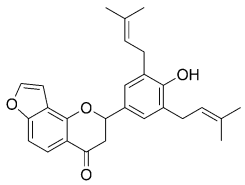

485

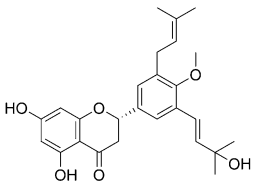

486

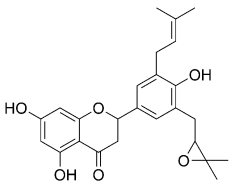

487

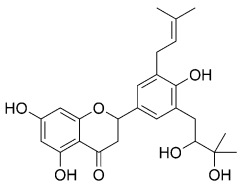

488

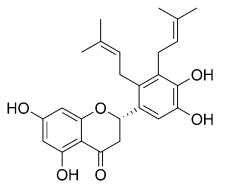

489

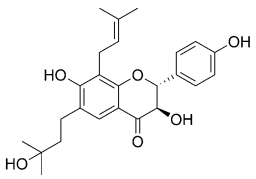

490

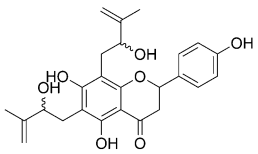

491

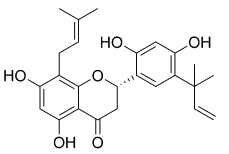

492

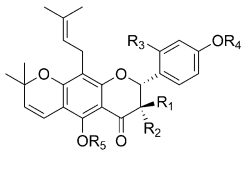

	R_1	R_2	R_3	R_4	R_5
493	OH	H	H	Me	H
494	OH	H	H	H	H
495	H	OH	H	H	H
496	H	OH	OH	Me	H
497	OH	H	OH	H	H

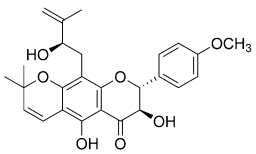

498

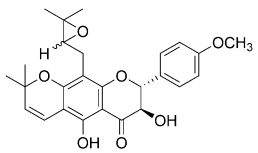

499

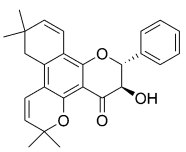

500

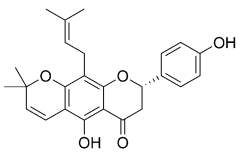

501

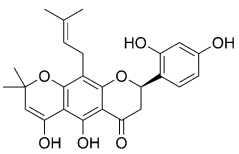

502

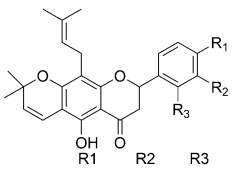

	R1	R2	R3
503	OMe	H	OH
504	OH	OH	H

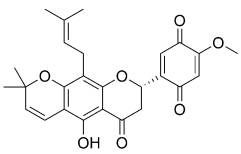

505

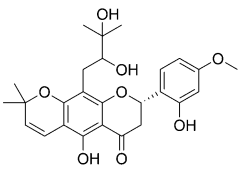

506

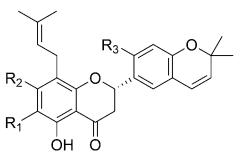

	R1	R2	R3
507	H	OMe	OH
508	Me	OH	OMe

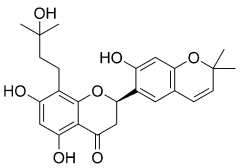

509

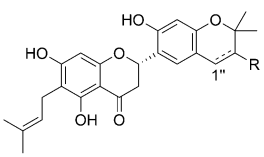

510	R=H	$\Delta^{1''}$
511	R=β-OH	

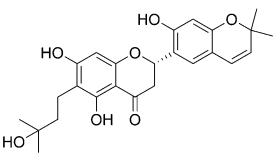

512

Fig. 8 (continued)

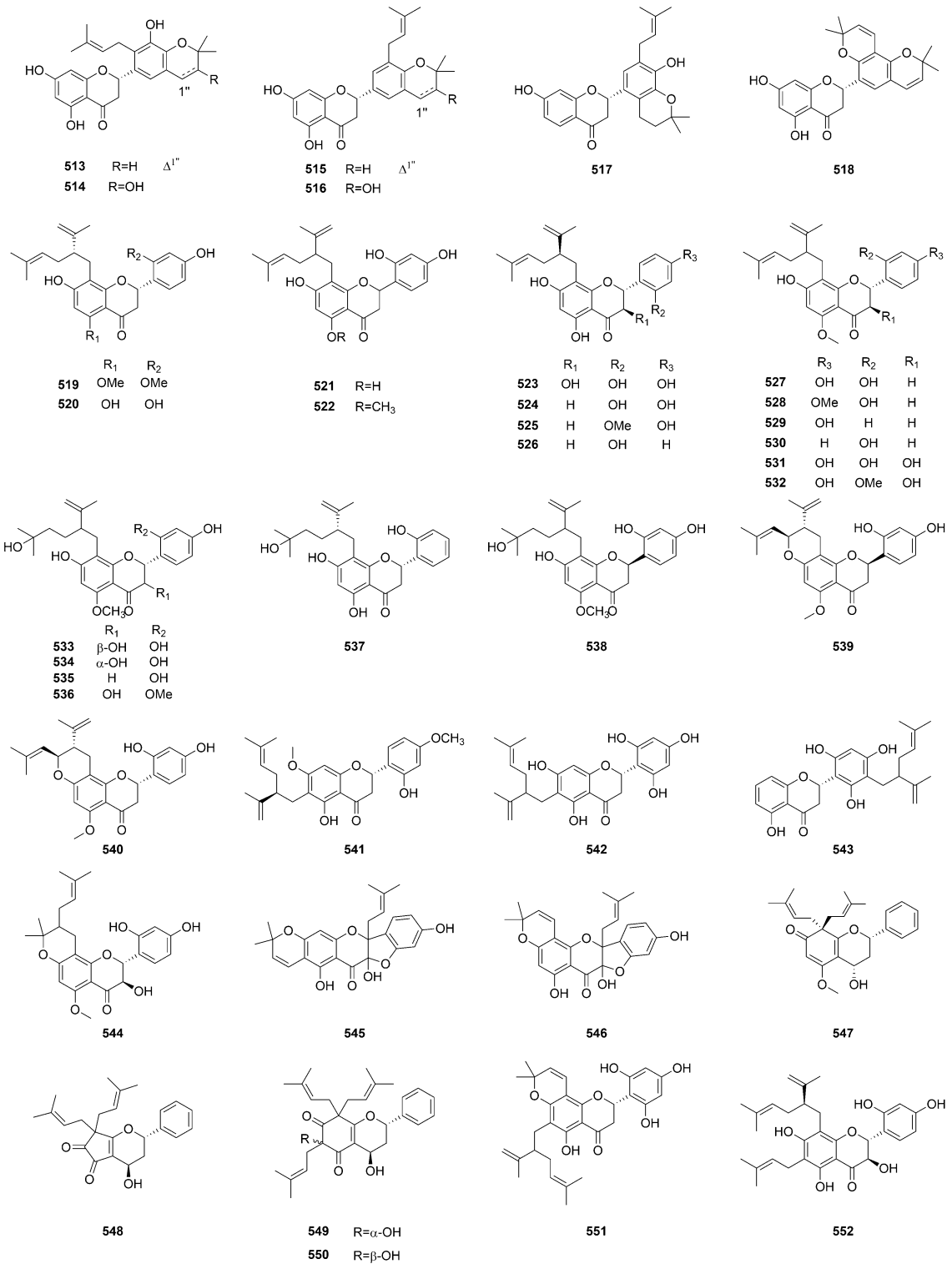

Fig. 8 (continued)

tomentosa led to the isolation of twelve natural geranylated flavonoids. Two flavonoids, diplacone (**374**) and 3′-*O*-methyl-5′-hydroxydiplacone (**375**) each bearing an unmodified geranyl side chain, possessed the strongest antiproliferative activities against THP-1 with IC_{50} values of 9.31 and 12.61 μM, respectively. The geranylated flavanones exhibited significantly greater cytotoxicity than the corresponding non-geranylated flavanones, taxifolin,

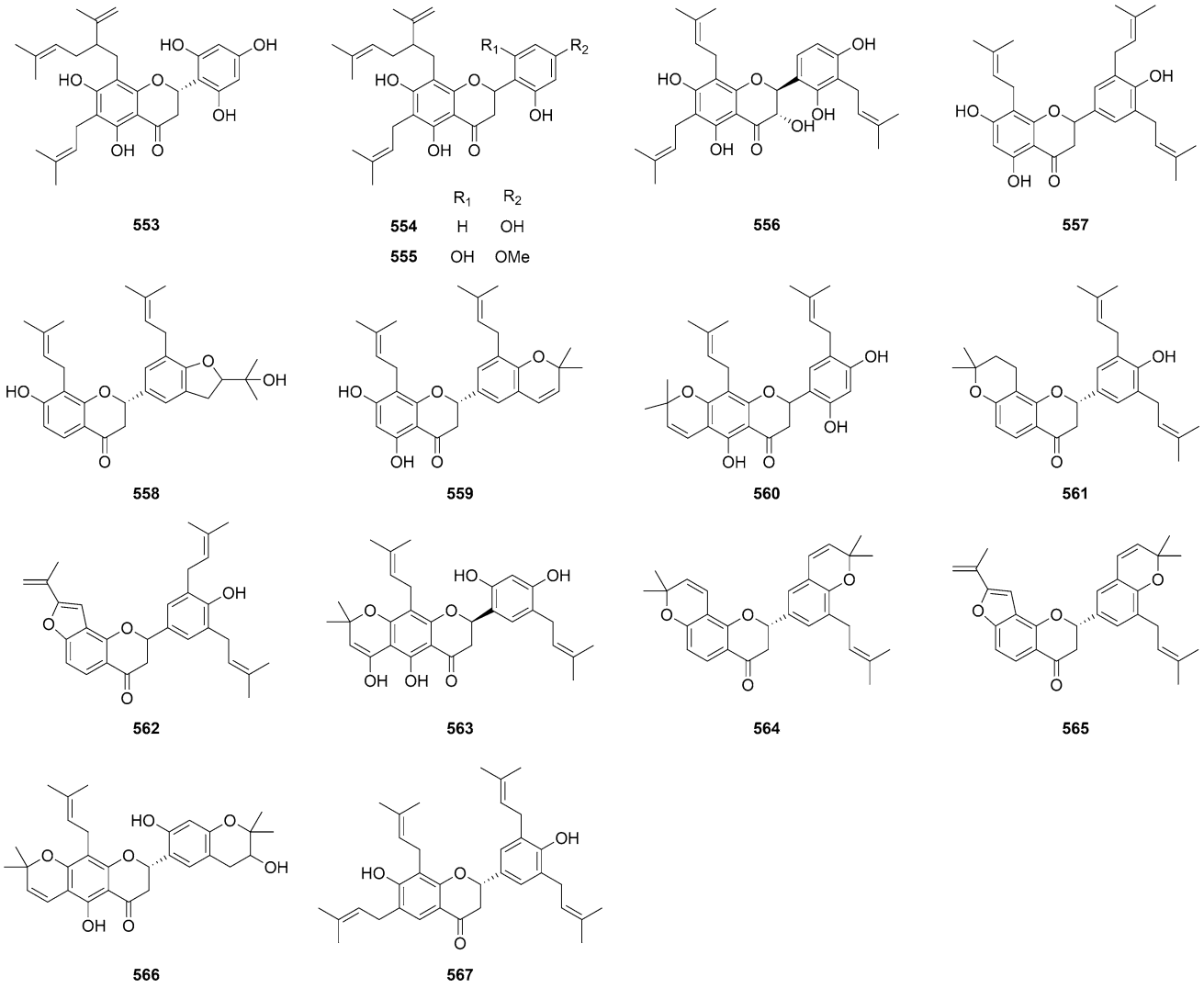

Fig. 8 (continued)

naringenin, and hesperetin, which suggested that the presence of a geranyl side chain is a crucial structural requirement for the cytotoxic effect of flavanones. The addition of a methoxy group on ring B decreased the activity of tomentone B (**409**) as compared to tomentone II (**410**), and of 3′-*O*-methyl-5′-hydroxyisodiplacone (**424**) as compared to **374** (Molčanová et al. 2021). Kuwanon E (**434**), isolated from the roots of *Morus alba*, also inhibited the proliferation of THP-1 human monocytic leukemic cells with an IC_{50} value of 4.0 μM (Zelová et al. 2014). In addition, 6-Farnesyl-3′,4′,5,7-tetrahydroxyflavanone (**449**), isolated from *Macaranga triloba*, strongly inhibited the growth of HeLa and HL-60 cells with IC_{50} values of 1.3 and 3.3 μg/mL, respectively (Zakaria et al. 2012). Calycinigin A (**543**), a C-3′ lavandulylated flavonone, exhibited an antiproliferative effect against HeLa cells with an IC_{50} value of 9.7 μM (Win et al. 2012).

Several diprenylated flavonones show potential antiproliferative activities against different cancer cells. 6,8-Diprenyl-4′-methyl-naringenin (**452**), isolated from the fruits of *Macaranga balansae*, showed cytotoxic activity against PanC1, A549, KB, and Lu-1 cell lines with IC_{50} values ranging from 7.89 to 22.81 μM (Mai et al. 2020). Lonchocarpol A (**457**) and dorsmanine I (**504**) from the stems of *Derris ferruginea* inhibited the growth of MRC-5 and KB cells with an IC_{50} value range of 6.2–23.8 μM (Morel et al. 2013). Maackiaflavanone (**463**) and 5-hydroxysophoranone (**482**) exhibited cytotoxicity against HeLa and SK-MEL-5 cells. The IC_{50} values of **463** were 8.2 and 6.5 μM, whereas the IC_{50} values of **482** were 12 and 7.7 μM, respectively. However, the structurally similar analogues, isomaackiaflavanone A (**465**), isomaackiaflavanone B (**473**), and abyssinone V (**479**), exhibit weak cytotoxicity against HeLa and SK-MEL-5 cells with IC_{50}

value range of 16–36 μM suggesting that 8-prenyl side chain promotes the cytotoxicity, and methoxy at C-2′ on the B ring decreased the cytotoxicity (Veselova et al. 2017). Sanggenol Q (**480**), isolated from the root bark of *Morus alba*, showed cytotoxicity against HepG2 cells with an EC_{50} value of 6.94 μM (Jung et al. 2015). Three diprenylated flavonoids, addisoniaflavanones I (**487**) and II (**488**) and 5,7-dihydroxy-5′-prenyl-[2″,2″-(3″-hydroxy)-dimethylpyrano]-(5″,6″:3′,4′)flavanone (**516**) isolated from *Erythrina addisoniae*, showed higher toxicity to H4IIE hepatoma cells than the monoprenyl-substituted flavonoids, with EC_{50} values of 5.25, 8.5, and 14.7 μM, respectively. Both **487** and **488** induced apoptosis via caspase-3 and -7 activation (Passreiter et al. 2015).

Xanthohumol (**579**) (Fig. 9), a prenylated chalcone isolated from *H. lupulus*, exhibited diverse bioactivities. It exhibited cytotoxic activity against WI-38, J774, HepG2, MG-63, HT-29, and SW620 cell lines with IC_{50} values of 19.5, 9.6, 7.1, 29.4, 12.0, and 25.0 μM, respectively (Bocquet et al. 2019; Harish et al. 2021; Hudcová et al. 2014). Two structurally similar chalcones sanjuanolide (**582**) and sanjoseolide (**583**), isolated from *D. frutescens*, show different cytotoxic activities against PC-3 and DU 145 prostate cancer cells. It was noted that **582** was 3.2- and 3.6-fold more potent than **583** against PC-3 and DU 145 cells, respectively. These compounds differ only by the replacement of a 2,3-dihydroxy-3-methyl-3-butenyl group in **583** by a 2-hydroxy-3-methyl-3-butanyl group in **582**, which suggested the hydroxylation of prenyl side chain decrease the cytotoxicity (Shaffer et al. 2016). 3-Hydroxy-4-methoxylonchocarpin (**601**) is a prenylated chalcone from the seeds of *Millettia pachycarpa* and exhibited cytotoxicity against K562 cells with an IC_{50} value of 2.4 μg/mL (Su et al. 2012). Gemichalcone B (**602**) is from the twigs of *Artocarpus nigrifolius* and showed strong cytotoxicity against SiHa cells with an IC_{50} value of 8.7 μM (Liu et al. 2018b).

Chalcones (**607**, **608**, **613–615**, and **666–670**) (Figs. 9 and 10) from *Desmodium renifolium* and *D. podocarpum* exhibited cytotoxicity against NB4, A549, SHSY5Y, PC3, and MCF-7 cells (Li et al. 2014a, b; Qin et al. 2015b). Artonin ZA-1 (**607**) and artonin ZA-2 (**608**) exhibited cytotoxicity against these human tumor cells with IC_{50} values ranging from 5.8 to 10 μM. Renifolin C (**613**) showed cytotoxicity against NB4 and PC3 cells with IC_{50} values of 6.4 and 8.5 μM, respectively. 2′,4-Hydroxy-3,4′-dimethoxychalcone (**614**) inhibited SHSY5Y, PC3, and NB4 cells with IC_{50} values of 3.8, 3.6, and 4.2 μM, respectively, whereas 2′,3-hydroxy-4,4′-dimethoxychalcone (**615**) exerted cytotoxicity against A549, PC3, and MCF-7 cells with IC_{50} values of 3.5, 6.8, and 6.2 μM, respectively. Renifolins D–H (**666–670**) each bearing a five-membered carbocycle showed cytotoxicity against these cancer cell lines with IC_{50} values ranging from 2.2 to 9.7 μM.

Kanzonol C (**644**) and hedysarumine F (**645**) showed cytotoxicity against A549 cells with IC_{50} values of 9.67 and 7.79 μM, respectively, whereas **644** exhibited cytotoxic activity against HCT116 cells with an IC_{50} value of 8.85 μM (Liu et al. 2018c). Flemiphilippinone C (**689**) bearing two prenyl moieties at C-3′ was isolated from the roots of *Flemingia philippinensis*. It exhibited antiproliferative activity against PC-3, Bel-7402, and CaEs-17 with GI_{50} values of 14.12, 1.91, and 2.58 μM, respectively. Mechanistically, **689** increased S/G2 arrest and induced apoptosis in Bel-7402 cells through a mitochondria-related pathway (Kang et al. 2016).

Gancaonin G (**729**) (Fig. 11) is from *Glycyrrhiza uralensis* and exhibited cytotoxicity against SW480 cells with an IC_{50} value of 9.84 μM (Tang et al. 2016). 4′-Hydroxy-5,7-dimethoxy-6-(3-methyl-2-butenyl)-isoflavone (**730**), gancaonin N (**731**), isopiscerythrone (**732**), viridiflorin (**733**), and ficucaricone D (**741**) exhibited cytotoxicity against five human cancer cell lines HL-60, SMMC-7721, A-549, MCF-7, and SW480, with IC_{50} values ranging from 0.42 to 8.48 μM (Liu et al. 2019c). Eleven prenylated isoflavones (**690**, **736**, **749**, **757**, **778**, **795**, **796**, **813**, **847**, **848**, and **870**) and two coumaronochromones (**887** and **888**) from the fruits of *Ficus altissima* were evaluated for their antiproliferative activities against three human tumor cell lines (HepG2, MCF-7, and MDA-MB-231) through MTT assay. Ficusaltin B (**848**), isolupalbigenin (**847**), and lupinalbin D (**888**) exhibited more effective cytotoxic activities to tested cell lines, which speculated that the prenyl substituent at C-3′ of the B ring was the active group in these isolated compounds. The structurally similar analogue isowigtheone (**778**) bearing only one prenyl substituent at C-3′ was inactivated. It suggested that the simultaneous presence of a prenyl group at C-6 or C-8 in the A ring and a prenyl group at C-3′ in B ring might be essential for those prenylated isoflavones to exert obvious anti-proliferative effects. For prenylated coumaronochromones, once the position of prenyl group changed to C-6 as lupinalbin B (**887**), the anti-proliferative activity against tumor cell lines would significantly reduce (Yao et al. 2021). Auriculasin (**818**) from the roots of *Flemingia philippinensis* exhibited an antiproliferative effect against PC-3 cells with a GI_{50} value of 8.33 μM. However, eriosematin, a chromone derivative, showed no activity ($GI_{50} > 100$ μM) which suggested B ring with 3′,4′-dihydroxy group in **818** would play an important role in inhibiting the growth of PC-3 cells (Kang et al. 2016). Flemiphilippinin G (**822**) and 5,7,3′-trihydroxy-2′-(3-methylbut-2-enyl)-4′,5′-(3,3-dimethylpyrano) isoflavone (**867**) showed cytotoxicity against MCF-7, A549, and HepG2 cells with IC_{50} values ranging from 4.8 to 24.8 μM (Fu et al. 2012). Tephrosin (**893**), *cis*-(6aβ,12aβ)-hydroxyrotenone (**894**), and rotenone (**895**), isolated from *Indigofera spicata*, exhibited cytotoxicity against HT-29, 697 human acute lymphoblastic leukemia

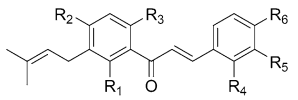

	R_1	R_2	R_3	R_4	R_5	R_6
568	OH	OH	H	OH	H	OH
569	H	OH	OH	H	OH	OH
570	OH	OH	OH	H	H	OH
571	OH	OMe	H	H	OH	OH
572	OH	OH	H	H	OH	OH
573	H	OMe	H	H	OH	OH
574	H	OH	H	H	OH	OH
575	OH	OH	H	H	H	OH
576	OH	OMe	H	H	H	OH
577	OH	OMe	OH	H	H	OH
578	OH	OH	H	H	OH	H
579	OH	OH	OMe	H	H	OH

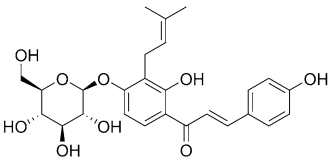

580

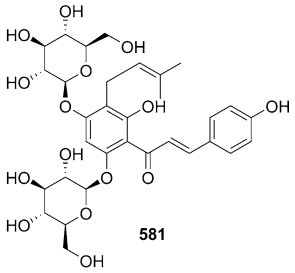

581

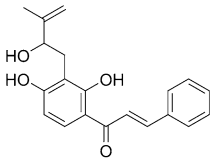

582

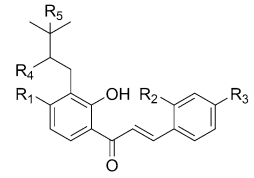

	R_1	R_2	R_3	R_4	R_5
583	OH	H	H	OH	OH
584	OMe	H	OH	H	OH
585	OMe	H	OH	OH	H
586	OH	OH	OH	OH	OH

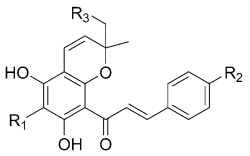

	R_1	R_2	R_3
587	Me	H	OH
588	Me	OMe	H
589	H	H	H
590	Me	OH	H

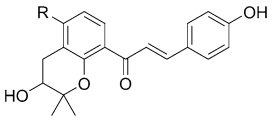

591 R=OH
592 R=OMe

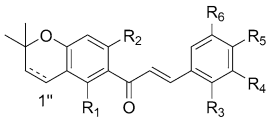

	R_1	R_2	R_3	R_4	R_5	R_6	
593	OH	H	H	OH	OH	H	
594	OH	H	H	H	OH	H	$\Delta^{1''}$
595	OH	H	H	H	OMe	H	$\Delta^{1''}$
596	H	OH	H	H	OH	H	$\Delta^{1''}$
597	H	H	OH	H	OH	H	$\Delta^{1''}$
598	OH	H	H	OH	OH	H	$\Delta^{1''}$
599	OH	H	H	H	OH	H	$\Delta^{1''}$
600	OH	OMe	H	H	OH	H	$\Delta^{1''}$
601	OH	H	H	H	OMe	OH	$\Delta^{1''}$

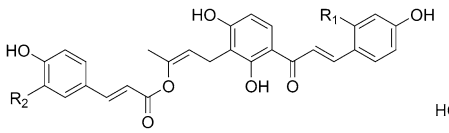

	R_1	R_2
602	H	H
603	H	OMe
604	OH	OMe
605	OH	H

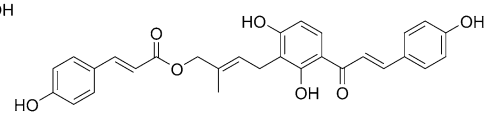

606

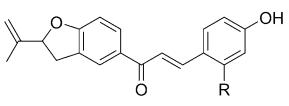

607 R=H
608 R=OH

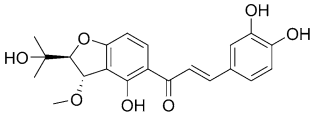

609

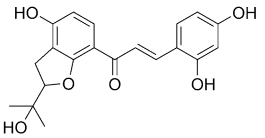

610

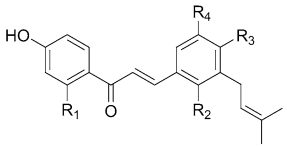

	R_1	R_2	R_3	R_4
611	H	OMe	OH	H
612	OH	H	OMe	H
613	OH	H	OMe	OH

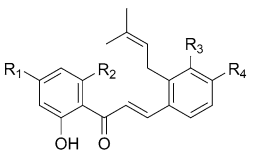

	R_1	R_2	R_3	R_4
614	OMe	H	OMe	OH
615	OMe	H	OH	OMe
616	OH	OH	OH	OH
617	OH	OH	OMe	OH

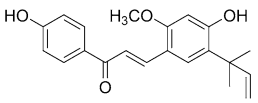

618

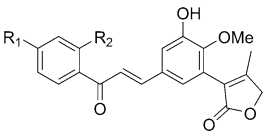

	R_1	R_2
619	OMe	H
620	OH	OH

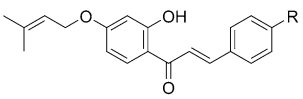

621 R=OH
622 R=H

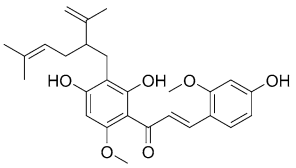

623

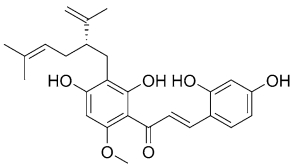

624

Fig. 9 Chemical structures of prenylated chalcones (**568–657**)

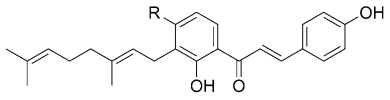

625 R=OH
626 R=OMe

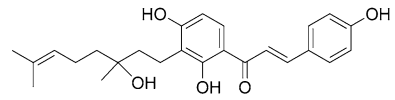

627

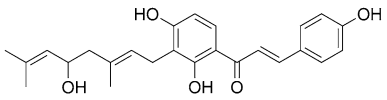

628

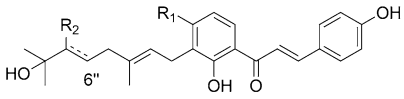

	R_1	R_2
629	OH	H
630	OH	OH
631	OMe	H
632	OH	H $\Delta^{6''}$

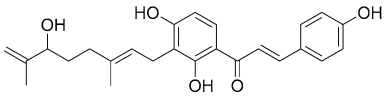

633

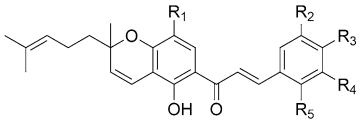

	R_1	R_2	R_3	R_4	R_5
634	OMe	H	H	OH	OH
635	OMe	OH	H	H	OH
636	OH	H	H	H	OH
637	OH	OH	H	H	OH
638	H	H	OH	H	H

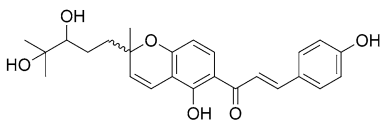

639 (-)
640 (+)

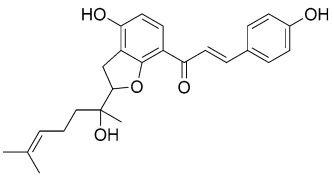

641

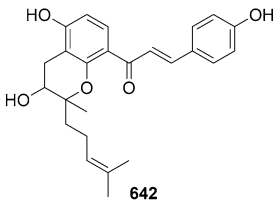

642

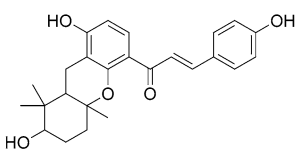

643

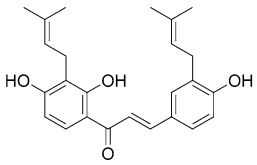

644

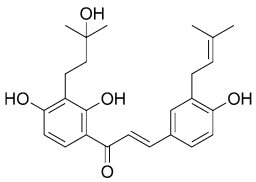

645

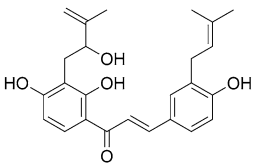

646

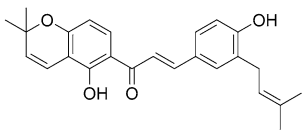

647

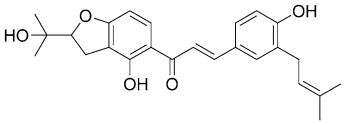

648

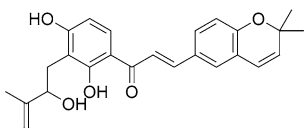

649

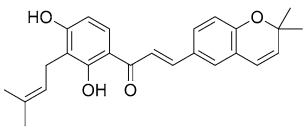

650

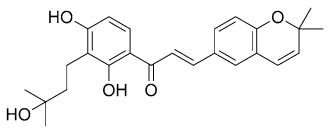

651

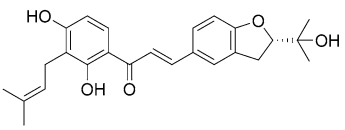

652

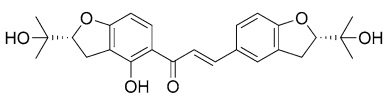

653

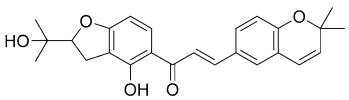

654

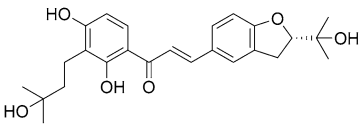

655

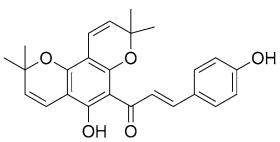

656

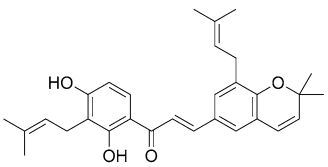

657

Fig. 9 (continued)

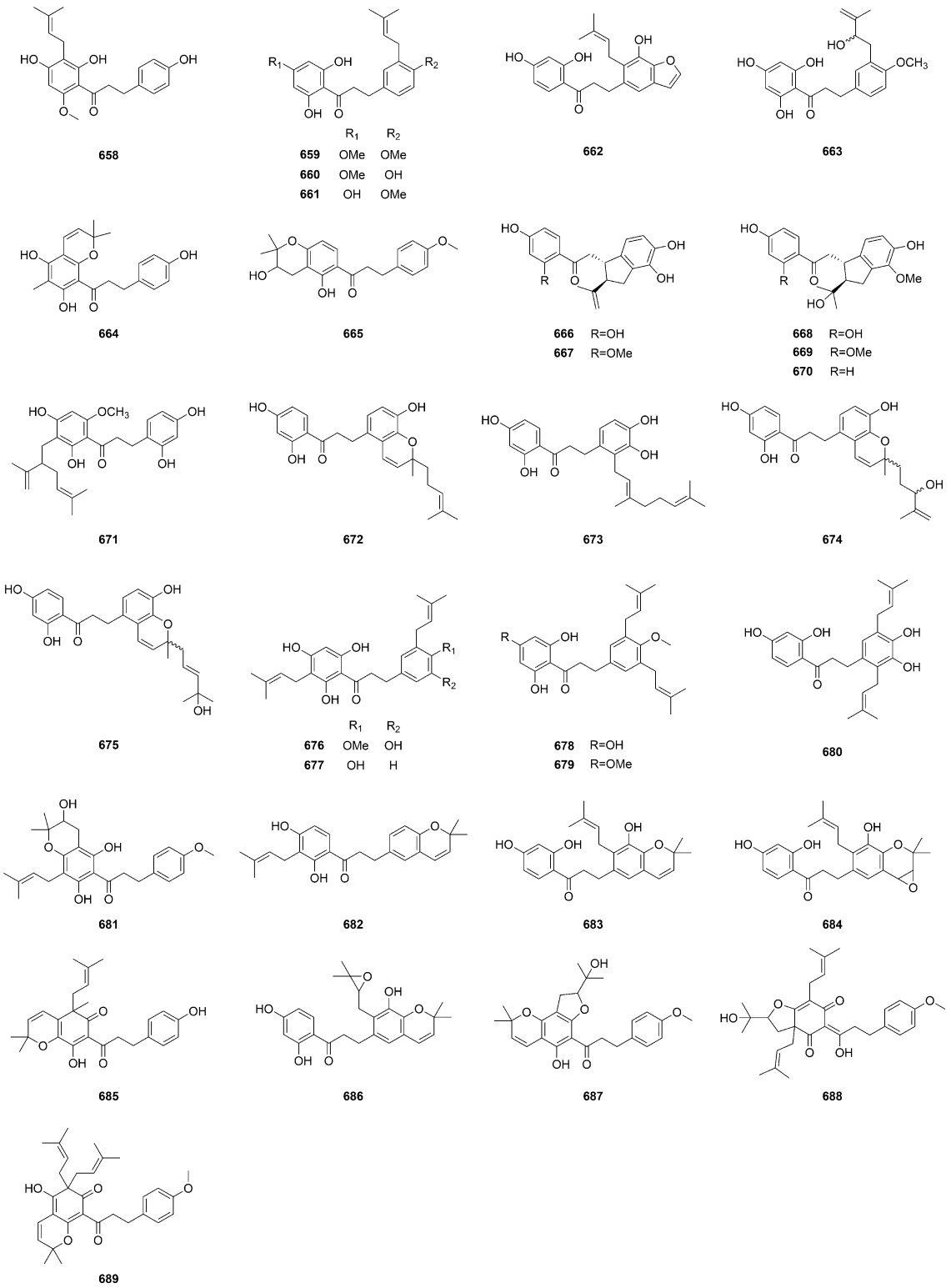

Fig. 10 Chemical structures of prenylated dihydrochalcones (**658–689**)

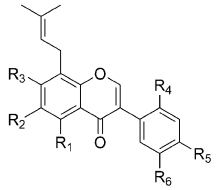

	R_1	R_2	R_3	R_4	R_5	R_6
690	OH	H	OH	H	OH	H
691	H	H	OH	OH	OH	H
692	OH	H	OH	H	OH	OH
693	OH	H	OH	OH	OH	H
694	OH	H	H	H	OH	H
695	H	H	OMe	H	OMe	H
696	H	H	OH	H	OH	H
697	H	OMe	OH	OMe	OMe	OMe
698	OH	H	OH	H	OMe	H
699	OH	$(CH_2)_2OH$	OH	H	OH	OH

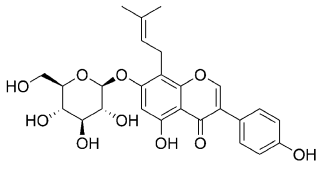

700

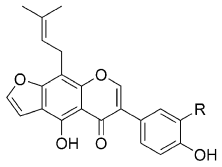

701 R=OH
702 R=H

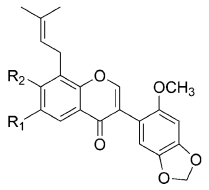

	R_1	R_2
703	H	OMe
704	OMe	OH

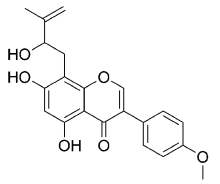

705

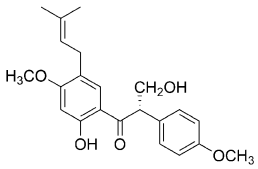

706

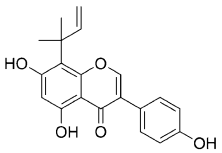

707

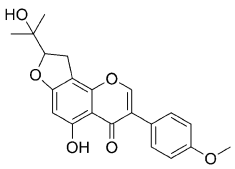

708

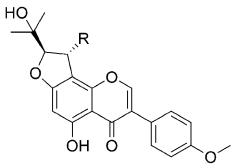

709 R=OH
710 R=OMe

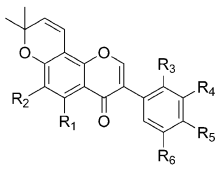

	R_1	R_2	R_3	R_4	R_5	R_6
711	H	H	H	H	OMe	H
712	H	OMe	H	H	OMe	H
713	H	OMe	H	OMe	OMe	H
714	OH	H	H	H	OMe	H
715	OH	H	H	H	OH	H
716	H	OMe	OMe	H	OMe	OMe
717	H	OMe	OMe	H	-OCH$_2$O-	
718	H	OMe	H	H	-OCH$_2$O-	
719	H	H	OMe	H	-OCH$_2$O-	

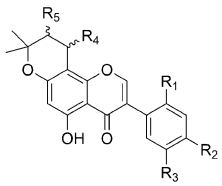

	R_1	R_2	R_3	R_4	R_5
720	H	OMe	H	H	OH
721	H	OMe	OMe	α-OH	α-OH
722	OMe	OMe	OMe	OH	OH

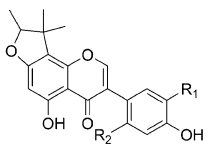

	R_1	R_2
723	H	H
724	H	OH
725	OH	H

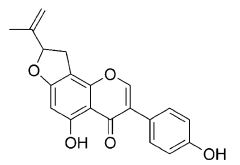

726

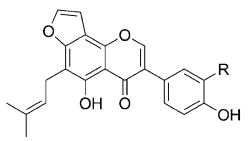

727 R=OH
728 R=H

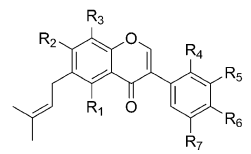

	R_1	R_2	R_3	R_4	R_5	R_6	R_7
729	OH	OMe	H	H	H	OH	H
730	OMe	OMe	H	H	H	OH	H
731	OH	OH	H	OH	H	OMe	H
732	OH	OH	H	OH	H	OH	OMe
733	OH	OH	H	OMe	H	OH	OMe
734	OH	OH	H	H	H	OH	H
735	OH	OH	H	OH	H	OH	H
736	OH	OH	OAc	H	OH	OH	H
737	OH	OH	H	H	H	OMe	H
738	OH	OH	H	H	OH	OH	H
739	OH	OH	H	H	OH	OMe	H
740	OH	OH	$(CH_2)_2OH$	H	OH	OH	H
741	OMe	OMe	H	H	H	OMe	H

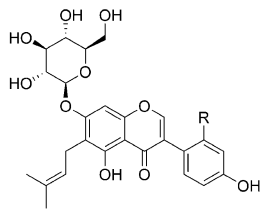

742 R=H
743 R=OH

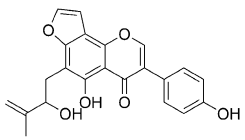

744

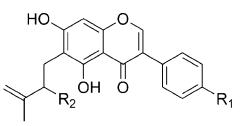

	R_1	R_2
745	OMe	OH
746	OH	OH
747	OH	=O

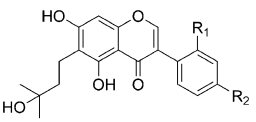

	R_1	R_2
748	H	OH
749	OH	OMe

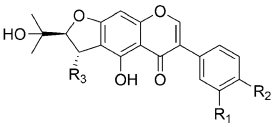

	R_1	R_2	R_3
750	H	OH	OMe
751	OH	OMe	OMe
752	OH	OMe	OH
753	H	OH	H
754	H	OMe	H

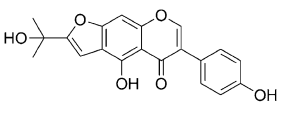

755

Fig. 11 Chemical structures of prenylated isoflavones (**690–908**)

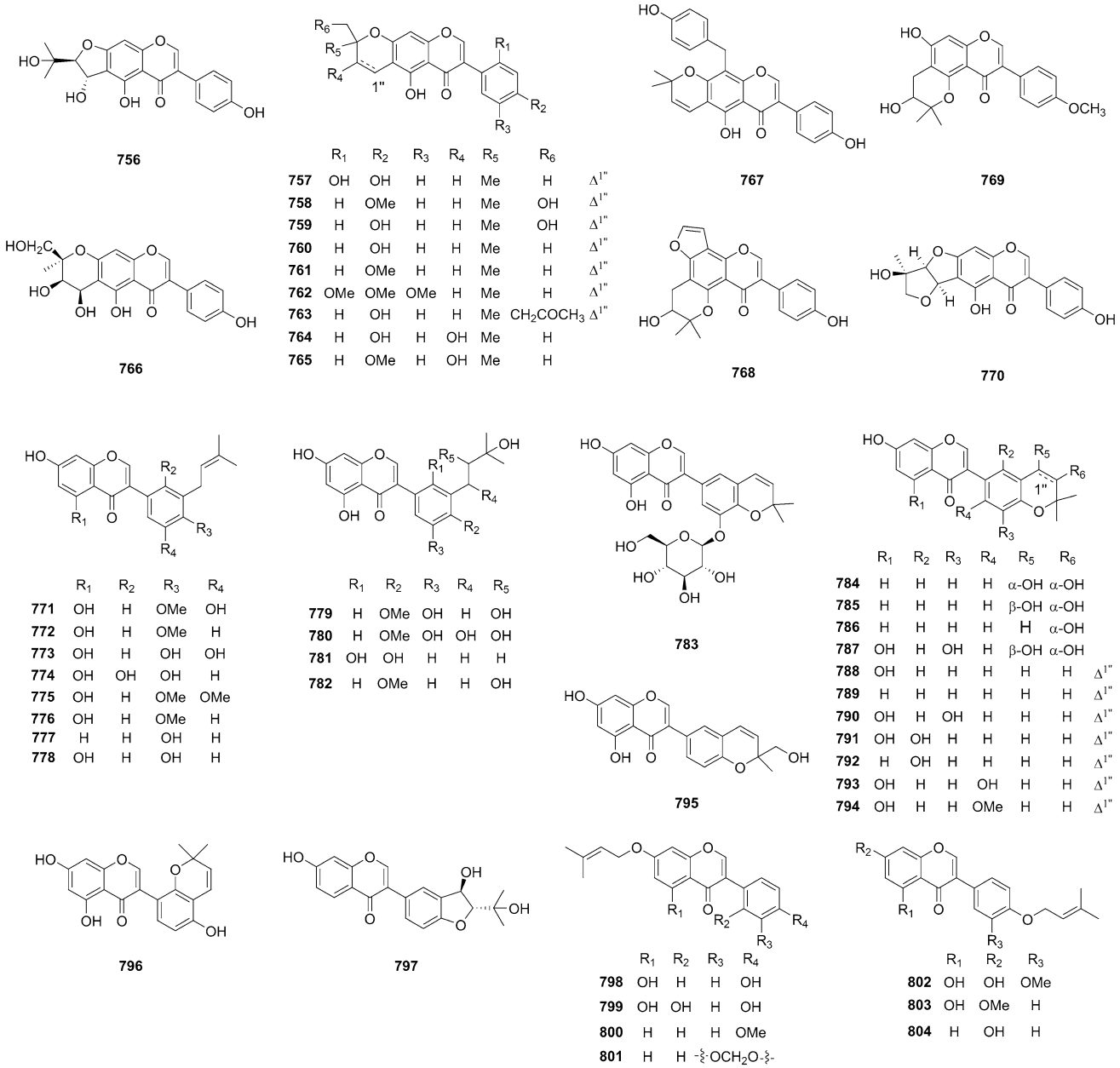

Fig. 11 (continued)

and Raji human Burkitt's lymphoma cells with IC_{50} values ranging from 0.1 to 9.0 μM. Additionally, **894** (IC_{50} 0.1 μM against HT-29 cells) and **895** (IC_{50} 0.1 μM against HT-29 cells) did not show obvious toxic effects on normal CCD-112CoN cells, with IC_{50} values over 100 μM (Bueno Perez et al. 2013).

The prenylated flavans (**909**, **916–927**, **932**, and **935–942**) (Fig. 12), isolated from the stem and root bark of *Daphne giraldii*, were evaluated their cytotoxicity against Hep3B cells. Among them, **919–921**, **926**, **927**, and **935–937** exhibited cytotoxicity against Hep3B cells with an IC_{50} value range of 5.15–9.66 μM (Sun et al. 2016a; Li et al. 2016). By comparing two similar flavans daphnegiravans A (**917**) and B (**918**), the presence of a methoxyl connected to the pyran ring reduced the cytotoxicity against all tested cancer cell lines (MCF-7, Bcap37, HepG2, Hep3B, and A549). The activity of the compound possessing a 2,2-dimethylpyran was greater than that of 2, 2-dimethyldihydropyran and furan substituents according to the IC_{50} values of daphnegiravans K (**920**), J (**926**), and I (**927**). A comparison of the activity data between daphnegiravan H (**925**) and **926** indicated that the cyclization between the prenyl and hydroxyl moieties in ring B produced a significant improvement in the reduction of cancer cell growth. This also supported that **917** and **924**

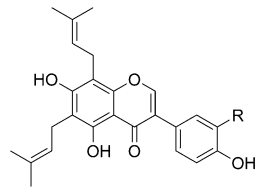

805 R=H
806 R=OMe
807 R=OH

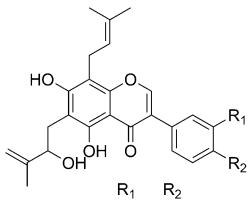

	R_1	R_2
808	OH	OH
809	H	OH

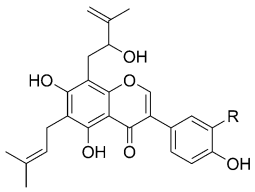

810 R=H
811 R=OH

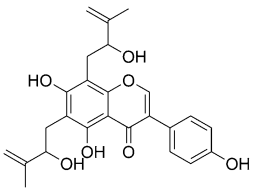

812

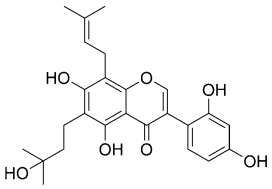

813

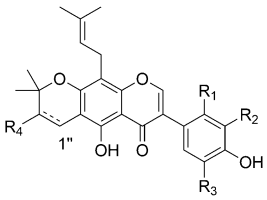

	R_1	R_2	R_3	R_4	
814	H	H	H	H	$\Delta^{1''}$
815	OH	H	H	H	$\Delta^{1''}$
816	H	H	H	OH	
817	H	OH	H	OH	
818	H	H	OH	H	$\Delta^{1''}$

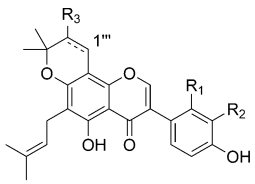

	R_1	R_2	R_3	
819	H	H	H	$\Delta^{1'''}$
820	H	OH	H	$\Delta^{1'''}$
821	OH	H	H	$\Delta^{1'''}$
822	H	H	OH	

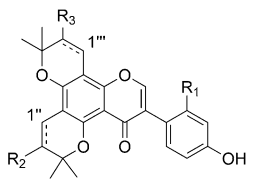

	R_1	R_2	R_3	
823	H	OH	OH	
824	H	H	H	$\Delta^{1'''}$
825	H	OH	H	$\Delta^{1'''}$
826	OH	H	H	$\Delta^{1'''}$ $\Delta^{1''}$

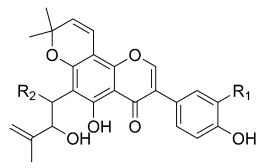

	R_1	R_2
827	H	H
828	OH	=O

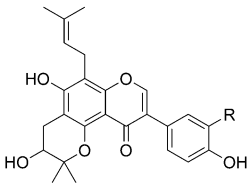

829 R=OH
830 R=H

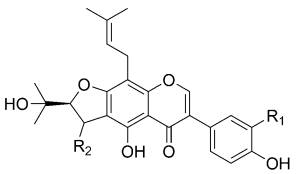

	R_1	R_2
831	OH	H
832	H	OMe
833	OH	OMe
834	H	H

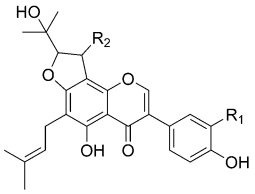

	R_1	R_2
835	OH	H
836	H	H
837	H	OMe

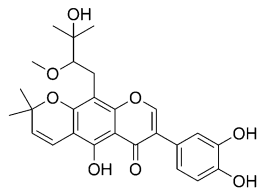

838

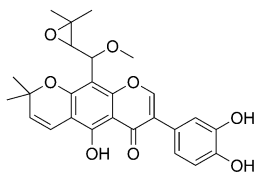

839

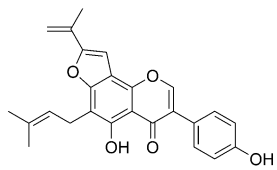

840

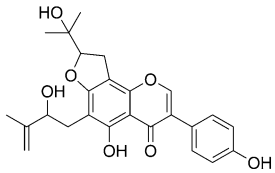

841

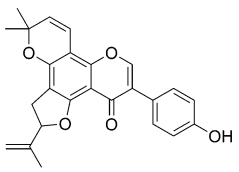

842

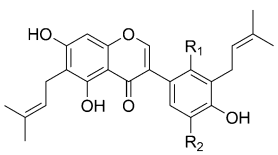

	R_1	R_2
843	OH	H
844	H	H
845	H	OH

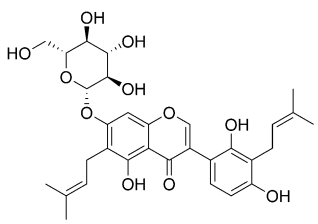

846

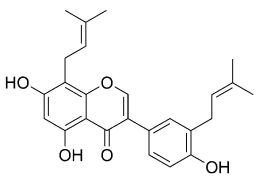

847

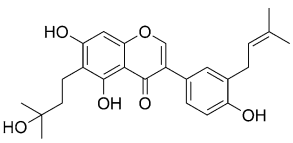

848

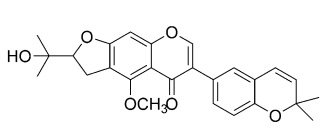

849

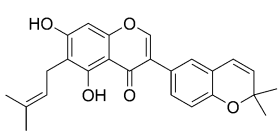

850

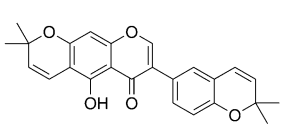

851

Fig. 11 (continued)

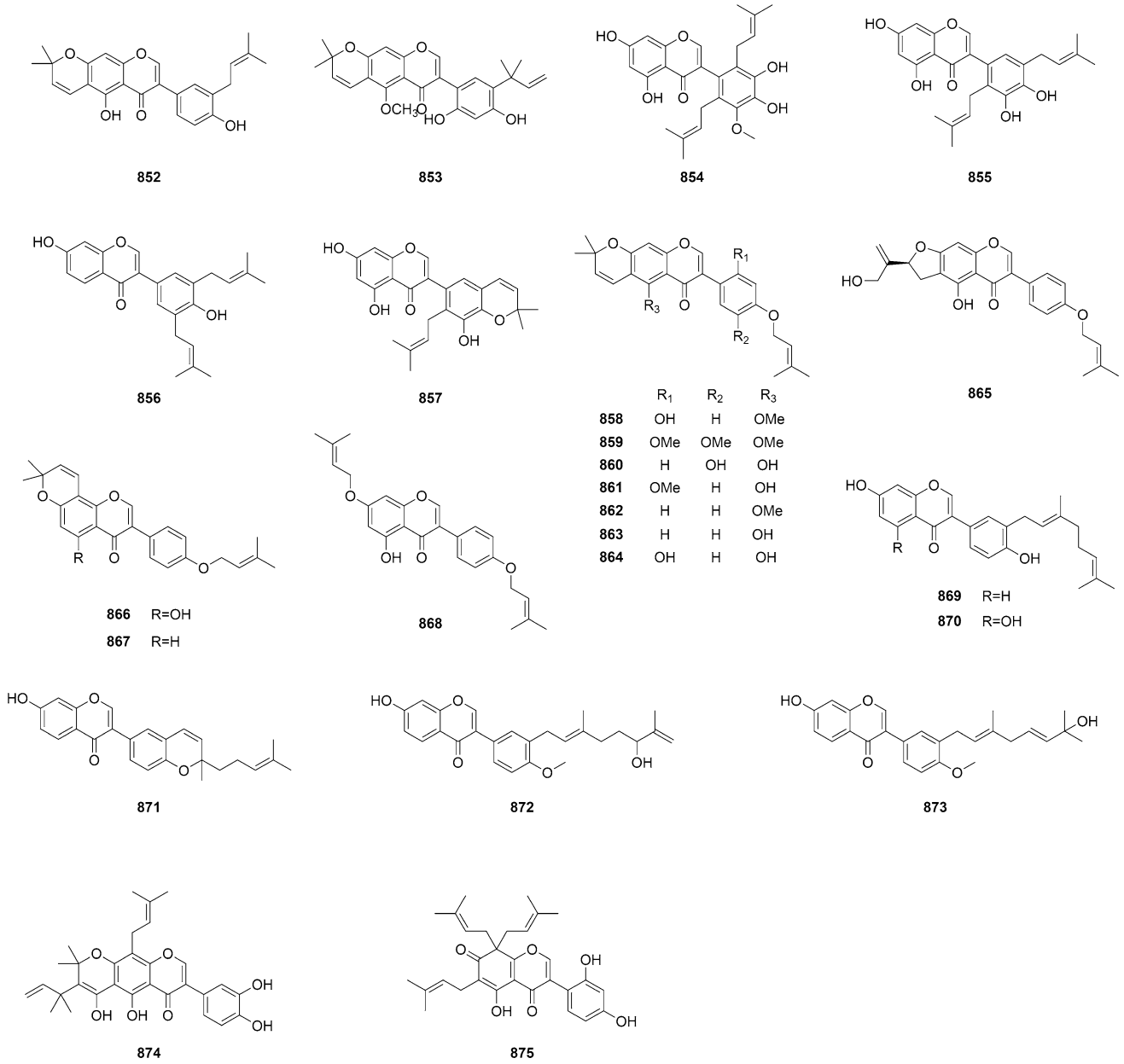

Fig. 11 (continued)

with a pyran or dihydropyran ring produced more potent inhibition than (2 S)-7,4′-dihydroxy-3′-prenylflavan (**916**) and (2 S)-kazinol I (**932**), respectively (Sun et al. 2016a).

Glyurallin A (**966**) (Fig. 13) is from *Glycyrrhiza uralensis* and exhibited cytotoxicity against SW480 cells with an IC_{50} value of 10.86 μM (Tang et al. 2016). Thonningine A (**996**), asthonningine B (**997**), indicanine A (**998**), ficucaricones A (**999**) and B (**1000**), 3′′,4′′-dihydrothonningine C (**1001**), and indicanine B (**1004**) showed promising cytotoxic effects towards five human cancer cell lines HL-60, SMMC-7721, A-549, MCF-7, and SW480, with IC_{50} values ranging from 0.18 to 18.76 μM (Liu et al. 2019c). Alopecurone J (**1011**) (Fig. 14) exhibited cytotoxic activities against HeLa, HCT116, A2780, and A549 cells with IC_{50} values ranging from 9.97 to 30.91 μM. (Soltani et al. 2020). Sanggenon E (**1025**) is from *Morus nigra* and showed cytotoxicity against THP-1 human monocytic leukemic cells with an IC_{50} value of 4.0 μM. (Zelová et al. 2014).

According to the cytotoxic activities of aforementioned compounds, the general SARs of prenylated flavonoids was summarized in Figs. 15 and 16.

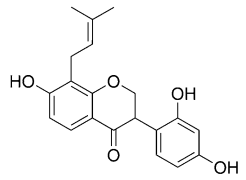

876

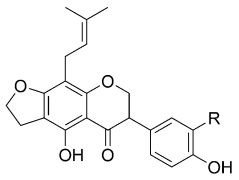

877 R=OH
878 R=H

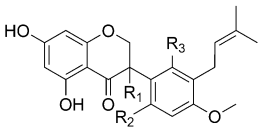

	R_1	R_2	R_3
879	OH	H	OMe
880	H	OMe	H
881	H	H	OMe

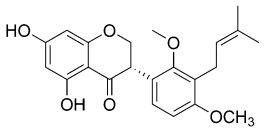

882

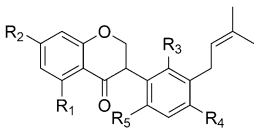

	R_1	R_2	R_3	R_4	R_5
883	H	OH	H	OH	OMe
884	OH	OMe	H	OH	OMe
885	OH	OH	OMe	OH	H
886	OH	OH	OH	OMe	H

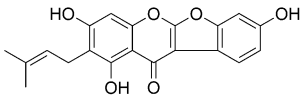

887

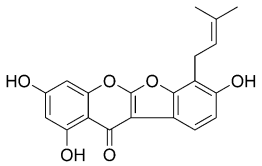

888

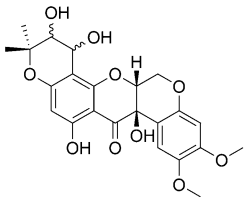

889 trans
890 cis

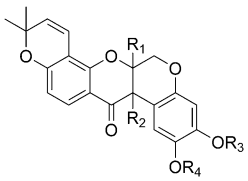

	R_1	R_2	R_3	R_4
891	α-H	α-H	Me	Me
892	β-H	β-OH	$-CH_2-$	
893	β-H	β-OH	Me	Me

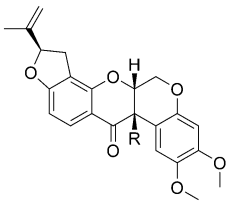

894 R=OH
895 R=H

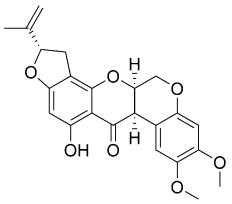

896

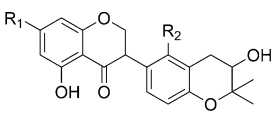

	R_1	R_2
897	OMe	OMe
898	OH	OH

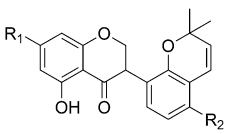

	R_1	R_2
899	OMe	OMe
900	OH	OH

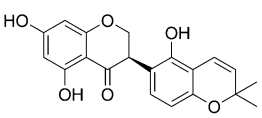

901

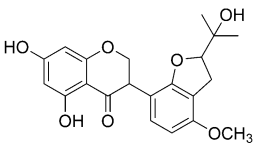

902

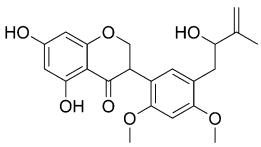

903

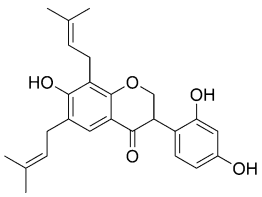

904

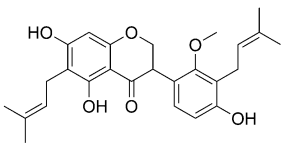

905

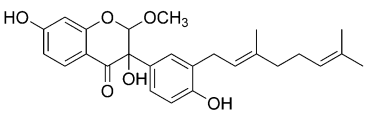

906

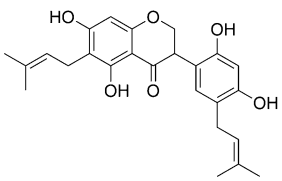

907

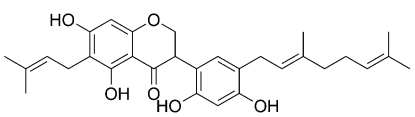

908

Fig. 11 (continued)

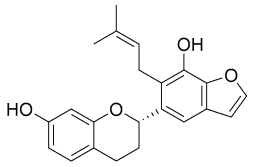

909

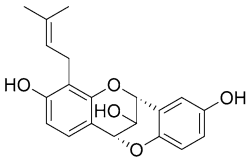

910

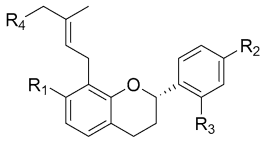

	R_1	R_2	R_3	R_4
911	OMe	OH	OH	OH
912	OH	OH	OH	H
913	OMe	OH	OH	H
914	OH	OMe	OH	H
915	OH	OH	H	H

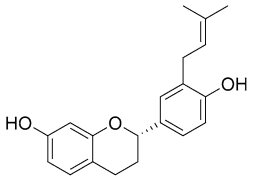

916

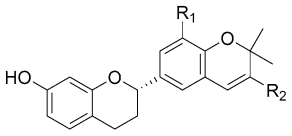

	R_1	R_2
917	H	H
918	H	OMe
919	OH	H

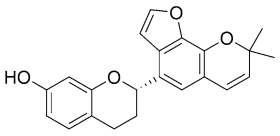

920

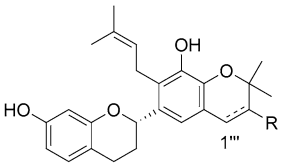

921 R=OH $\Delta^{1'''}$
922 R=OMe $\Delta^{1'''}$
923 R=H

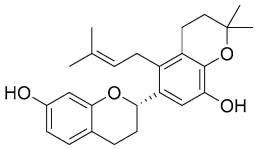

924

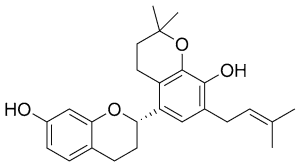

925

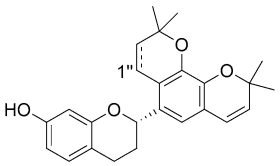

926
927 $\Delta^{1''}$

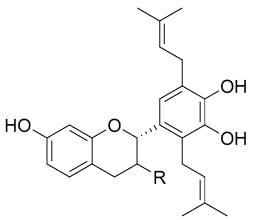

928 R= β-OH
929 R= H

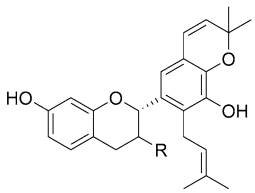

930 R= β-OH
931 R= H

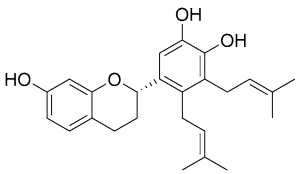

932

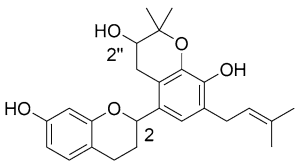

	C-2	C-2"
933	R	R
934	R	S
935	S	R
936	S	S

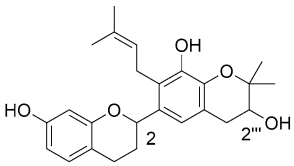

	C-2	C-2'''
937	R	R
938	S	R
939	R	S
940	S	S

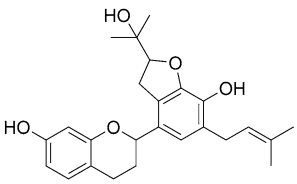

941 2S
942 2R

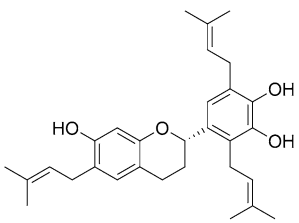

943

Fig. 12 Chemical structures of prenylated flavans (**909–943**)

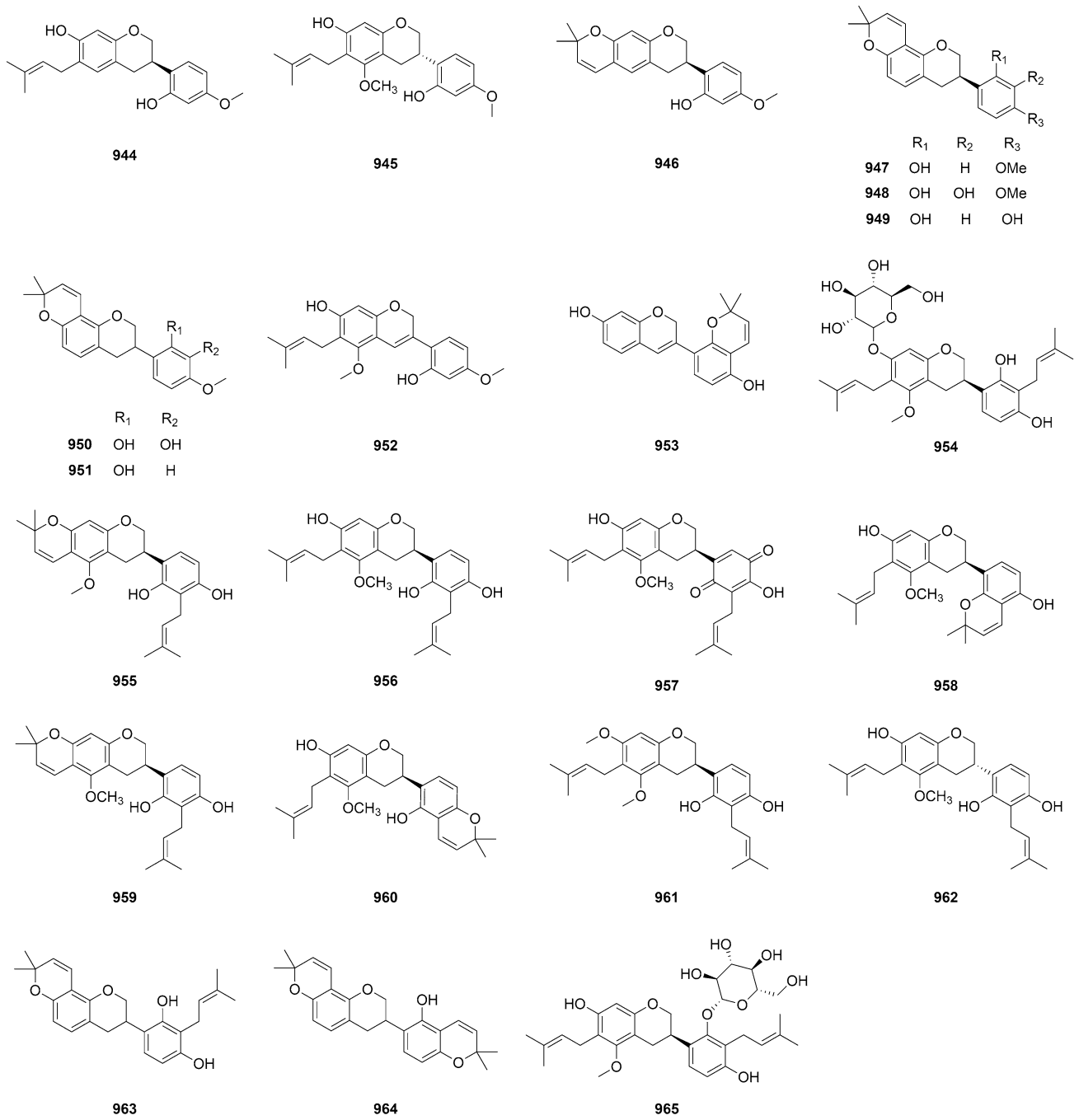

Fig. 13 Chemical structures of prenylated isoflavans (**944–1005**)

Prenylated flavonoids with anti-inflammatory activity

Inflammation is a primary pathological process involved in the progression of various diseases. Many prenylated flavonoids exhibited promising anti-inflammatory activities and regulated the expression of various inflammatory cytokines and related proteins, such as nitric oxide (NO), TNF-α, interleukins (ILs), induced NO synthase (iNOS), and NF-κB, etc. Anti-inflammatory effect of *Epimedium grandiflorum* was attributed to the presence of prenylflavonoid glycosides. The prenylated flavones desmethylicaritin (**5**), icariside II (**15**), epimedigrandioside A (**21**), and korepimeosides A (**22**) and B (**23**) from *Epimedium grandiflorum* possessed inhibitory activities against NF-κB and iNOS with IC_{50} values ranging from 16.6 to 26.5 μM and

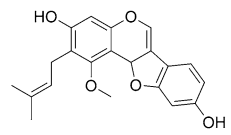

966

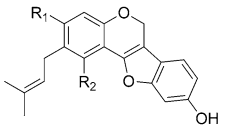

	R_1	R_2
967	OH	OMe
968	OMe	H
969	OH	H

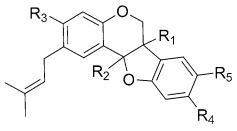

	R_1	R_2	R_3	R_4	R_5
970	OH	H	OH	OH	H
971	α-H	α-H	OMe	OH	H
972	OH	H	OMe	OH	H
973	α-OH	α-H	OH	$-OCH_2O-$	

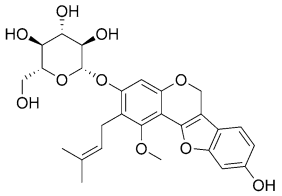

974

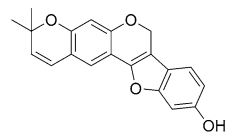

975

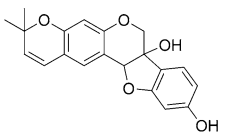

976

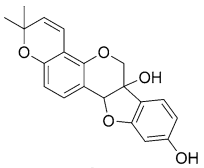

977

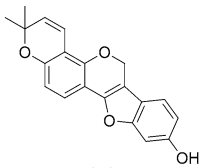

978

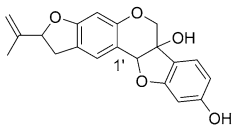

979

980 $\Delta^{1'}$

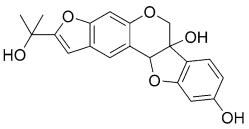

981

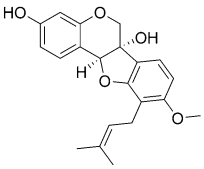

982

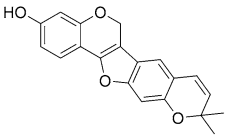

983

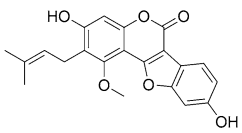

984

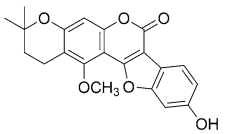

985

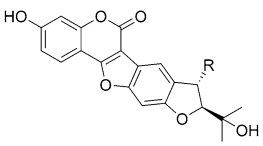

986 R = OH

987 R = H

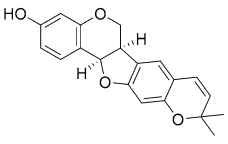

988

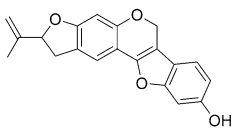

989

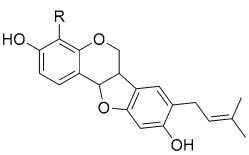

990 R=H

991 R=OH

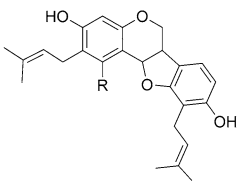

992 R=H

993 R=OMe

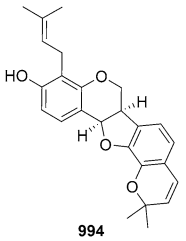

994

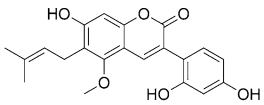

995

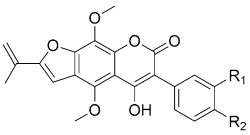

	R_1	R_2
996	$-OCH_2O-$	
997	H	OMe

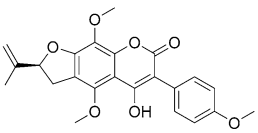

998

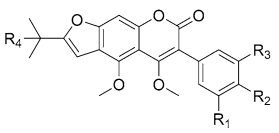

	R_1	R_2	R_3	R_4
999	OH	OMe	H	OH
1000	OH	$-OCH_2O-$		OH
1001	H	OMe	OMe	H

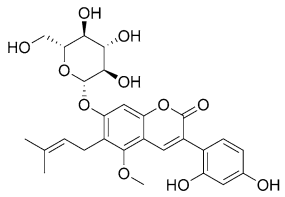

1002

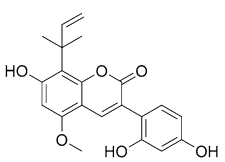

1003

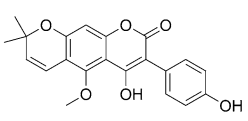

1004

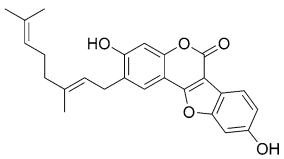

1005

Fig. 13 (continued)

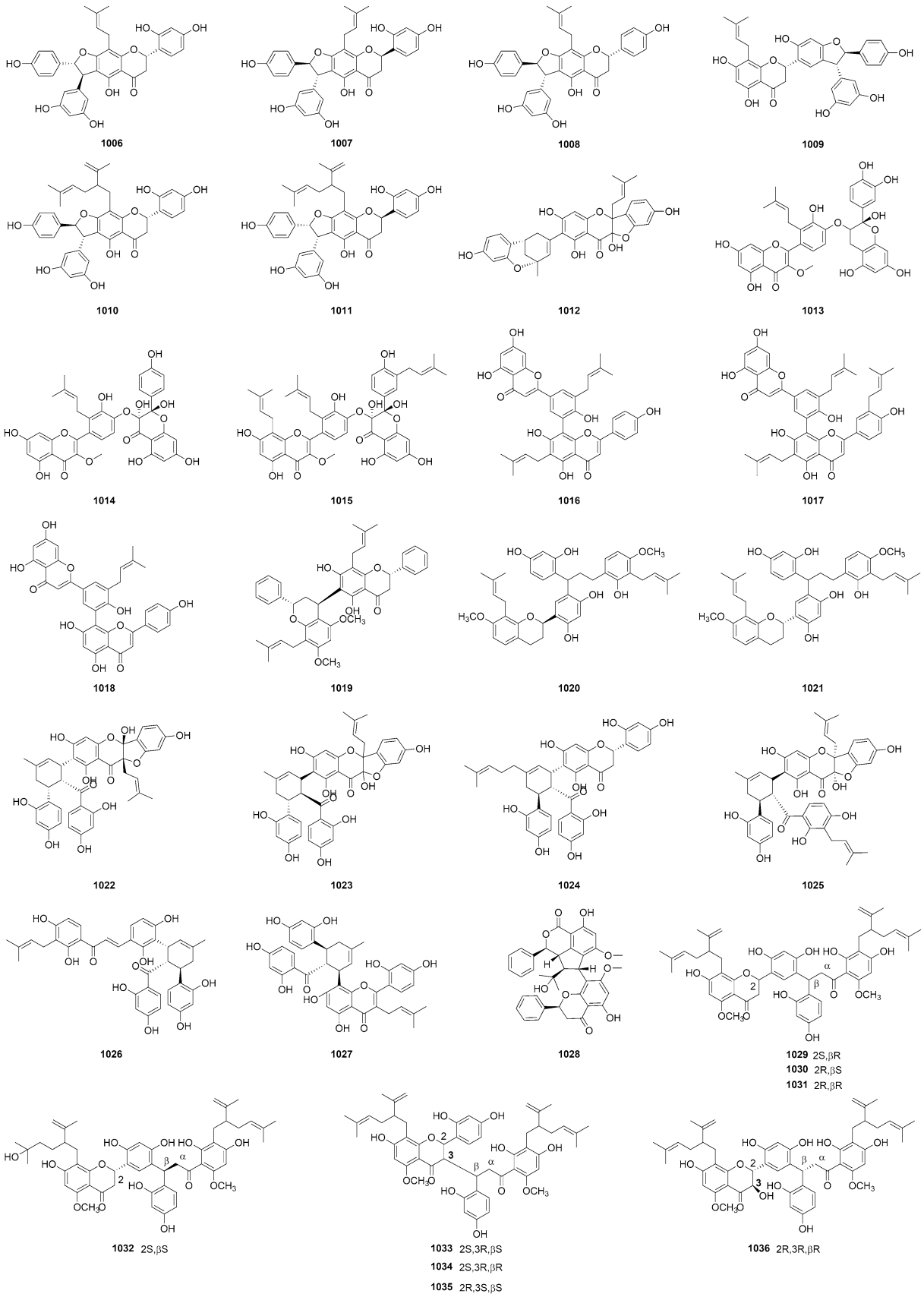

Fig. 14 Chemical structures of prenylated flavonostilbenes and biflavonoids **(1006–1036)**

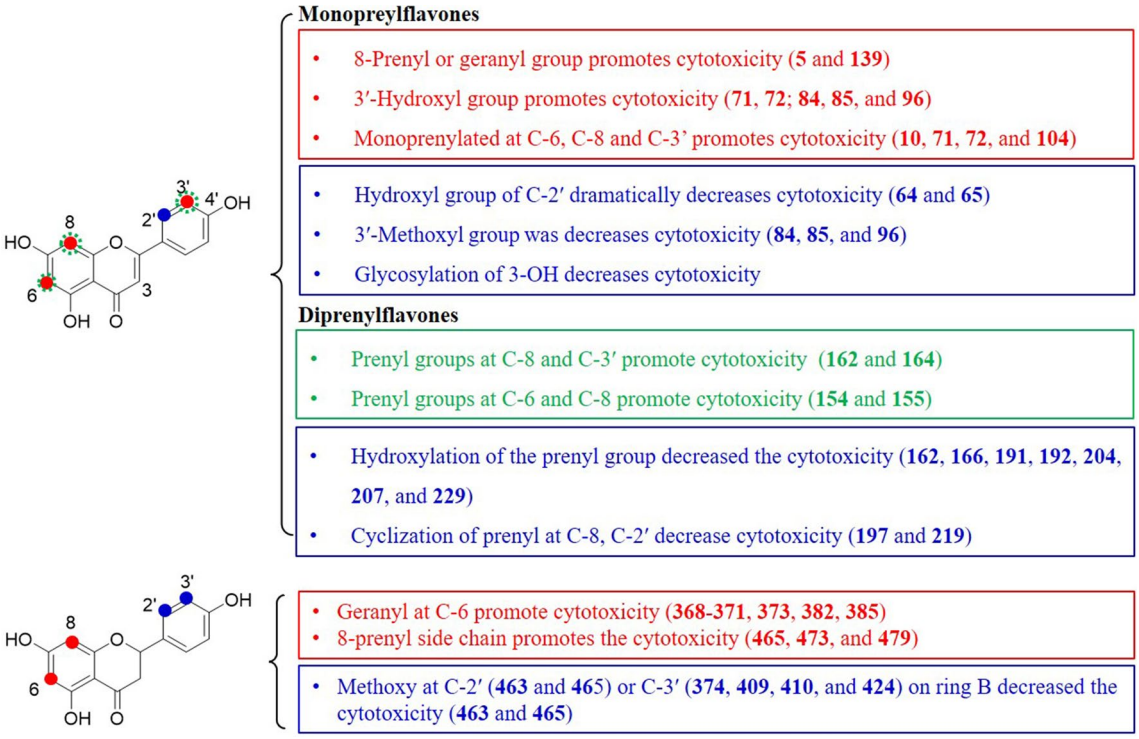

Fig. 15 SARs of prenylated flavonoids with cytotoxicity (I)

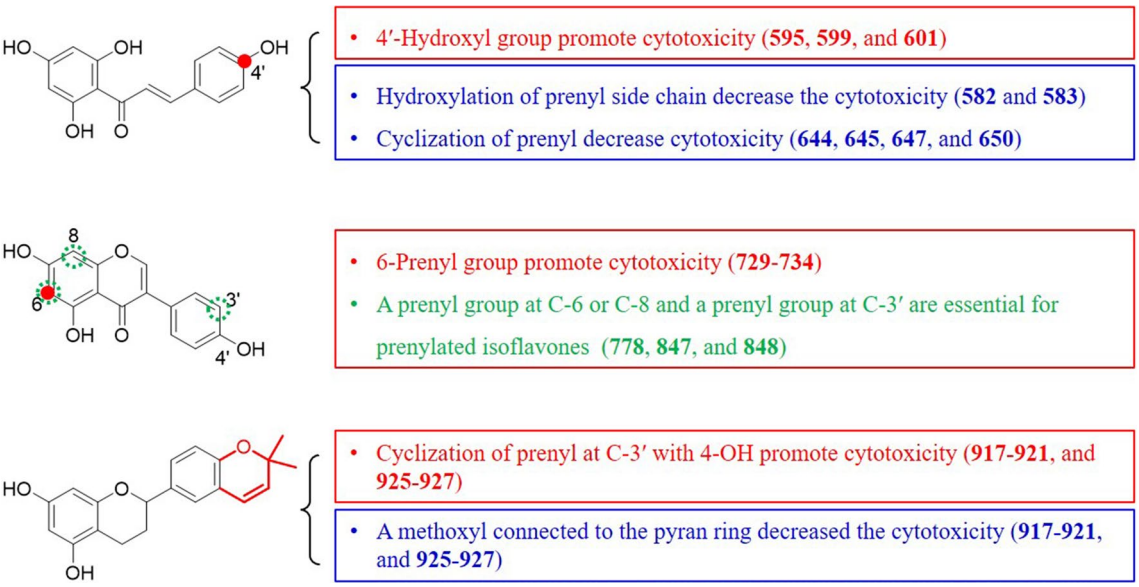

Fig. 16 SARs of prenylated flavonoids with cytotoxicity (II).

14.0 to 17.5 μM, respectively. Epimedoside (**19**), epimedokreanoside II (**20**), and epimedins I (**40**), K (**41**), and L (**42**) also exhibited inhibitory activities of iNOS with IC_{50} values of 14–30 μM, respectively, however, they did not show any effect on NF-κB or transcription factor Sp-1 (Zulfiqar et al. 2017).

Morus alba has long been used in traditional Chinese medicine and the root bark of *M. alba*, named Sang-bai-pi, is listed as an important herb medicine in Chinese Pharmacopoeia. The prenylated flavones, albanin D (**146**), (7″*R*)-(−)-6-(7″-hydroxy-3″,8″-dimethyl-2″,8″-octadien-1″-yl)apigenin (**147**), 10-oxomornigrol F (**190**), **204**,

2-(2,4-dihydrophenyl)-5-hydroxy-8-(hydroxymethyl)-8-methyl-3-(3-methyl-2-butenyl)-(9CI) (**205**), and mulberranol (**225**), and one chalcone, morachalcone A (**575**), isolated from the twigs of *Morus alba*, showed inhibitory activities against NO production with IC_{50} values of 2.2 to 5.3 μg/mL in LPS-treated RAW 264.7 cells. Compounds **146**, **147**, **190**, **225**, and **575** reduced LPS-induced iNOS expression in a concentration-dependent manner. In addition, compounds **146**, **190**, and **225** significantly suppressed LPS-induced expression of COX-2 protein (Tran et al. 2017). Treatments of kuwanon T (**176**), **204**, **434**, sanggenol A (**435**), sanggenon A (**545**), sanggenon M (**546**), and kuwanon G (**1027**) at a dose of 100 μg/mL strongly inhibited the production of IL-6 with the inhibition values ranging from 90.9 to 99.1% in TNF-α stimulated MG 63 cells (Chang et al. 2019). Sanggenol L (**431**), isolated from the root bark of *Morus alba*, showed inhibitory effect against NO production with an IC_{50} value of 12.5 μM in LPS-treated RAW 264.7 macrophages (Qin et al. 2015a).

Six cyclized geranylflavonoids (**237**–**242**) were isolated from the rhizomes of *Helminthostachys zeylanica*. (10*R*,11 *S*)-ugonin S (**237**), ugonin V (**238**), ugonin W (**239**), and ugonin Y (**240**) exhibited NO inhibition with IC_{50} values of 19.7, 18.0, 7.0, and 6.7 μM, respectively (Huang et al. 2017). Nymphaeol A (**386**), 3′-geranyl-naringenin (**437**), isonymphaeol-B (**438**), and nymphaeols B (**445**) and C (**446**), isolated from *Okinawa propolis*, repressed NO production with IC_{50} values ranging from 2.4 to 7.0 μM and inhibited COX-2 activity with IC_{50} values ranging from 11.74 to 24.03 μM in LPS-treated RAW 264.7 cells (Shahinozzaman et al. 2018).

The geranylated flavonoids from *Paulownia tomentosa* were evaluated for their ability to inhibit cyclooxygenases (COX-1 and COX-2). Mimulone (**369**), 3′,4′-*O*-dimethyl-5′-hydroxydiplacone (**370**), **374**, **375**, and tomentodiplacone O (**411**) showed significant effects on COX-1 and COX-2 inhibition with IC_{50} values range of 1.8–26.3 μM, comparable with the positive control ibuprofen with IC_{50} values of 6.3 μM for COX-1, and 4.2 μM for COX-2, respectively. Compound **411** showed greater selectivity against COX-2 than ibuprofen, which is a relatively nonselective COX inhibitor. According to the SARs of the geranylated flavonoids, the unmodified prenylated side chain and substitution of ring B appeared to be crucial for the COX inhibitory activity of flavanones. What's more, these geranylated flavonoids were also evaluated for their inhibitory activities against 5-lipoxygenase (5-LOX). **374**, **375**, 3′-*O*-methyl-5′-methoxydiplacone (**371**), tomentone (**408**), and paulownione C (**415**) show inhibitory activities with IC_{50} values of 0.05–2.46 μM. Compounds **374** and **375** both bearing two hydroxy groups on the ring B and an unmodified geranyl side chain showed inhibitory activities against 5-LOX almost 10 times greater than the positive control zileuton (IC_{50} value: 0.35 μM) (Hanáková et al. 2017). Additionally, **369** also named bonannione A was isolated from *Macaranga denticulata* (Zhang et al. 2016). Another study assayed the geranylated flavonoids (**373**, **379**–**382**, **394**–**398**, and **400**–**406**) from the fruits of *Paulownia tomentosa* were tested for inhibitory effect on human neutrophil elastase (HNE) in vitro which stimulates the release of inflammatory cytokines such as IL-6, IL-8, and other cytokines, exacerbating the inflammatory process. 3′-*O*-methyldiplacone (**373**), 6-geranyl-5,7,3′,5′-tetrahydroxy-4′-methoxyflavanone (**379**), prokinawan (**395**), tomentin J (**396**), isopaucatalinone B (**398**), and tomentin A (**400**) displayed potent inhibition with IC_{50} values of 7.8, 3.3, 6.7, 6.3, 2.4, and 8.4 μM, respectively, showing more potent than the non-prenylated flavones quercetin (IC_{50}: 14.3 μM), luteolin (IC_{50}: 12.7 μM), and apigenin (IC_{50}: 46.1 μM). The activities of the geranylated flavonoids indicated a positional requirement for the geranyl derivatives. However, hydroxylation at C-3 and methoxylation at C-5′ might tend to reduce the HNE inhibitory potencies (Ryu et al. 2017).

A series of prenylated flavonoids (**154**, **501**–**503**, **665**, **681**, **687**, **805**–**807**, **818**, **819**, **855**, **857**, and **874**) from the roots of *Flemingia philippinensis* were evaluated for their HNE inhibitory activity. The results indicate that HNE inhibitory activity was significantly affected by subtle changes in the respective structures of the prenylated flavonoids. The 4′-hydroxy group in flavanones strongly affected the inhibition by comparing lupinifolin (**501**) (IC_{50} = 13.3 μM) and flemichin D (**502**) (IC_{50} = 5.3 μM) with khonklonginol H (**503**) (IC_{50} = 110.2 μM). 8-γ,γ-Dimethylallylwighteone (**805**) (IC_{50} = 6.0 μM) with two prenyl groups on the A-ring was 9 times more effective than the non-prenylated compound genistein (IC_{50} = 51.4 μM), which suggested the prenylation at the A-ring plays a pivotal role in HNE inhibition. Similar prenylation effects were also observed for flemingsin (**806**) (IC_{50} = 12.0 μM) and osajin (**819**) (IC_{50} = 26.0 μM). A comparison of 6,8-diprenylorobol (**807**) (IC_{50} = 1.3 μM) with **819** (IC_{50} = 26.0 μM) showed that the catechol motif of the B-ring significantly influences HNE inhibition. However, prenylation on the B-ring diminished the inhibitory activity by comparing genistein (IC_{50} = 51.4 μM) with 5,7,3′,4′-tetrahydroxy-2′,5′-di(3-methylbut-2-enyl) isoflavone (**855**) (IC_{50} = 213.1 μM) (Kim et al. 2018).

The prenylated chalcones (**646**, **648**, **653**–**655**, and **647**) were isolated from the roots of *Hedysarum gmelinii* and showed NO inhibition activities with IC_{50} values ranging from 3.25 to 18.18 μM in LPS-treated BV-2 cells. Among them, hedysarumine B (**648**), paratocarpin F (**654**), and hedysarumine G (**655**) exhibited higher activities than the positive control dexamethasone (IC_{50}: 9.47 μM), with IC_{50} values of 5.12, 8.48, and 3.25 μM, respectively (Liu et al. 2018c).

Fruits of *Ficus carica* have been consumed as a very popular health-promoting fruit worldwide since ancient times. A series of prenylated isoflavone derivatives were separated from the fruits of *F. carica*. Among these isolated compounds, **730**, **741**, and **997–1000** showed stronger inhibitory effects against NO production with IC_{50} values below that of positive control hydrocortisone, while the other compounds (**732–734**, **996**, **1001**, and **1004**) exhibited weaker inhibitory effects against NO production by comparison with that of hydrocortisone. The compounds with the hydrogen atom at C-3′, the 2-propan-2-ol group at C-2″, and the furan ring were more likely to hold significant inhibitory effects against NO production by comprehensive analysis of the structures and the inhibitory activities of **997**, **996**, **1001 − 1000**, and **1004**. The compounds with a *para*-disubstituted benzene ring were more likely to possess potent inhibitory effects against NO production by comparing the structures of **730–734** (Liu et al. 2019c).

Two diprenylated isoflavones, **819** and pomiferin (**820**), isolated from the fruit of *Maclura pomifera*, exhibited inhibitory activities against NF-κB with IC_{50} values of 12.0 and 13.0 μg/mL in SW1353 cells and against iNOS with values of 7.2 and 6.4 μg/mL in LPS-treated macrophages, respectively. Compounds **819** and **820** also enhanced the activity of NAG-1 by 1.8- and 1.5-fold increases at 6.0 μM, respectively, whereas **820** inhibited intracellular oxidative stress with an IC_{50} of 3.3 μg/mL (Abourashed et al. 2015). A prenylated flavonostilbene cajanusflavanol A (**1028**) featuring a unique highly functionalized cyclopenta[1,2,3-*de*]isobenzopyran-1-one tricyclic core possessed inhibitory effect against NO production with an IC_{50} value of 13.62 μM (He et al. 2018).

Prenylated flavonoids with antihyperglycemic activity

Postprandial hyperglycaemia is an important risk factor in the onset and development of type 2 diabetes. Inhibition of α-glucosidase would delay the digestion as well as absorption of carbohydrates, which consequently, suppress the postprandial hyperglycaemia. Prenylation of flavonoids increased the potency of α-glucosidase inhibition. 6-Prenylquercetin (**70**) and **71** from *Glycyrrhiza uralensis* leaves showed α-glucosidase inhibitory activities with IC_{50} values of 3.7 and 21.3 μg/mL, respectively (Fan et al. 2019). Hirtacoumaroflavonoside (**77**) act as a noncompetitive α-glucosidase inhibitor with an IC_{50} value of 22 μM (Sheliya et al. 2015). Hirtaflavonoside B (**157**) showed α-glucosidase inhibitory activity with an IC_{50} value of 71 μM and acted in a mixed noncompetitive inhibitory pattern (Sheliya et al. 2015). **207** and dioxycudraflavone A (**229**) also exhibited α-glucosidase inhibitory activities with IC_{50} values of 23.2 and 25.27 μM, respectively (Li et al. 2018). 6-Prenyleriodictyol (**266**), 6-prenylnaringenin (**267**), and 5′-prenyleriodictyol (**312**) showed α-glucosidase inhibitory activities with IC_{50} values of 27.5, 15.4 and 53.4 μg/mL, respectively (Fan et al. 2019). Three 8-prenylflavonones euchrenone a7 (**279**), 8-prenylnaringenin (**280**), and isoxanthohumol (**281**) from *Morus alba* and *H. lupulus* showed inhibition activities against α-glucosidase with IC_{50} values of 6.28, 50, and 40 μM, respectively (Wang et al. 2022; Yang et al. 2012). 4′,1″-Dihydroxy-3′-methoxy-6,7-furanflavanone (**349**) is from the seeds of *Psoralea corylifolia* and exhibited inhibitory activity on α-glucosidase with an IC_{50} value of 53.1 μM, lower than the positive control acarbose (IC_{50} = 214.5 μM) (Fei et al. 2020). Four geranylated flavonones nymphaeol A (**367**), **437**, **438**, and **445**, isolated from *Okinawa propolis*, strongly suppressed *in vitro* α-glucosidase enzyme activity with IC_{50} values of 3.77–5.66 μM (Shahinozzaman et al. 2018). Kushenols E (**460**), L (**461**), and A (**526**) inhibited α-glucosidase activity with IC_{50} values of 24.6, 32.6, and 50.6 μM, respectively. **460** showed an uncompetitive inhibitory pattern, whereas **461** and **526** had a noncompetitive binding mechanism (Kim et al. 2017). Kushenol B (**554**) inhibited α-glucosidase activity in an uncompetitive inhibitory pattern with an IC_{50} value of 11.0 μM (Kim et al. 2017). **579** showed α-glucosidase inhibitory activity with an IC_{50} value of 47 μM below that of positive control acarbose (IC_{50} = 58 μM) (Wang et al. 2022). 5,3′,4′-trihydroxy-1″-methoxy-6,7-furanbavachalcone (**609**) is from the seeds of *Psoralea corylifolia* and exhibited inhibitory activity on α-glucosidase with an IC_{50} value of 90.3 μM. The IC_{50} value of the positive control acarbose was 214.5 μM (Fei et al. 2020). A phytochemical investigation of *Masclura tricuspidata* leaves resulted in the isolation of 47 prenylated isoflavonoids. They were evaluated for their α-glucosidase inhibitory and anti-glycation activities. Most isoflavonoids showed good inhibitory activity against α-glucosidase, with IC_{50} values of < 30.0 μM. Among the isolates, gancaonin M (**698**), millewanin G (**808**), erysenegalensein E (**810**), and cudracusisoflavone L (**812**) showed strong α-glucosidase inhibition with IC_{50} values of 8.2, 3.2, 4.2, and 8.9 μM, respectively. The prenylated isoflavonoids were further divided into one linear prenyl moiety, two linear prenyl moieties, one cyclized prenyl moiety, and two prenyl moieties with one linear and one cyclized type. Comparing the type of prenyl group, the inhibitory activity was stronger in isoflavonoids with linear prenyl group than cyclized ones. The addition of the hydroxyl group to the prenyl group increased the inhibitory effects, while the addition of the OCH_3 group caused a decrease in the inhibitory effect. The molecular docking analysis also supported the aforementioned speculation (Jo et al. 2021).

Peroxisome proliferator-activated receptor-γ (PPAR-γ) belongs to the nuclear hormone receptor superfamily that

function as ligand-inducible transcription factors modulating the expression of target genes involved in controlling glucose homeostasis, lipid metabolism and inflammation. 22 prenylated flavonoids, isolated from *Psoralea corylifolia*, were screened on the PPAR-γ agonist activity. Bavachin (**273**), bavachinin (**277**), 4′-*O*-methylbavachalcone (**573**), broussochalcone B (**574**), and corylifol A (**869**) exhibited potent PPAR-γ agonist activation from 6.16-fold to 13.12-fold at a test concentration of 25 μM. Substituting methoxyl at C-7 of A-ring to hydroxyl, such as **273** and **574**, reduced PPAR-γ agonist activation compared to **277** and **573**, indicating that the methoxyl in the C-7 position of A-ring is crucial for PPAR-γ agonist activity. Isobavachin (**289**) and isobavachalcone (**575**) show less PPAR-γ agonist activity than **273** and **574**, suggesting that the prenyl in the C-6 position of A-ring may contribute to their agonist activities. **573** and **574** showed less PPAR-γ agonist activity than **273** and **274**, which indicated that the C-ring structure is an important determinant for PPAR-γ agonist activity, opening the C-ring results in remarkably lower activity. In addition, the cyclization of the prenyl group on the A-ring and B-ring also markedly reduced PPAR-γ agonist activity (Fig. 17) (Ma et al. 2016).

Protein tyrosine phosphatase 1B (PTP1B), a negative regulator in the insulin signaling pathway, was evidenced as a promising drug target for type 2 diabetes. The prenylated flavonoids, macarangin (**143**), bonannione A (**337**), bonanniol A (**378**), (2*E*)-1-(5,7-dihydroxy-2,2,6-trimethyl-2 *H*-benzopyran-8-yl)-3-(4-methoxyphenyl)-2-propen-1-one (**588**), (2*E*)-1-(5,7-dihydroxy-2,2-dimethyl-2 *H*-benzopyran-8-yl)-3-phenyl-2-propen-1-one (**589**), and laxichalcone (**656**), from *Macaranga denticulate* showed potential inhibitory activities against PTP1B in vitro with an IC_{50} value of 22.7, 14.0, 15.2, 48.8, 19.3, and 20.7μM, respectively (Zhang et al. 2016). **166**, cudraflavone C (**167**), cudraflavanone D (**472**), and euchrestaflavanone C (**510**) derived from the roots of *Cudrania tricuspidate*, showed PTP1B inhibitory activities with IC_{50} values of 13.6, 9.4, 5.7, and 12.3 μM, respectively (Quang et al. 2015). Five prenylated flavonoids, morunigrol A (**174**), **204**, cudraflavone B (**228**), and morunigrols C (**248**) and B (**249**), from *Morus nigra* exhibited PTP1B inhibitory activity with IC_{50} values of 12.5, 22.1, 20.0, 7.7 and 5.3 μM, respectively (Qu et al. 2021).

Aldose reductase mediates the first step of the "polyol pathway" by reducing glucose to sorbitol through a NADPH-dependent reaction. Under hyperglycemic conditions, it tended to cause excessive accumulation of sorbitol which might finally promote the formation of advanced glycation end-products (AGEs) by decrease the cell's antioxidative capabilities. The AGEs could lead to diabetic complications, such as microangiopathies, nephropathies, retinopathies, peripheral neuropathies and cataract. Aldose reductase inhibitors possessed the potential to prevent or control the onset of these diabetic complications. **280**, **281**, and **579** are potent tight-binding inhibitors of human aldose reductase AKR1B1 with IC_{50} values of 0.81, 0.57, and 9.11 μM and Ki values of 0.30, 0.17, and 5.29 μM, respectively, using glyceraldehyde as a generic substrate. The IC_{50} and Ki values of three inhibitors against AKR1B1 were 1.87, 0.88, and 29.17μM, and 0.71, 0.34, and 15.08 μM, respectively, when applied glucose as a generic substrate. **280** and **579** inhibited AKR1B1 in a non-competitive fashion, whereas **281** displayed the typical pattern of an uncompetitive inhibitor. All three inhibitors exhibit a 4′-OH group which indicated a 4′-OH group is crucial for the inhibition of AKR1B1. **280** (IC_{50} = 0.81 μM) exhibited an inhibitory potency that is 7.6 times greater as compared to that of **267** (IC_{50} = 6.2 μM), applying glyceraldehyde as substrate. It suggested that prenyl moiety at the C-8 position played an important role in aldose reductase inhibition. The efficacy of **280** (IC_{50} = 1.87 μM) and **281** (IC_{50} = 0.88 μM) is 15–34 times greater than that of **579** (IC_{50} = 29.17 μM), which indicated that the C-ring structure is an important determinant for aldose reductase inhibition, opening C-ring results in remarkably lower activity (Seliger et al. 2018; Shim et al. 2009). A series of prenylated isoflavoinds (**698**, **705**, **727**, **745**, **760**, **799**, **808**, **809**, **832**–**834**, and **835**) from *M. tricuspidata* leaves efficiently inhibited methylglyoxal- or glyoxal-induced AGEs formation, which can be considered as promising candidates for the treatment of several diabetic complications (Jo et al. 2021).

Prenylated flavonoids with antioxidant activity

6-Prenylated-3,5,7,4′-tetrahydroxy-2′-methoxyflavonol (**69**), isolated from *Chlorophora regia*, exhibited remarkable

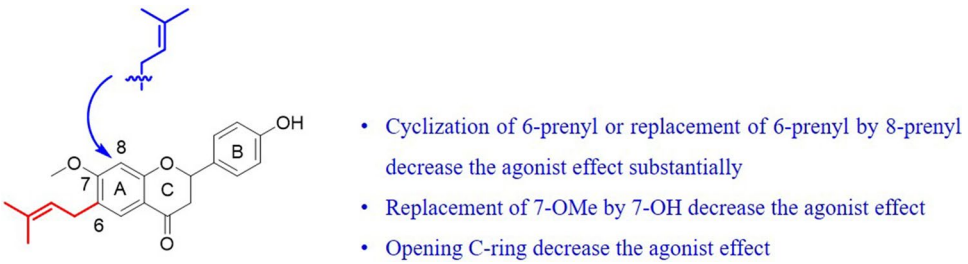

Fig. 17 SARs of prenylated flavonoids with PPARγ agonist activity

free radical scavenging properties with an IC_{50} value of 2.8 μg/mL (Kyekyeku et al. 2016). **70**, 5′-prenylquercetin (**102**), **266**, **312**, and 8-[(*E*)-3-hydroxymethyl-2-butenyl]-eriodictyol (**323**) from *Glycyrrhiza uralensis* leaves scavenged DPPH radicals with an EC_{50} value of 2.4, 3.6, 5.2, 8.7, and 2.3 μg/mL (Fan et al. 2019). **72** exhibited weak DPPH scavenging activity with an IC_{50} value of 0.34 mg/mL (ascorbic acid as a positive control, IC_{50} = 0.07 mg/mL) (Kırmızıbekmez et al. 2015). The prenylated flavnoids (**84**, **267**, **308**, and **332**) and several non-prenylated flavonoids isolated from *Eleocharis tuberosa* were evaluated for antioxidant activity by the reducing power assay and DPPH radical scavenging assay. The result indicated that the flavonoids, **84**, eleocharins C (**308**), and B (**332**), with a 3′,4′-dihydroxylated B ring had strong antioxidant activity, and the activity decreased when the hydroxyl of B-ring was substituted with methoxy. The prenylation of flavonoids did not affect the antioxidant activity of flavonoids (Luo et al. 2014). Elastixanthone (**97**), **202**, and cycloartobiloxanthone (**217**) identified in the bark of *Artocarpus elasticus*, displayed significant scavenging activity for DPPH with an IC_{50} value of 21.6, 11.5, and 40.0 μg/mL (Ramli et al. 2016). Artocarpin (**169**), 3′-hydroxycycloartocarpin (**182**), and pyranocycloartobiloxanthone A (**232**) are from the leaves and heartwoods of *Artocarpus anisophyllus* and showed DPPH radical scavenging activity with SC_{50} values of 140.0, 152.9, and 20.2 μg/mL, respectively. (Abdul Lathiff et al. 2015). The antioxidant activities of sixteen prenylated flavonoids from *Artocarpus altilis* were assessed to scavenge DPPH, ABST, and superoxide anions. Artogomezianon (**179**) and isocycloartobiloxanthone (**230**) exhibited ABTS activities with IC_{50} values of 36.9 and 7.2 μM, respectively, while **179** had an IC_{50} value of 39.7 for superoxide anion scavenging activity. Artoflavone A (**209**), hydroxyartoflavone A (**210**), and **230** showed DPPH scavenging activities, with IC_{50} values of 53.5, 20.9, and 33.9 μM, respectively (Lan et al. 2013). A diprenylflavone, 3,5,2′,4′-tetrahydroxy-6″,6″-dimethylpyrano(2″,3″:7,6)-8-(3‴,3‴-dimethylallyl) flavone (**195**), from the roots of *Eriosema chinense* show strong DPPH scavenging activities with an IC_{50} value of 35 μM (Thongnest et al. 2013). Cycloheterophyllin (**258**) and 2′,4′-dihydroxy-3,4-(2″,2″-dimethylchromeno)-3′-prenyldihydrochalcone (**688**) showed antioxidant activity towards DPPH with SC_{50} value of 102.8 and 223.8 μM (Abdullah et al. 2017). Mildbone (**341**) and mildbenone (**593**) were from *Erythrina mildbraedii* and showed potent DPPH scavenging activities with IC_{50} values of 20.2 and 28.5 μM, stronger than the positive control (BHA, IC_{50} value: 44.2) (Ali et al. 2012). Two derivatives, 1-(2,4-dihydroxyphenyl)-3-[8-hydroxy-2-methyl-2-(4-methyl-3-pentenyl)-2 H-1-benzopyran-5-yl]-1-propanone (**672**) and 2-geranyl-2′,3,4,4′-tetrahydroxydihydrochalcone (**673**), from *Artocarpus altilis* showed DPPH scavenging activities with IC_{50} values of 82.2 and 82.4 μM, respectively (Huong et al. 2012). Excelsanone (**694**) and 6,8-diprenylgenistein (**805**) from *Erythrina excelsa* possessed actives for DPPH radical scavenging with IC_{50} values of 1.31 and 0.07 mg/mL, respectively (Gbaweng et al. 2020). Thonningiisoflavone (**781**) is from *Ficus thonningii* and showed strong DPPH radical scavenging activity with an IC_{50} value of 65.5 μM (Fongang et al. 2015). Iconisoflavan (**945**), iconisoflaven (**952**), licorisoflavan A (**961**), (3 *S*)-licoricidin (**962**), and glycycoumarin (**995**), isolated from the roots of *Glycyrrhiza iconica*, exhibited weak DPPH scavenging activity with IC_{50} values of 0.29, 0.18, 0.56, 0.32, and 0.47 mg/mL, respectively (ascorbic acid as a positive control, IC_{50}: 0.07 mg/mL) (Kırmızıbekmez et al. 2015).

Sophoflavanones A (**539**) and B (**540**) from the roots of *Sophora flavescens* exhibited antioxidant activities against Fe^{2+}/cysteine-induced toxicity at a concentration of 0.1 μM with inhibitory values of 71.65% and 72.49%, respectively (vitamin C as a positive control:87.83%) (Zhu et al. 2018). The diprenylisoflavones 5,7,3′,4′-tetrahydroxy-6,8-diprenylisoflavone (**807**) and **818** from *Flemingia philippinensis* showed antioxidant activities with ferric reducing antioxidant power values of 4338 and 2977 μmol/g, respectively (Fu et al. 2012).

In general, the antioxidant activity of prenylated flavonoids shows a close relationship with the number and position of hydroxyl groups. The catechol motif of B ring had strong antioxidant activity, and the activity decreased when the hydroxyl of B-ring was substituted with methoxy. Additionally, the prenylation of flavonoids did not affect the antioxidant activity of flavonoids.

Prenylated flavonoids with antibacterial activity

Compound **204** showed a potent antibacterial effect by disrupting the phospholipid-repair system and inhibiting the phosphatidic acid biosynthesis pathway of *Staphylococcus aureus* (Pang et al. 2019). (±)-5,4′-dihydroxy-2′-methoxy-6′,6″-dimethypyraro-(2″,3″:7,8)-6-methylflavanone (**338**) from the traditional Chinese medicine *Tripterygium wilfordii* showed significant antimicrobial activities against *S. aureus* and methicillin-resistant *S. aureus*, with IC_{50} values of 2.60 and 2.07 μg/mL, respectively. Another compound **467** exhibited antimicrobial activities against *Cryptococcus neoformans*, *Pseudomonas aeruginosa*, vancomycin-resistant *Enterococcus faecalis*, and methicillin-resistant *S. aureus* with IC_{50} values of 2.95, 8.59, 4.32, and 4.47 μg/mL, respectively (Chen et al. 2017). **501** inhibited the growth of *S. aureus* with MIC and MBC values of 8 and 16 μg/mL, respectively, by damaging the bacterial cytoplasmic membrane (Yusook et al. 2017). **501** resisted the activity of multidrug resistant enterococci with antibiofilm-producing activity, increasing membrane permeability and causing loss of salt tolerance (Sianglum et al. 2019). **579** possessed antimicrobial

activities against *S. aureus* (T28.1, T25.10, T26A4, 08143), *Trypanosoma brucei*, and *Leishmania mexicana* with MIC values of 6.8–55.0 μM (Bocquet et al. 2019).

Several monoprenylated isoflavonoids exhibited potent natural antifungal against *Z. parabailii* acting by severely compromising the membrane integrity, fifteen (**690**, **734**, **735**, **777**, **778**, **949**, **951–953**, **968–970**, **975**, **978**, and **989**) of which showed moderate to good antifungal activity against *Z. parabailii* (MIC $\leq$ 50 μg/mL) at pH 6.5. Wighteone (**734**), luteone (**735**), and glabridin (**949**) showed the highest antifungal activities with MICs of 3.13–6.25, 12.5, and 6.25–12.5 μg/mL. The fungicidal activity of **734** and **949** was 4–8 times higher than that of polygodial (MIC 50 μg/mL) at pH 6.5, the most potent natural agent against *Z. parabailii* reported so far. However, the diprenylated isoflavones (**805** and **854**) and diprenylated flavonone (**466**) did not exert any antifungal activity (MIC $\gg$ 25 μg/mL). A brief SARs of prenylated flavonoids was shown in Fig. 18 (Kalli et al. 2022). The isoflavans licoricidin (**956**), **961**, and licorisoflavans C – E (**958–960**) showed marked antibacterial activities against *P. gingivalis* with MIC value range of 1.56 – 12.5 μg/mL. Cyclization of a single prenyl group could reduce the activity against *P. gingivalis* by comparing the MIC values of **958–960** with those of **956** and **961** (Villinski et al. 2014). The prenylated isoflavans (**945**, **952**, **962**, and **961**) from the roots of *Glycyrrhiza iconica* showed antimicrobial activity against *Salmonella typhimurium* ATCC 13,311 with MIC values of 2–16 μg/mL (Kırmızıbekmez et al. 2015).

Prenylated flavonoids with antimalarial activity

The prenylated flavonoid scaffolds can be considered as promising skeletons for antiplasmodial activity. Monoprenylated flavonones, 4′-*O*-Methyl-sigmoidin B (**290**), abyssinin II (**291**), sigmoidin B (**292**), abyssinoflavone IV (**322**), exhibited antiplasmodial activity with IC_{50} values of 4.37, 6.87, 7.14, and 7.96 μM, respectively. Diprenylated flavonone, sigmoidin A (**477**), abyssinin III (**489**), sigmoidin F (**513**) and abyssinoflavone V (**514**), exhibited antiplasmodial activity with IC_{50} values 3.02, 2.32, 2.29, and 9.51 μM, respectively. However, sigmoidins C (**345**) and D (**346**), and erylatissin G (**347**) show weak antiplasmodial activity, indicating that cyclization of the prenyl side chain would dramatically decrease the antiplasmodial activity (Tuenter et al. 2019). Tripteryols B (**467**) and A (**508**) from *Tripterygium wilfordii* were active against chloroquine-sensitive D6 and resistant W2 clones of *Plasmodium falciparum* with IC_{50} values in the range of 3.15–4.63 μg/mL. A novel flavan-4-ol analogue rhodiflavan C (**548**) bearing an unprecedented five-membered A-ring bearing two prenyl groups at C_8 and a pair of rare diastereomers rhodiflavans A (**549**) and B (**550**) possessing a chromene-5,7-dione unit and three prenyl substitutions at the A ring were isolated from *Tephrosia rhodesica*. They exhibited antiplasmodial activity against the 3D7 strain of *Plasmodium falciparum* with an IC_{50} values of 7.0, 7.3, and 5.7 μg/mL (Atilaw et al. 2020).

Other active prenylated flavonoids

Methoxycyclocommunol (**113**) and cudraflavone C (**167**), isolated from the bark of *Artocarpus integer*, exhibited strong PGE2 inhibitory activity with IC_{50} values of 4.3 and 0.07 μM, respectively, in LPS-treated human whole blood (Shah et al. 2016). Kushenol X (**141**), Kurarinone (**522**) and kushenol C (**523**), 2-[(2′-(1-Hydroxy-1-methylethyl)-7′-(3-methyl-2-butenyl)-2′,3′-dihydrobenzofuran)-5-yl]-7-hydroxy-8-(3-methyl-2-butenyl)chroman-4-one (**558**) exhibited dose-dependently inhibitory activities of hCE 2 with IC_{50} values of 3.05, 1.46, 2.61, and 1.13 μM, respectively, and were proven to be uncompetitive inhibitors with Ki values of 1.72, 1.73, 0.79, and 1.59 μM and Km values of 5.41, 2.08 3.10, and 2.74 μM, respectively. Comparison

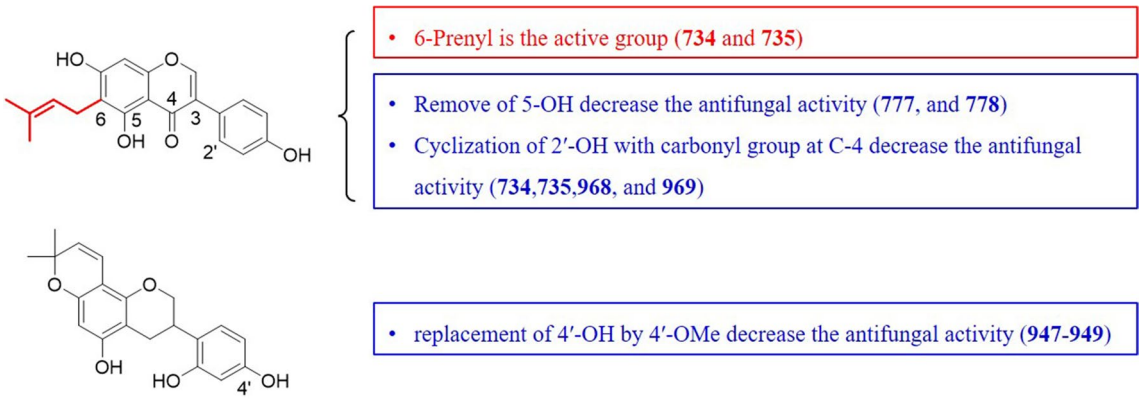

Fig. 18 SARs of prenylated flavonoids with antifungal activity against *Z. parabailii*

of their structures and molecular docking results suggested the hydroxy groups of C-4′ and C-7 and ketone carbonyl group at C-4 in flavonoids were important for their inhibitor activities. (Song et al. 2019).

Tyrosinase inhibitors are important substances to treat abnormal pigmentation disorders, such as melasma, age spots and sites of actinic damage, arising from the accumulation of an excessive level of epidermal pigmentation. Artogomezianone (**179**) and cudraflavone A (**231**) repressed melanin production by suppressing tyrosinase activity with IC_{50} values of 84.8 and 88.4 μM, respectively (Lan et al. 2013). **232** inhibited tyrosinase activity with an IC_{50} value of 60.5 μg/mL (Abdul Lathiff et al. 2015). Artonin M (**261**) is from the dried heartwood of *Artocarpus altilis* and repressed melanin production by suppressing tyrosinase activity with an IC_{50} value of 74.1 μM (Lan et al. 2013). **279** is from the leaves of *Morus alba* and significantly inhibited tyrosinase activity, with an IC_{50} value of 0.26 μM (Yang et al. 2012). Morusyunnansins E (**911**) and F (**912**) from the leaves of *Morus yunnanensis* significantly inhibited mushroom tyrosinase with IC_{50} values of 1.43 and 0.15 μM, respectively (Hu et al. 2012). Sigmoidin B (**292**) and **477** are from the stem barks of *Erythrina latissimi* and exhibited antigenotoxic activity with IC_{50} values of 52.5 and 44.1 μM, respectively. (Zarev et al. 2017). (2 *S*)-2′,4′-Dihydroxy-5′-(1‴,1‴-dimethylallyl)-8-prenylpinocembrin (**492**) exhibited strong anti-tyrosinase activity with an IC_{50} value of 2.32 μM (Peralta et al. 2014). **579** was proven to have a protective effect against HUVEC injury caused by Ang II by improving cell viability from 53.9 to 74.9% (Zhang et al. 2017).

Histone deacetylases (HDAC) are enzymes that cleave acetyl groups from acetyl-lysine residues in histones and various nonhistone proteins. Both acetylation and deacetylation of histones play a fundamental role in the epigenetic regulation of gene expression, and disruption of the balance between histone acetyltransferases and HDACs causes many disorders and metabolic diseases. Alopecurone J (**1011**) exerted strong histone deacetylase (HDAC) inhibitory activity in HeLa and HCT116 cells with IC_{50} values of 3.85 and 0.08 μM, respectively. The molecular docking results indicated that **1011** could bind to the active pocket of HDAC8, and the resveratrol group of **1011** had hydrophobic interactions with residues Phe 152 and His 143, whose hydroxyl moieties bear metal coordination with Zn^{2+} (Soltani et al. 2020).

Pharmacological activity

Members of the prenylated flavonoids, such as icariin, icaritin, and xanthohumol, are promising candidates for diverse diseases. The pharmacological activities of the active prenylated flavonoids obtained from plant sources are summarized in this review.

Anticancer activity

Glabratephrin (**58**) was proposed as an effective and safe compound able to reverse doxorubicin resistance mediated by Pgp in triple negative breast cancers. It increased doxorubicin accumulation and cytotoxicity in triple negative breast cancer cells with high levels of Pgp, without adding significant additional toxicities to doxorubicin treatment. Glycine 185 of Pgp was identified as a critical residue mediating the reduced catalytic efficacy of Pgp elicited by compound **58** in a site-directed mutagenesis experiment. In addition, **58** was predicted to bind two residues, Pha 322 and Gln 721, by *in silico* molecular docking (Abd–Ellatef et al. 2022). 6-Prenylapigenin (**64**) suppressed the proliferation of HeLa cells via the MAPK and Akt signaling pathways. Compound **64** increased the protein levels of p-JNK and p-p38, and reduced the expression of p-Akt and p-ERK (Ye et al. 2021). 2-methoxy-2′,4′,4,6-tetrahydroxy-5-lavanduly dihydrochalcone (**671**) could significantly activate autophagic flux and trigger ROS release in HepG2 cells. However, it did not affect the main proteins of the apoptosis signaling pathway (Yang et al. 2021). A new prenylated flavone (**165**), isolated from *Daphne giraldii*, selectively inhibited the proliferation of hepatocellular carcinoma (HCC) cells by activating the p38/MAPK pathway without apparent cytotoxicity to normal human cells. It also repressed tumor growth in a nude mouse xenograft model without significantly affecting body weight or pathology characteristics. Mechanistically, **165** resulted in G0/G1 arrest and apoptosis by downregulating the expression of cyclin E1, CDK2, and CDK4 and promoting the cleavage of caspase 3 and PARP in HCC cells. It aggravated p38 phosphorylation and attenuated JNK phosphorylation which were abrogated by SB203580, a p38/MAPK-specific inhibitor, and exacerbated by SP600125, a JNK/MAPK-specific inhibitor, indicating **165**-induced apoptosis in a p38/MAPK dependent manner (Wang et al. 2017a). A further mechanistic study indicated that **165**-induced p38-dependent apoptosis was related to oxidative and nitrosative stress in HCC cells (Shang et al. 2018). **169**-induced primary glioblastoma cell apoptosis was mediated by the activation of the mitochondrial pathway involving mitochondrial depolarization, ROS production, cytochrome c release, Bad and Bax upregulation, and Bcl-2 downregulation. The **169**-induced ROS generation activated Akt and ERK1/2 phosphorylation which resulted in PARP cleavage and caspase-3, -7, and − 9 activation (Lee et al. 2018). Norartocarpin (**173**) was identified as an Nrf2 activator and prevented oxidative insults in human lung epithelial cells. **173** upregulated the protein levels of Nrf2 and its downstream genes NAD(P)H quinone oxidoreductase 1 (NQO1) and γ-glutamyl cysteine synthetase (GCLM) by facilitating the nuclear translocation of Nrf2 and enhancing Nrf2 protein stability (Yang et al. 2019). **204** is from the root bark of *Morus australis* and effectively

inhibited the proliferation and survival of epithelial ovarian cancer (EOC) cells in vitro and repressed tumor growth in vivo. It resulted in paraptosis-like cell death, a novel mode of nonapoptotic programmed cell death that is characterized by extensive cytoplasmic vacuolation due to dilation of the endoplasmic reticulum (ER) and mitochondria and lack of apoptotic hallmarks. **204** also resulted in an obvious enhancement of mitochondrial Ca^{2+} levels, accumulation of endoplasmic reticulum stress markers, generation of ROS, and depletion of $\Delta\psi m$ in EOC cells. **204**-induced paraptosis-like cell death was supposed to relate to overloaded mitochondrial Ca^{2+} causing mitochondrial swelling and dysfunction for the treatment of voltage-dependent anion channel inhibitor, 4,4′-diisothiocyanostilbene-2,2′-disulfonic acid, which reversed the aforementioned effect in vitro and in vivo (Xue et al. 2018). In addition, **204** was found to be a promising candidate for cancer treatment, including lung cancer. It induced mitochondria-dependent apoptosis through chromatin condensation, PARP cleavage, mitochondrial membrane potential (MMP) loss, cytochrome c release, Bax/Bcl-2 dysregulation, and caspase-3 cleavage. It also caused a pro-autophagic effect, accompanied by an increased level of LC3-II and a decreased level of SQSTM1/p62. **204** enhanced intracellular ROS levels, inhibited PI3K/Akt signaling and activated the JNK and ERK pathways, which was confirmed by treatment with the corresponding enzyme inhibitors (Wang et al. 2020c). **202**, derived from the stem bark of *Artocarpus elasticus*, suppressed breast cancer cell viability by inducing caspase-dependent apoptosis. **202** enhanced the release of total ROS and polarized the mitochondrial membrane. It upregulated the expression of cytochrome c, Bax, caspase-7 and -9, and p21 and downregulated the expression of MAPK and cyclin D at the transcriptional and translational levels. **202** also repressed an inhibitor of apoptosis, livin, to avoid preceding chemotherapeutic resistance and apoptosis evasion (Etti et al. 2017a, b). **267** inhibited the voltage-gated potassium channel Kv1.3 with an estimated value of the half-blocking concentration of 5.76 μM in Jurkat T cells and exhibited more effective inhibition of Kv1.3 channels than the nonprenylated compounds, acacetin, chrysin, baicalein, wogonin, and luteolin. **266** showed low cytotoxicity to Jurkat T cells, which indicated that the channel inhibition might be involved in its anti-proliferative and pro-apoptotic effects (Teisseyre et al. 2018). **281** can diminish melanoma cell viability due to autophagy and caspase-dependent apoptosis in the B16-F10 murine melanoma model. **281** abolished the metastatic potential of a melanoma subclone by disrupting integrin signaling and inhibited the development of lung metastatic foci in tumor-challenged animals (Krajnović et al. 2019). In addition, **281** was identified as a noncompetitive inhibitor with a different binding site than acarbose. It bound to α-glucosidase in allosteric sites via hydrogen bonds, hydrophobic, van der Waals, and electrostatic forces. The binding of **281** to α-glucosidase affected the tertiary structure of α-glucosidase by changing the hydrophobicity around Tyr and Trp residues. After binding **281**, the binding sites of α-glucosidase formed a stable α-helix, which is involved in forming stable hydrogen bonds with the Asn241 residue (Wang et al. 2022). **460** inhibited autophagy-modulating activity by exhibiting autophagosome maturation by blocking the degradation of EGFP puncta in HeLa cells stably expressing EGFP-mRFP-LC3B. It also reduced lysosomal activity and cathepsin maturation by disrupting lysosomal positioning, subsequently inducing apoptosis. Valosin-containing protein (VCP)/p97 was proven to be a potential target protein of **460** in regulating lysosomal positioning for autophagy maturation (Kwon et al. 2020). **522** suppressed the TGF-β-induced epithelial-mesenchymal transition (EMT) of lung epithelial cells. **522** suppressed the phosphorylation of Smad2/3 and Akt induced by TGF-β1 in lung epithelial cells and lung tissues treated with BLM. Oral administration of **522** attenuated fibrotic changes in lung tissues, including the accumulation of collagen, and improved mechanical pulmonary functions (Park et al. 2021).

579, a prenylated chalcone from hops, exhibited diverse anti-cancer activities, such as anti-chronic myelogenous leukemia, anti-breast cancer, and anti-glioma cell activities, but the anti-cancer mechanisms are different. **579** inhibited the proliferation, induced S phase cell cycle arrest, and stimulated apoptosis in K562 cells. It degraded BCR-ABL in a concentration- and time-dependent manner involving the activation of caspase and inhibition of autophagy and the ubiquitin proteasome system in K562 cells (Lu et al. 2019). **579** inhibited the survival of breast cancer cells by modulating the Notch signaling pathway in vivo and in vitro. It not only downregulated cell viability and induced G0/G1 cell cycle arrest and apoptosis in MCF-7 and MDA-MB-231 cells, but also reduced the activation of the Notch signaling pathway and apoptotic regulators Bcl-2, Bcl-extra large, and caspase 3 (Liu et al. 2016; Sun et al. 2018b). **579** induced reversal of drug resistance via the inhibition of ABCB1-mediated transport of doxorubicin, stimulating ABCB1 ATPase activity and acting as a substrate of ABCB1. **579** bound to the ABCB1 transmembrane domain, which resulted in less protein and ligand position fluctuation, and **579** synergized with the ABCB1 substrate colchicine (Liu et al. 2018a). **579** induced glioma cell autophagy and inhibited tumor growth in vivo through the Akt/mTOR/S6K pathway and MAPK cascade (Lu et al. 2015). **579** induced apoptosis in human malignant glioblastoma cells and the mechanism was related to the increase in ROS species and activation of MAPK pathways, and **579** activated caspase-3 and −9 and PARP cleavage (Festa et al. 2011). **579** decreased the proliferation of TPC1 cancer cells by inducing DNA fragmentation and promoting cell cycle arrest (Carvalho et al. 2018). The chemoprotective effect of **579** was investigated in vitro in the metabolically

competent HepG2 cell line. The results indicated that **579** could act as a scavenger of AFBO, preventing DNA adduct formation and DNA damage induction (Štern et al. 2021). **579** impaired the PMA-driven migratory and invasive capacity of A549 cells by decreasing the level of MMP-9 expression and concomitantly increasing TIMP-1 protein expression, a specific blocker of PRO-MMP-9 activation. **579** decreased the PMA-induced production of VEGF and TGF-β. Furthermore, **579**-treatment counteracted the PMA-induced EMT of A549 cells by upregulating of E-cadherin and α-E-catenin and downregulating of *N*-cadherin, vimentin, and snail-l expression (Slawinska-Brych et al. 2021). **579** significantly induced glioblastoma multiforme cell death and enhanced temozolomide cytotoxicity. Mechanistically, **579** downregulated replication factor C subunit 2 (RFC2), a DNA repair-related gene, which was overexpressed in glioblastoma multiforme patients and tumors. MicroRNA-4749-5p, a **579**-upregulated microRNA, was identified to target the RFC2 3′ UTR and inhibit RFC2 expression (Ho et al. 2020). **579** inhibited esophageal squamous cell carcinoma (ESCC) cell proliferation in vitro and in vivo by targeting keratin (KRT)-18, which was highly expressed in patient ESCC tissues. Knockdown or overexpression of KRT18 protein abrogated or enhanced the anti-proliferative activity of **579**, respectively. **579** could attenuate KRT18 protein expression. However, it did not change the KRT18 mRNA levels. **579** also induced apoptosis and cell cycle arrest at the G1 phase, which was associated with the modulation of the expression of related markers, including cyclin D1, cyclin D3, cleaved-PARP, Bcl-2, cytochrome c, and Bax (Yin et al. 2020).

818, isolated from *Flemingia philippinensis*, promoted apoptosis and diminished tumor growth by suppressing PI3K/Akt/mTOR signaling through an ROS-mediated caspase-independent pathway. It caused selective apoptotic cell death in LNCaP prostate cancer cells by elevating DNA fragmentation, the sub-G1 cell population, c-PARP, the Bax/Bcl-2 ratio, AIF and endonuclease G. **818** decreased the phosphorylation of Akt, mTOR and PI3K. However, auriculasin-induced apoptosis did not result in caspase-3, -8, and −9 activation (Cho et al. 2018). Isoangustone A (**845**) was proven to be an agonist of AMPK, an important signaling molecule that regulates cell energy homeostasis and autophagy. **845** inhibited mitochondrial respiratory capacity, activated autophagic signaling and induced a complete autophagic flux in colorectal cancer cells in a concentration-dependent manner. It also enhanced AMPK and ACC phosphorylation and increased LC3-I&II protein levels in vivo and in vitro in a concentration- and time-dependent manner (Tang et al. 2021). BAS-4, isolated from *Brosimum acutifolium*, showed potential activity against glioma through the apoptosis pathway mediated by ΔΨm loss and Akt pathway disruption. It inhibited migration and invasion and induced apoptosis via mitochondrial damage, ΔΨm loss, cell cycle arrest, and Akt phosphorylation suppression in glioma cells. However, it did not induce cytotoxicity in primary glial cells (Maués et al. 2019). **949** suppressed the tumor formation in the hepatoma xenograft model in vivo without statistically significant changes in body weight. It was proven to restrain the migration and invasion of human hepatocellular carcinoma cells by inhibiting the phosphorylation of ERK1/2 and JNK1/2 rather than inhibiting their proliferation. **949** suppressed the protein and mRNA expression of MMP9 by affecting the expression of the NF-κB and AP-1 transcription factors (Hsieh et al. 2014). Two prenylated dihydroisoflavones, sigmoidin I (**883**) and bidwillon A (**904**), and two prenylated pterocarpans, 6α-hydroxyphaseollidin (**982**) and sophorapterocarpan A (**990**), exhibited promising cytotoxic effects to diverse sensitive cell lines (CCRF-CEM, MDA-MB-231-*pcDNA*, HCT116, U87MG, and HepG2) with an IC_{50} value range of 3.36–29.48 μM and drug-resistant cancer cell lines [CEM/ADR5000, MDA-MB-231-*BCRP*, HCT116 ($p53^{-/-}$), U87MG, and ΔEGFR] with an IC_{50} value range of 4.60-30.98 μM, and did not exhibit obvious cytotoxicity to the normal cell line AML12, with the IC_{50} values greater than 98.02 μM (Kuete et al. 2014). **982** induced apoptosis in CCRF-CEM cells mediated by the activation of effector and initiator caspases, including caspase-3, -7, -8, and −9, breakdown of MMP and increase in ROS production, whereas the apoptotic process induced by abyssinone IV (**483**), **883**, and **990** was alleviated by the loss of MMP and the increase in ROS production (Kuete et al. 2014). A brief summary of the anti-cancer mechanisms of the active ingredients is listed in Table 5..

Anti-inflammatory activity

169 prevented skin damage from UVB irradiation-induced photodamage in hairless mice, probably due to its antioxidant and anti-inflammatory properties. Treatment with **169** at topical doses of 0.05% and 0.1% showed a significant photoprotective effect by decreasing histopathological changes, such as desquamation, epidermal thickening and sunburn cell formation. It exhibited a significant effect by decreasing levels of ROS and lipid peroxidation which have been used as markers of oxidative stress for evaluating UVB irradiation induced skin damage. In addition, **169** downregulated the inflammatory proteins cPLA2 and COX-2 to decrease the levels of TNF-α and IL-1β (Lee et al. 2013). **169** had a potential therapeutic effect on skin wounds by accelerating the inflammatory phase and increasing myofibroblast differentiation, proliferation and migration of fibroblasts and keratinocytes, collagen synthesis and maturation, re-epithelialization, and angiogenesis. It accelerated inflammatory progression and subsequently decreased persistent inflammation. **169** increased collagen production and increased human fibroblast proliferation and migration by activating

Table 5 Anti-cancer mechanism of active ingredients

No	Ingredient	Models	Result/Mechanism	References
58	Glabratephrin	MDA-MB-231 and murine mammary JC cells	↑Doxorubicin accumulation and cytotoxicity, bind Phe 322 and Glu 721	Abd–Ellatef et al. (2022)
64	6-prenylapigenin	HeLa cells	↑p-PARP, ↑p-JNK, ↑p-p38, ↓p-Akt, ↓p-ERK	Ye et al. (2021)
165	Daphnegiravone D	Hep3B and HepG2 cells Male BALB/c nude mice	Apoptosis, ↑G0/G1 arrest, ↓cyclin E1, CDK2, and CDK4, ↑cleaved-caspase-3 and -PARP, ↓p-p38/MAPK, ↓p JNK. Negative results: cyclin D1, p-ERK	Wang et al. (2017a)
		Hep3B and HepG2 cells	Apoptosis, ↑MDA, ↓SOD and GSH-Px, ↑iNOS, ↑c-PARP, ↑Bax/Bcl-2 ratio, ↑caspase-3	Shang et al. (2018)
169	Artocarpin	U87 and U118 cells BALB/cA-nu (nu/nu)	↑Caspase-3, -7, and -9 activities, ↑c-PARP, ↑NADPH oxidase activity, ↑Bad, ↑Bax, ↑cytochrome c, ↓Bcl-2, ↑Akt, ↓p-ERK1/2. Negative results: JNK1/2, p38 MAPK	Lee et al. (2018).
173	Norartocarpin	Hepa 1c1c7, MDA-MB-231, Beas-2B cells	↑Nrf2, ↑NQO1, ↑GCLM, ↑GSH, ↓intracellular ROS	Yang et al. (2019)
202	Artonin E	MDA-MB 231 cells	Apoptosis, ↑G2/M arrest, ↑sub G0/G1 phase, ↑mRNA of caspase-7, -8, and -9, and P21, ↓mRNA of cyclin E, ↑HSP 27, ↑phospho S46 and S392, ↑SMAC, ↑TRAIL, ↑HO-1, ↑pro-caspase 3, ↓HSP 60 and 70, ↓livin, ↓Bcl-2, ↓Bcl-x, ↓phospho S15, ↓cIAP-2, ↓c-caspase 3. Negative results: p53	Etti et al. (2017a)
		MCF-7 cells	Apoptosis, ↑membrane blebbing, ↑chromatin condensation, ↑nuclear fragmentation, ↑caspase 9, ↑caspase 8 only at 30 μM, ↑ROS, ↑G0/G1 phase, ↑mRNA of cytochrome c, Bax, caspase-7 and -9, and p21, ↓mRNA of MAPK and cyclin, ↓PON2, ↓Bcl-x, ↓xIAP, ↓Bad, ↓Bcl-2, ↓survivin, ↓livin, ↓Hsp 27, ↑Hsp 60 and 70, ↑cell cycle regulatory protein p21, ↑Bax	Etti et al. (2017b)
204	Morusin	A2780, SKOV-3, and HO-8910 cells	Autophagy, ↑cytoplasmic vacuolization, ↑LC3 puncta, ↑LC3-II/LC3-I ratio, ↓p62 at 6 h, ↑p62 after 12 h, ↑precursor forms of cathepsin B and cathepsin D, ↓mature forms of cathepsin B and cathepsin D, ↑BiP, ↑C/EBP-homologous protein, ↑IRE1α, ↑p-eIF2α, ↓AIP-1/Alix protein, ↑mitochondrial Ca^{2+}, ↓$\Delta\psi$m, ↑ROS. Negative results: c-PARP, caspase-3, and -9	Xue et al. (2018)
		A549 and NCI–H292 cells	Apoptosis and autophagy, ↑c-PARP, ↑caspase-3 and -9, ↑mitochondrial depolarization, ↓mitochondrial membrane potential, ↑cytochrome c translocation, ↑Bax, ↓Bcl-2, ↓Bcl-X_L, ↑LC3-II, ↓SQSTM1, ↓p-Akt, ↑p-JNK, ↑p-ERK, ↑ROS, ↓p-p65	Wang et al. (2020c)
281	Isoxanthohumol	Murine metastatic melanoma B16-F10 cells, female inbred C57BL/6 mice	Apoptosis and autophagic, ↓cell migration, invasion, and adhesion, ↓integrin α-6, ↓FAK, ↓vinculin, ↓Rho kinase, ↓α-SMA, ↓β-Actin, ↓diameter per nodule, ↓HMGB1, ↑S100, ↓Ki-67	Krajnović et al. (2019)
487 **488**	Addisoniaflavanone I Addisoniaflavanone II	H4IIE cells	Apoptosis, ↑caspase-3 and -7, ↑nuclear fragmentation	Passreiter et al. (2015)
460	Kushenol E	HeLa and HCT116 cells	Autophagy, ↑EGFP-LC3B–positive puncta, ↑LC3B-II, ↑p62, ↓lysosomal activity, ↓cathepsin B and cathepsin D maturation, ↑cPARP1 and γ-H2AX, ↑annexin V binding and PI uptake, ↑VCP/p97	Kwon et al. (2020)

Table 5 (continued)

No	Ingredient	Models	Result/Mechanism	References
522	Kurarinone	Male BALB/c mice, Male BALB/c mice	↓COLIα 1, ↓N-cadherin, ↓α-SMA, ↓p-Smad2/3, ↓p-Akt, ↓Epithelial-mesenchymal transition, ↓TFG-β1, ↓IL-17, ↓RORγt mRNA	Park et al. (2021)
579	Xanthohumol	K562 and K562/ADR cells	Autophagy, ↑S arrest, ↓G0/G1 and G2/M, ↓BCR-ABL, ↓p-BCR-ABL, ↑LC3-II, ↑p62, ↑ubiquitinated proteins, ↑Hsp70, ↑c-caspase-3 and -9, ↑c-PARP	Lu et al. (2019)
		Human MCF-7, MDA-MB-231, HEK-293T, h-TERT-BJ, MCF-10A, and murine 4T1 cells, female BALB/c mice	Apoptosis, ↓Hes1 and Hey1 transcription, ↓c-Myc and surviving, ↓EGFR, ↑MIF, ↑c-caspase-3, ↑c-PARP, ↓Notch1, ↓Ki-67, ↑survivin	Liu et al. (2016)
		MCF-7/ADR cells	↓Bcl-2, ↓pro-caspase-3, ↑Bax, ↑c-PARP, ↑γ-H2AX, ↑S and G2/M arrest, ↓G0/G1 arrest, ↓ABCG2. Negative results: β-catenin and ALDH	Sun et al. (2018b)
		MCF-7/ADR cells	↓DOX efflux, ↑intracellular Rho123, ↓efflux of ABCB1, Bound close to residues Phe 336, Phe 983, Ala 980, Phe 728, Asn 842, Tyr 953, and Phe 732 of ABCB1	Liu et al. (2018a)
		U87 glioma cells	Autophagy, ↑conversion of LC3-I to LC3-II, ↑p62 degradation, ↓phosphorylation of Akt, mTOR, and S6K, ↑caspase-3 activation, ↑c-PARP, ↑phosphorylation of p38, ERK, and JNK	Lu et al. (2015)
		T98G and U87-MG cells	Apoptosis, ↑caspase-3 and -9, ↓PARP, ↓Bcl-2, ↑mitochondrial depolarization, ↑ROS, ↑p-ERK1/2, ↑p-p38. ↑JNK, ↑SAPK. Negative results: JNK/SAPK	Festa et al. (2011)
		TPC-1 cells	↑caspase-3 and -7, ↑S arrest, ↓G1 arrest	Carvalho et al. (2018)
		A172 and U87-MG cells	↓RFC2, ↑miR-4749-5p	Ho et al. (2020)
		KYSE30, KYSE70, KYSE410, KYSE450, and KYSE510 cells	apoptosis, ↑G1 arrest, ↓cyclinD1, cyclinD3, ↑c-PARP, ↑cytochrome c, ↑Bax, ↓Bcl-2, ↓KRT18 and Ki67 protein. Negative results: mRNA of KRT18	Yin et al. (2020)
818	Auriculasin	LNCaP-FGC and RWPE-1 cells	Apoptosis, ↑DNA fragmentation and chromatin condensation, ↑Bax, ↓Bcl-2, ↑c-PARP, ↑release of AIF and endonuclease G proteins, ↓PI3K, ↓p-Akt, ↓p-mTOR, ↓p-p70s6k, ↑ROS. Negative results: caspase-3, -8, and -9	Cho et al. (2018)
845	Isoangustone A	SW480, LOVO, and SW620 cells	Autophagy and apoptosis, ↑LC3 lipidation, ↑p62 degradation, ↓p-Akt, ↓p-mTOR, ↓p-4EBP1, ↑p-AMPK, ↑ACC, ↑p-ULK1, ↓mitochondrial respiration, ↑LC3-I&II	Tang et al. (2021)
/	BAS-4	C6 glioma cells	Apoptosis, ↓C6 scratch migration and C6 colony formation, ↓$\Delta\Psi$m, ↓Akt	Maués et al. (2019)
949	Gabridin	Huh7 and Sk-Hep-1 cells	↓protein and mRNA expressions of MMP9, ↓c-Fos, ↓c-Jun, ↓p-IκB, ↓p-ERK1/2, ↓p-JNK 1/2. Negative results: PI3K/Akt, p38	Hsieh et al. (2014)

the p38 and JNK pathways, whereas it increased the proliferation and migration of human keratinocytes through the ERK and p38 pathways and augmented human endothelial cell proliferation and tube formation through the Akt and p38 pathways (Yeh et al. 2017). **190** exerts its anti-inflammatory effect by activating the Nrf2/HO-1 pathway and may be a potential Nrf2 activator. It inhibited the LPS-induced production of NO, TNF-α, and IL-1β *in vitro* in RAW264.7 and mouse bone marrow-derived macrophages. **190** suppressed the expression of iNOS, COX-2, TNF-α, and IL-6 in LPS-induced RAW264.7 cells. Mechanistically, **190** induced OH-1 mRNA and protein expression by activating Nrf2 through the p38 MAPK pathway. When HO-1 was inhibited, the anti-inflammatory effect of **190** was significantly abrogated (Tran et al. 2018). **228**, a large amount of prenylated flavonoid in the roots of *Morus alba*, was identified as a COX-2 and COX-1 inhibitor and decreased the expression and secretion of TNF-α by blocking the translocation of the NF-κB in THP-1 human monocytic leukemia cells (Hošek et al. 2011). Cudraflavanone B (**275**) suppressed the production of IL-6 and TNF-α and inhibited NF-κB signaling pathway by restraining the expression of iNOS and COX-2 in LPS-induced RAW264.7 and BV2 cells. In addition, **275** inhibited the phosphorylation of mitogen-activated protein kinase, an extracellular signal-regulated kinase, signaling pathways in these LPS-stimulated cells (Ko et al. 2021). Sophoraflavanone M (**286**) reduced LPS-induced production of inflammatory mediators NO, IL-6, TNF-α, and MCP-1, and the expression of these mediators at the mRNA level in the LPS-primed RAW264.7 cell line. **286** inhibited the NF-κB signaling pathway by suppressing the phosphorylation and degradation of IκBα and the translocation of p65. **286** also suppressed JNK phosphorylation to dampen AP-1 transcriptional activity (Han et al. 2021). Neougonin A (**416**) from *Helminthostachys zeylanica* reduced the production of the inflammatory mediators TNF-α, PGE2, NO, IL-1β, and IL-6 and the inflammation-related proteins iNOS and COX-2 via the suppression of the NF-κB signal transduction pathway in LPS-induced macrophage RAW264.7 cells. **416** inhibited the phosphorylation of IκBα and blocked the translocation of NF-κB/p65 into the nucleus. However, it had no effect on JNK, ERK1/2, or p38MAPK phosphorylation (Cao et al. 2016). **472** exhibited a potential antineuroinflammatory effect and inhibited NO production activity with an IC_{50} value of 6.28 in LPS-treated BV2 microglial cells. Mechanistically, it remarkably suppressed the protein expression of iNOS and COX-2. **472** also decreased the production of proinflammatory cytokines (IL-6, TNF-α, IL-12, and IL-1β), blocked the nuclear translocation of NF-κB p50 and p65 by interrupting the degradation and phosphorylation of IκB-α, and inhibited NF-κB binding. In addition, **472** suppressed the phosphorylation of JNK and p38 (Kim et al. 2016). **523** dose-dependently suppressed the production of inflammatory mediators, including NO, PGE2, IL-6, IL1β, MCP-1, and IFN-β, in LPS-stimulated RAW264.7 macrophages, demonstrating the inhibition of STAT1, STAT6, and NF-κB activation. It augmented the activity of Nrf2 transcription, which was responsible for the upregulation of HO-1 expression and its activity. **523** activated the endogenous antioxidant defense system involving glutathione, superoxide dismutase, and catalase in tert-butyl hydroperoxide (tBHP)-induced oxidative stress HaCaT cells, which was relative to upregulated activation of Nrf2 and Akt in the PI3K-Akt signaling pathway (Cho et al. 2020). Sophoraflavanone G (**527**) inhibited LPS-induced production of NO and PGE2 by downregulating the expression of iNOS and COX-2 in LPS-induced RAW264.7 cells. It also decreased the mRNA and protein expression levels of the proinflammatory cytokines TNF-α, IL-6, and IL-1β. Mechanistically, **527** decreased the levels of phosphorylated PI3K and Akt, and attenuated the expression of phosphorylated JAK and STAT. In addition, it upregulated HO-1 expression via nuclear translocation of Nrf2 (Guo et al. 2016b). Compared with the chronic, unpredictable, mild stress-exposed group, the levels of IL-6, IL-1β, and TNF-α in the hippocampus were significantly reduced, and the quantity of 5-HT and NE was increased considerably in the **527**-treatment model. **527** upregulated the expression of PI3K, Akt, mTOR, 70S6K, BDNF, and Trkb (Wang et al. 2020b). SPF1 was identified as a potent ligand for RXR, a target related to Alzheimer's disease. SPF1 potentiated the effect of T0901317, a liver X receptor ligand, on reducing proinflammatory cytokine mRNA levels. It efficiently reduced the mRNA expression levels of IL-1β and IL-6 in vitro. SPF1 increased ATF3 mRNA levels in RAW264.7 cells. However, SPF1 did not affect ATF3 mRNA induction in LPS-treated RAW264.7 cells since ATF3 is also induced by LPS (Wang et al. 2019).

Compound **579** alleviated oxidative damage and accelerated diabetic wound healing via Nrf2 activation in vitro and in vitro. It augmented Nrf2 expression and accelerated diabetic wound healing. **579** caused AMPKα activation and covalent modification of Keap1, which were related to the stabilization and translocation of Nrf2 (Lu et al. 2022). **579** possessed a potential protective effect on LPS-treated depressive-like symptoms mediated by inflammation and oxidative stress. Pretreatment with **579** at doses of 10 and 20 mg/kg reversed the behavioral impairments prophylactically, as was obvious in the forced swimming test and tail suspension test, without affecting locomotion, and the 20 mg/kg dose improved anhedonic behavior, as observed in the sucrose preference test. **579** prevented LPS-induced neuroinflammation and oxido-nitrosative stress in a dose-dependent manner. It reduced activated gliosis via attenuation of Iba-1 and GFAP, and the expression of phosph-NF-κB and caspase-3 and enhanced the expression of Nrf2 and HO-1 in the hippocampus (Rahman et al. 2021).

A brief summary of the anti-inflammatory mechanisms of the active ingredients is listed in Table 6.

Neuroprotective activity

Neurons are damaged following prolonged exposure to high concentrations of corticosterone and one of the main mechanisms underlying neuronal injury is apoptosis. Icariin (**26**) protected neurons from damage in hippocampal neuronal cells by protecting them against apoptosis. **26** blocked p38 MAPK phosphorylation, improved mitochondrial membrane potential, and inhibited caspase-3 activation. **26** stimulated mitochondrial activity by upregulating the cortical expression of SIRT1 and PGC-1α and prevented brain ischemic nerve injury (Zhu et al. 2010; Liu et al. 2011). **26** could be used to treat poststroke dementia. It ameliorated the damage in central cholinergic circuit histone acetylation homeostasis by enhancing CREB phosphorylation in the central cholinergic circuits. **26** decreased the levels of acetylcholine and choline acetyltransferase compared with those without **26**-treatment (Wang et al. 2013). **522** alleviated the clinical symptoms of Parkinson's disease and some other neurodegenerative diseases. It was proven that **522** played a functional role in dopamine receptor subtypes, $V_{1A}R$, $5\text{-}HT_{1A}R$, and hMAOs. **522** could bind well to dopamine receptor subtypes, unfolding antagonist behavior on D_1R (IC_{50}: 42.1 μM) and agonist effects on D2LR and D4R (EC_{50} 22.4 and 71.3 μM, respectively). **522** suppressed hMAO isoenzymes in a modest and nonspecific manner (Prajapati et al. 2021). **579** acted at $GABA_A$ receptors in the hippocampal nerve terminals to downregulate the Ca^{2+} influx by N- and P/Q-type Ca^{2+} channels, which subsequently suppressed the Ca^{2+}-calmodulin/PKA cascade to reduce the evoked glutamate release. **579** reduced the frequency of miniature excitatory postsynaptic currents without affecting their amplitude (Chang et al. 2016). In addition, **579** reduced infarct volume and improved neurobehavior, mediated by inhibition of inflammatory responses, apoptosis, and platelet activation. **579** decreased the expression of HIF-1α, TNF-α, iNOS, and caspase-3, which were associated with middle cerebral artery occlusion-induced focal cerebral ischemia (Yen et al. 2012). Morachalcone D (**586**) and morachalcone E (**610**), two prenylated flavonoids with similar structures isolated from mulberry leaves, exerted protective effects against glutamate- and erastin-induced HT22 cell death. **586** had more potential than **610** in preventing oxytosis and ferroptosis. **586** attenuated glutamate- and erastin-induced neurotoxicity in a dose-dependent manner at concentrations between 20 μM and 50 μM. However, it had no significant protective effect against neurotoxicity below 15 μM. Mechanistically, the protective effect of **586** was related to the prevention of ROS production, glutathione depletion, and active Fe^{2+} iron accumulation. **586** upregulated the expression of genes involved in antioxidant defense, including GPx4, CAT, SOD2, Nrf2, HMOX1 and SLC7A11. The activation of Nrf2 and HO-1 might play an important role in the neuroprotective effect of **586** against oxidative stress (Wen et al. 2020). A brief summary of the neuroprotective mechanisms of the active ingredients was listed in Table 7..

Anti-diabetic and anti-obesity activity

(3,5,4′-trihydroxy-8,3′-dimethoxy-7-(3-methylbut-2-enoxy) flavone (**121**), a 7-*O*-prenylated flavonoid from the leaves of *Melicope lunuankenda*, induces insulin release by acting on pancreatic β-cells in STZ-induced diabetic rats. It ameliorated the derailed blood glucose levels, liver glycogen, and serum biological parameters at a dose of 10 mg/kg in STZ-induced diabetic rats. In vitro, **121** induced insulin release in RIN 5 F cells, which supported its action on pancreatic β-cells. Moreover, **121** did not show any conspicuous toxic symptoms at a dose of 500 mg/kg in the acute toxicity test. (George et al. 2015). **949** stimulated glucose uptake through the AMPK pathway in L6 myotubes. It increased glucose uptake accompanied by the translocation of GLUT4 to the plasma membrane. **949** required at least 4 h to increase glucose uptake, whereas it significantly decreased glycogen and increased lactic acid within 15 min. The **949**-induced glucose uptake was abrogated by an AMPK inhibitor or siRNA. However, the inhibitors of PI3K and Akt did not block this progress. Therefore, **949** alleviated the effect of glucose intolerance by AMPK-dependent GLUT4 translocation in the plasma membrane of mouse skeletal muscle (Sawada et al. 2014). **579** had anti-obesity benefits. It decreased the production of dysfunctional fatty acid oxidation and ROS, through mitochondrial uncoupling and stress response induction, and inhibited respiration in a ROS-dependent manner at higher concentrations (Kirkwood et al. 2013). **579** also significantly decreased plasmic purine metabolites, glucose levels, energy metabolites, and body weight in vivo (Legette et al. 2013; Paraiso et al. 2021). The seed extract of *Psoralea corylifolia* was rich in prenylated flavonoids, which reduced body weight and fat mass in a dose-dependent manner. It prevented obesity by increasing browning and activating thermogenic genes to increase energy expenditure and stimulating thermogenesis in subcutaneous white adipose tissue and brown adipose tissue. It induced browning in white adipose tissue, increased p-AMPKα1/2 and p38, and increased brown adipose tissue activity and the differentiation of 3T3-L1 cells by increasing the expression of uncoupling protein 1 and other thermogenic genes. In addition, it improved insulin sensitivity and prevented hepatic steatosis by increasing lipid oxidation and secretion in HFD-fed mice

Table 6 Anti-inflammatory mechanism of active ingredients

No	Ingredient	Models	Result/Mechanism	References
169	Artocarpin	Male hairless mice	↓ROS, TNF-α and IL-1β, COX-2, cPLA2	Lee et al. (2013)
		C57BL/6 mice, human fibroblast, human keratinocyte, HUVEC cells	↑α-SMA, ↓C5/C5a, TIMP-1, MCP-1, MIP-1α, MIP-2, IL-16, and IL-1β, ↑collagen I, ↑collagen III on day 7, ↑TGF-β, ↑α-SMA, ↑p-p38 and p-JNK, ↑co-localization of p38 or JNK and vimentin, ↑Akt, ERK and p38 in keratinocytes, ↑co-localization of phosphorylated ERK or p38 and CK14, ↑CD31, ↑phosphorylated of Akt, ERK, and p38 in HUVECs, ↑co-localization of phosphorylated Akt or p38 and CD31 in HUVECs Negative results: Akt and ERK in human fibroblast, JNK in HUVECs	Yeh et al. (2017)
190	10-oxomornigrol F	RAW264.7 cells	↓NO, IL-1β, IL-6, and TNF-α, ↓protein and mRNA of iNOS and COX-2, ↓mRNA of IL-6 and TNF-α, ↑protein and mRNA of HO-1, ↑mRNA of NQO1 and GCLC, ↑Nrf2, ↑p-p38 MAPK. Negative results: ERK1/2, JNK, Akt	Tran et al. (2018)
228	Cudraflavone B	THP-1 cells, COX-1, COX-2 enzyme	↓mRNA of TNF-α, ↓COX-1, ↓COX-2, ↑ZFP36 ↓chemokine CCL2, ↓iNOS, ↓PGE2	Hošek et al. (2011)
275	Cudraflavanone B	RAW264.7 and BV2 cells	↓IL-6 and TNF-α, ↓iNOS, COX-2, ↓p-IκBα, ↓translocation of NF-κB p65, ↓ERK	Ko et al. (2021)
286	Sophoraflavanone M	RAW264.7 cells, mouse peritoneal macrophage	↓NO, ↓iNOS activity, ↓protein and mRNA of iNOS, IL-6, TNF-α, and MCP-1, ↓p-IκBα, ↓translocation of NF-κB p65, ↓JNK, ↓AP-1 Negative results: ERK and p38	Han et al. (2021)
416	Neougonin A	RAW 264.7 Macrophage	↓NO, ↓iNOS, ↓COX-2, ↓PGE2, ↓TNF-α, IL-1β, and IL-6, ↓ERK1/2, JNK, and p38 MAPK, ↓p-IkBα, ↓p-p65	Cao et al. (2016)
472	Cudraflavanone D	BV2 Microglial cells	↓TNF-α, IL-1β, IL-6, IL-12, ↓COX-2, ↓p-IkBα, ↓translocation of p50 and p65, ↓p-JNK and p38 Negative results: p-ERK	Kim et al. (2016)
523	Kushenol C	RAW 264.7 and HaCaT cells	↓NO, iNOS, PGE2, IL-6, IL-1β, IFN-β, and MCP-1, ↓p-STAT1, p-STAT6, ↑SIRT1, ↓p-NF-κB, NF-κB-DNA binding activity, ↑HO-1, ↓Nrf2 and ↑Nrf2 DNA binding activity in LPS-treated RAW264.7 cells, ↓ROS, ↑GSH, SOD, catalase, ↑Nrf2 and p-Akt in HaCaT cells	Cho et al. (2020)
527	Sophoraflavanone G	RAW264.7 cells	↓NO, PGE2, ↓protein and mRNA of iNOS, COX-2, TNF-α, IL-6, and IL-1β, ↓p-Akt, p-PI3K, ↓p-STAT3, p-JAK, ↑HO-1, ↑nuclear translocation of Nrf2, ↓Keap1. Negative results: PIAS1 and PIAS3	Guo et al. (2016a).
		Adult male BALB/C mice	↓IL-6, IL-1β, TNF-α, ↑5-HT, ↓noradrenaline, ↑p-PI3K, p-Akt, p-mTOR, p-P70S6K, BDNF, Trkb, PSD95, GluR1 Negative results: JNK, and p38	Wang et al. (2020b)
	SPF1	RAW264.7 cells, Male C57BL/6J mice	↓mRNA of IL-1β, IL-6, TNF-α, iNOS, and COX-2, ↑RXR/LXR heterodimer if combination of SPF1 and LXR agonist, ↑mRNA of ATF3 in RAW264.7 cells without LPS, ↓translocation of p65 Negative results: mRNA of ATF3 in LPS-treated RAW264.7 cells	Wang et al. (2019)

Table 6 (continued)

No	Ingredient	Models	Result/Mechanism	References
579	Xanthohumol	HaCaT cells, HUVECs (STZ)-induced diabetic rat	↑Nrf2, ↑TrxR1, ↑HO-1, ↑SOD1, ↑p-AMPKα Negative results: ERK, Akt	Lu et al. (2022)
		Adult BALB/c male mice	↓TNF-α, IL-6, and IL-1β, ↓Iba-1, GFAP, p-NF-κB, ↓ROS in serum, ↓NO and MDA in hippocampus, ↑Nrf2 and HO-1, ↓caspase-3	Rahman et al. (2021)

(Liu et al. 2019a). A brief summary of the anti-diabetic and anti-obesity mechanisms of the active ingredients was listed in Table 7..

Cardioprotective activity

26 ameliorated left ventricular dysfunction and cardiac remodeling by downregulating the activity of MMP-2 and MMP-9 in rats with congestive heart failure. It could alleviate apoptosis by regulating the Bcl-2/Bax axis, inhibiting the levels of TNF-α, noradrenaline, angiotensin II and brain natriuretic peptide, and blocking the expression and activity of MMP-2 and MMP-9 (Song et al. 2011). **26** protected cardiomyocytes and apoptosis by inhibiting the JNK and p38 pathways. It prevented the phosphorylation of JNK and p38 and the protein expression levels of Bax and cleaved caspase-3 in Ang II-treated H9c2 cells but upregulated the expression of Bcl-2 (Zhou et al. 2014). **579** inhibited TGF-β1-induced cardiac fibroblast activation by mediating the PTEN/Akt/mTOR pathway. It inhibited the TGF-β1-induced proliferation, differentiation, and collagen overproduction of cardiac fibroblasts by inducing the expression of PTEN and phosphorylation of Akt and mTOR (Jiang et al. 2020). Moreover, **579** exerted a cardioprotective effect by upregulating PTEN expression and inhibiting the phosphorylation of Akt/mTOR in vivo (Sun et al. 2021). **579** was also identified as a cholesteryl ester transfer protein inhibitor that regulates cholesterol transfer between lipoproteins, leading to an increase in HDL cholesterol levels and decreasing the risk of atherosclerosis (Hirata et al. 2012). A brief summary of the cardioprotective mechanisms of the active ingredients is listed in Table 7..

Anti-osteoclastogenesis activity

26 inhibited osteoclastogenesis through the regulation of the RANKL-mediated MAPK/TRAF6/NF-κB/ERK signaling pathway and suppressed the activation of the p38 and JNK pathways. **26** suppressed bone resorption, ERK phosphorylation, IL-6, TNF-α, HIF-1α, and COX-2 and PGE_2 synthesis. **26** also reduced the size of osteoclast formation and diminished the activity of TRAP and ACP (Hsieh et al. 2011; Kim et al. 2018a). **579** inhibited osteoclastogenesis by modulating the RANKL signaling pathway. It inhibited multinucleated osteoclast formation and transcription factor expression of c-Fos and NFATc1 and suppressed RANKL-induced expression of TRAF6, GAB2, ERK, c-Src, PI3K, and Akt genes, as well as RANKL-induced activity of TRAP (Suh et al. 2013). On the other hand, it stimulated osteoblast differentiation through the p38 MAPK and ERK signaling pathways by modulating ALP activity and the expression of RUNX2 in a mesenchymal stem cell line (Jeong et al. 2011). A brief summary of the anti-osteoclastogenesis mechanisms of the active ingredients was listed in Table 7..

Other activities

949 inhibited dexamethasone-induced muscle atrophy via directly binding to the glucocorticoid receptor and inhibiting nuclear translocation of the glucocorticoid receptor. Moreover, **949** inhibited dexamethasone-induced phosphorylation of p38 and FoxO3a (Yoshioka et al. 2019).

492 exerted its antifungal activity on biofilms due to its antioxidant activity. It inhibited *Candida albicans* strain fluconazole-sensitive and *C. albicans* strain azole-resistant biofilms, with a prooxidant effect leading to the accumulation of endogenous oxidative metabolites and increased antioxidant defenses. COMSTAT analysis showed that biofilms treated with higher concentrations exhibited different diffusion distances that could change the flow inside the biofilm matrix (Peralta et al. 2018).

579 inhibited porcine reproductive and respiratory syndrome virus proliferation and decreased viral-induced oxidative stress by activating the Nrf2–HMOX1 pathway. It stimulated genes associated with the antioxidant response in the Nrf2 signaling pathway and upregulated the expression of Nrf2, HMOX1, GCLC, GCLM, and NQO1 in marc-145 cells (Liu et al. 2019b).

Safety

281 display none or remarkably low toxic effect on various non-cancerous cells (Krajnović et al. 2019). **579** exhibited a good safety profile without adverse effects on major organ function and homoeostasis and hepatotoxic effects in mice

Table 7 Other mechanism of active ingredients

Disease	No	Ingredient	models	Result/Mechanism	References
Neuroprotective activity	**26**	Icariin	Sprague–Dawley rat	↓LDH release, ↓caspase-3, ↓p38 MAPK Negative results: JNK1, ERK1/2	Zhu et al. (2010)
		Male Kunming mice	↑SIRT1 and PGC-1α, ↓ACh, ↑ChAT mRNA, ↑p-CREB	Liu et al. (2011) Wang et al. (2013)	
579	Xanthohumol	Male Sprague-Dawley rat	↓4-AP-evoked glutamate release, ↓intrasynaptosomal Ca^{2+}, ↓$Ca_v2.2$ and $Ca_v2.1$ channels, ↓mEPSCs. Negative results: synaptosomal membrane potential, G-proteins	Chang et al. (2016)	
		Male Wistar rat	↓Infarct volume, ↓TNF-α, ↓caspase-3, ↓HIF-1α, ↓iNOS, ↓platelet aggregation, ↓hydroxyl radical formation	Yen et al. (2012)	
586610	Morachalcone D morachalcone E	HT22 cells	Oxytosis and ferroptosis, ↓glutamate-induced oxytosis, ↓erastin-induced ferroptosis, ↓endogenous oxidative stress, ↓ROS, ↓GSH depletion, ↓accumulation of active Fe^{2+} ions, ↑GPx4, ↑CAT, ↑SOD2, ↑Nrf2, ↑HMOX1, ↑SLC7A11	Wen et al. (2020)	
Inhibit osteoclasts differentiation	**26**	Icariin	Osteoblasts cells, bone marrow cells	↓RANKL, ↑OPG, ↓protein and mRNA of IL-6 and TNF-α, ↓PGE2, COX-2, ↓ERK1/2, IκBα and p-p38 in osteoblasts, ↓p38 and JNK in osteoclasts co-culture, ↓HIF-1α	Hsieh et al. (2011)
		Raw264.7 cells	↓Osteoclast formation, ↓NF-κB activation, ↓IκBα degradation, ↓TRAF6, ↓p-ERK, ↓NFATc1, ↓c-Fos, RANK, TRAP, and Atp6v0d2 Negative results: p-JNK, p-p38, and p-Akt	Kim et al. (2018a)	
579	Xanthohumol	RAW264.7 cells	↓Osteoclast differentiation and function, ↓TRAF6 and GAB2, ↓ERK1, ↓c-Fos, NFATc1, ↓c-Src, PI3K, and Akt2, ↓carbonic anhydrase II, TCIRG, OSTM1, and CLCN7, ↓cathepsin K and MMP-9	Suh et al. (2013)	
Stimulates osteoblast differentiation	**579**	Xanthohumol	MC3T3-E1 and C2C12 cells, mouse preosteoblast cells and mouse mesenchymal stem cells	↑osteogenic differentiation, ↑ALP, collagen type Iα, BSP, OC, RUNX2, and Dlx5, ↑p-ERK and p-p38 MAPK,	Jeong et al. (2011)

Table 7 (continued)

Disease	No	Ingredient	models	Result/Mechanism	References
Cardioprotective	**26**	Icariin	Male Sprague–Dawley rat	↓TNF-α, noradrenaline, Ang II, and BNP, ↓MMP-2 and MMP-9 mRNA, ↓Bax, ↓cleaved caspase-3 and caspase-3 activity	Song et al. (2011)
			H9c2 cardiomyocyte	↓ANP and BNP in response to Ang II, ↓Ang II stimulation, ↓Bax and cleaved-caspase 3, ↑Bcl-2, ↓Ang II-induced ROS, ↓p-JNK and p-p38	Zhou et al. (2014)
579	Xanthohumol	Male Sprague-Dawley rat		↓Protein and mRNA of α-SMA, ↑Collagen-I and -III, ↓p-Smad3, ↑PTEN, ↓p-Akt, ↓p-mTOR	Jiang et al. (2020)
		Male C57BL/6 mice		↓ANP, ↓BNP, ↓cardiac fibrosis, ↑PTEN, ↓p-Akt, ↓p-mTOR	Sun et al. (2021)
Anti-diabetes	**121**	3,5,4′-trihydroxy-8,3′-dimethoxy-7-(3-methylbut-2-enoxy)flavone	STZ-induced type-2 diabetic rat	↓SGOT, ↓SGPT, ↓ALP, ↓serum urea, ↓total triglycerides, ↓total cholesterol, ↑HDLC,↑serum protein,↑serum insulin	George et al. (2015)
949	Glabridin	L6 myotube/Male ICR mice		↑Glucose uptake, ↑p-AMPK, ↑GLUT4 translocation, ↑p-AS160, ↑CaMKII *in vitro*, ↑p-ACC, ↓FAS	Sawada et al. (2014)
Inhibit muscle atrophy	**949**	Glabridin	C2C12 cells	↓MuRF1 and Cbl-b, ↓translocation of the glucocorticoid receptor, ↓p-FoxO3a, p-p38 Negative results: atrogin-1, FoxO1, mTOR, Akt	Yoshioka et al. (2019)
Antivirus	**579**	Xanthohumol	Marc-145 cells	↓PRRSV replication, ↑Nrf2, ↑HMOX1, ↑GCLC, ↑GCLM, ↑NQO1, ↑TXNIP, ↑TXNRD1, ↓ROS and MDA, ↑SOD and GSH	Liu et al. (2019b)

(Albini et al. 2006; Dorn et al. 2010). A safety study of oral **579** administration was carried out to evaluate the influence on fertility in Sprague Dawley rats. Treatment of **579** (100 mg/kg body weight per day or 0.5% xanthohumol in the diet) by gavage for 28 days did not cause any adverse effects on female reproduction and the development of offspring (Hussong et al. 2005). **820** and **895** can inhibit cancer cell proliferation at < 10 μM with no cytotoxicities to normal cells (Bueno Perez et al. 2013; Venturelli et al. 2016). It is worthy to mention that many functional foods and traditional herbal medicines are rich in prenylated flavonoids, indicating the safety of prenylated flavonoids.

Conclusion

In this review, the research progress on phytochemistry and pharmacological activity of prenylated flavonoids and plant resources in the past decade were comprehensively summarized. Prenylated flavonoids showed great potential in antitumor, anti-inflammatory, neuroprotective, anti-diabetic, anti-obesity, cardioprotective, and anti-osteoclastogenic activities. Due to the presence of the prenyl group, the bioavailability of prenylated flavonoids was improved and they had more potential in drug development than nonprenylated flavonoids. Several studies have confirmed that prenylation can increase the bioactivities of flavonoids. In this review, we made the best possible effort to summarize the available information and evidence. This review could be a useful tool in assisting researchers in discovering the new medicinal value of prenylated flavonoids.

Supplementary Information The online version contains supplementary material available at https://doi.org/10.1007/s12272-023-01443-4.

Acknowledgements The authors are grateful for the National Natural Science Foundation of China. (Grant Numbers: 81603255), grants from National Key Research and Development Program of China. (Grant Numbers: 2022YFC2804204) and High-Level Talent Special Support Plan of Zhejiang Province (Grant Numbers: 2019R52009).

Declarations

Conflict of interest The authors declare that there is no conflict of interest.

References

Abd-Ellatef GEF, Gazzano E, El-Desoky AH, Hamed AR, Kopecka J, Belisario DC, Costamagna C, Marie S, Fahmy MA, Abdel-Hamid SR, Riganti AZ C (2022) Glabratephrin reverses doxorubicin resistance in triple negative breast cancer by inhibiting P-glycoprotein. Pharmacol Res 175:105975. https://doi.org/10.1016/j.phrs.2021.105975

Abdul Lathiff SM, Jemaon N, Abdullah SA, Jamil S (2015) Flavonoids from *Artocarpus anisophyllus* and their bioactivities. Nat Prod Commun 10(3):1934578X1501000305. https://doi.org/10.1177/1934578x1501000305

Abdullah SA, Jamil S, Basar N, Abdul Lathiff SM, Mohd Arriffin N (2017) Flavonoids from the leaves and heartwoods of *Artocarpus lowii* King and their bioactivities. Nat Prod Res 31(10):1113–1120. https://doi.org/10.1080/14786419.2016.1222387

Abdullah I, Phongpaichit S, Voravuthikunchai SP, Mahabusarakam W (2018) Prenylated biflavonoids from the green branches of *Garcinia dulcis*. Phytochem Lett 23:176–179. https://doi.org/10.1016/j.phytol.2017.12.004

Abourashed EA, Abraha A, Khan SI, McCants T, Awan S (2015) Potential of horse apple isoflavones in targeting inflammation and tau protein fibrillization. Nat Prod Commun 10(9):1934578X1501000923. https://doi.org/10.1177/1934578x1501000923

Adam Suleiman MH (2015) Prenylated flavonoids from the stem wood of *Commiphora opobalsamum* (L.) Engl. (Burseraceae). J King Saud Univ Sci 27(1):71–75. https://doi.org/10.1016/j.jksus.2014.04.005

Ahn J, Kim Y-M, Chae H-S, Choi YH, Ahn H-C, Yoo H, Kang M, Kim J, Chin Y-W (2019) Prenylated flavonoids from the roots and rhizomes of *Sophora tonkinensis* and their effects on the expression of inflammatory mediators and proprotein convertase subtilisin/kexin type 9. J Nat Prod 82(2):309–317. https://doi.org/10.1021/acs.jnatprod.8b00748

Akashi T, Sasaki K, Aoki T, Ayabe S, Yazaki K (2009) Molecular cloning and characterization of a cdna for pterocarpan 4-dimethylallyltransferase catalyzing the key prenylation step in the biosynthesis of glyceollin, a soybean phytoalexin[1,[w]]. Plant Physiol 149(2):683–693. https://doi.org/10.1104/pp.108.123679

Akihisa T, Motoi T, Seki A, Kikuchi T, Fukatsu M, Tokuda H, Suzuki N, Kimura Y (2012) Cytotoxic activities and anti-tumor-promoting effects of microbial transformation products of prenylated chalcones from *Angelica keiskei*. Chem Biodivers 9(2):318–330. https://doi.org/10.1002/cbdv.201100255

Albini A, Dell'Eva R, Venè R, Ferrari N, Buhler DR, Noonan DM, Fassina G (2006) Mechanisms of the antiangiogenic activity by the hop flavonoid xanthohumol: NF-κB and akt as targets. FASEB J 20:527–529. http://www.fasebj.org/cgi/doi/https://doi.org/10.1096/fj.05-5128fje

Ali MS, Ali MI, Ahmed G, Afza N, Lateef M, Iqbal L, Waffo AFK, Ahmed Z (2012) Potent antioxidant and lipoxygenase inhibitory flavanone and chalcone from *Erythrina mildbraedii* Harms (Fabaceae) of cameroon. Z Naturforsch B 67(1):98–102. https://doi.org/10.1515/znb-2012-0116

Anh HLT, Tuan DT, Trang DT, Tai BH, Nguyen XN, Yen PH, Kiem PV, Minh CV, Duc TM, Kang HK, Kim YC, Kim YH (2017) Prenylated isoflavones from *Cudrania tricuspidata* inhibit NO production in RAW 264.7 macrophages and suppress HL-60 cells proliferation. J Asian Nat Prod Res 19(5):510–518. https://doi.org/10.1080/10286020.2016.1232253

Araya-Cloutier C, Vincken J-P, van de Schans MGM, Hageman J, Schaftenaar G, den Besten HMW, Gruppen H (2018) QSAR-based molecular signatures of prenylated (iso)flavonoids underlying antimicrobial potency against and membrane-disruption in Gram positive and Gram negative bacteria. Sci Rep 8(1):1–14. https://doi.org/10.1038/s41598-018-27545-4

Ateba SB, Njamen D, Ukowitz K, Zehl M, Kählig H, Hobiger S, Jungbauer A, Krenn L (2016) New flavonoids from the underground parts of *Eriosema laurentii*. Phytochem Lett 18:144–149. https://doi.org/10.1016/j.phytol.2016.10.003

Atilaw Y, Muiva-Mutisya L, Bogaerts J, Duffy S, Valkonen A, Heydenreich M, Avery VM, Rissanen K, Erdélyi M, Yenesew A (2020) Prenylated Flavonoids from the roots of Tephrosia rhodesica.

J Nat Prod 83(8):2390–2398. https://doi.org/10.1021/acs.jnatprod.0c00245
Bao S, Luo L, Wan Y, Xu K, Tan G, Fan J, Li S-M, Yu X (2021) Regiospecific 7-*O*-prenylation of anthocyanins by a fungal prenyltransferase. Bioorg Chem 110:104787. https://doi.org/10.1016/j.bioorg.2021.104787
Bartmańska A, Tronina T, Poplonski J, Milczarek M, Filip-Psurska B, Wietrzyk J (2018) Highly cancer selective antiproliferative activity of natural prenylated flavonoids. Molecules 23(11):29221–292214. https://doi.org/10.3390/molecules23112922
Bartmańska A, Tronina T, Poplonski J (2019) Biotransformation of a major beer prenylflavonoid - isoxanthohumol. Z naturforsch C. J Biosci 74(1–2):1–7. https://doi.org/10.1515/znc-2018-0101
Belofsky G, Aronica M, Foss E, Diamond J, Santana F, Darley J, Dowd PF, Coleman CM, Ferreira D (2014) Antimicrobial and antiinsectan phenolic metabolites of *Dalea searlsiae*. J Nat Prod 77(5):1140–1149. https://doi.org/10.1021/np401083g
Bocquet L, Sahpaz S, Bonneau N, Beaufay C, Mahieux S, Samaillie J, Roumy V, Jacquin J, Bordage S, Hennebelle T, Chai F, Quetin-Leclercq J, Neut C, Rivière C (2019) Phenolic compounds from *Humulus lupulus* as natural antimicrobial products: new weapons in the fight against methicillin resistant *Staphylococcus aureus, Leishmania mexicana* and *Trypanosoma brucei* strains. Molecules 24(6):1024. https://doi.org/10.3390/molecules24061024
Boozari M, Nejad Ebrahimi S, Soltani S, Tayarani-Najaran Z, Emami SA, Asili J, Iranshahi M (2019a) Absolute configuration and anti-cancer effect of prenylated flavonoids and flavonostilbenes from *Sophora pachycarpa*: possible involvement of wnt signaling pathway. Bioorg Chem 85:498–504. https://doi.org/10.1016/j.bioorg.2019.01.051
Boozari M, Soltani S, Iranshahi M (2019) Biologically active prenylated flavonoids from the genus *Sophora* and their structure-activity relationship-a review. Phytother Res 33(3):546–560. https://doi.org/10.1002/ptr.6265
Bueno Perez L, Li J, Lantvit DD, Pan L, Ninh TN, Chai H-B, Soejarto DD, Swanson SM, Lucas DM, Kinghorn AD (2013) Bioactive constituents of *Indigofera spicata*. J Nat Prod 76(8):1498–1504. https://doi.org/10.1021/np400567c
Cao L, Li R, Chen X, Xue Y, Liu D (2016) Neougonin A inhibits lipopolysaccharide-induced inflammatory responses via down-regulation of the NF-κB signaling pathway in RAW 264.7 macrophages. Inflammation 39(6):1939–1948. https://doi.org/10.1007/s10753-016-0429-9
Cao Y-G, Zheng X-K, Yang F-F, Li F, Qi M, Zhang Y-L, Zhao X, Kuang H-X, Feng W-S (2018) Two new phenolic constituents from the root bark of *Morus alba* L. and their cardioprotective activity. Nat Prod Res 32(4):391–398. https://doi.org/10.1080/14786419.2017.1309535
Carvalho DO, Freitas J, Nogueira P, Henriques SN, Carmo AM, Castro MA, Guido LF (2018) Xanthohumol inhibits cell proliferation and induces apoptosis in human thyroid cells. Food Chem Toxicol 121:450–457. https://doi.org/10.1016/j.fct.2018.09.021
Chang Y, Lin TY, Lu CW, Huang SK, Wang YC, Wang SJ (2016) Xanthohumol-induced presynaptic reduction of glutamate release in the rat hippocampus. Food Funct 7(1):212–226. https://doi.org/10.1039/c5fo01005e
Chang Y-S, Jin H-G, Lee H, Lee D-S, Woo E-R (2019) Phytochemical constituents of the root bark from *Morus alba* and their Il-6 inhibitory activity. Nat Prod Sci 25(3):268–274. https://doi.org/10.20307/nps.2019.25.3.268
Chen L, Duan Y, Li C, Wang Y, Tong X, Dai Y, Yao X (2013) Four new prenylated flavonoids from the roots of *Cudrania tricuspidata*. Magn Reson Chem 51(12):842–846. https://doi.org/10.1002/mrc.4020
Chen R, Xiao L, Zou J, Yin Y, Ou B, Li J, Wang R, Xie D, Zhang P, Dai J (2013) Regio- and stereospecific prenylation of flavonoids by *Sophora flavescens*. prenyltransferase Adv Synthesis Catal 355(9):1817–1828. https://doi.org/10.1002/adsc.201300196
Chen R, Gao B, Liu X, Ruan F, Zhang Y, Lou J, Feng K, Wunsch C, Li S-M, Dai J, Sun F (2016) Molecular insights into the enzyme promiscuity of an aromatic prenyltransferase. Nat Chem Biol 13:226–234. https://doi.org/10.1038/nchembio.2263
Chen Y, Zhao J, Qiu Y, Yuan H, Khan SI, Hussain N, Iqbal Choudhary M, Zeng F, Guo D-A, Khan IA, Wang W (2017) Prenylated flavonoids from the stems and roots of *Tripterygium wilfordii*. Fitoterapia 119:64–68. https://doi.org/10.1016/j.fitote.2017.04.003
Chien TV, Nguyen TA, Nguyen TT, Thao TTP, Loc TV, Sung TV (2019) Two new prenylated isoflavones from *Maclura cochinchinensis* collected in Hoa Binh province Vietnam. Nat Prod Res 33(2):212–218. https://doi.org/10.1080/14786419.2018.1443096
Cho H-D, Lee J-H, Moon K-D, Park K-H, Lee M-K, Seo K-I (2018) Auriculasin-induced ROS causes prostate cancer cell death via induction of apoptosis. Food Chem Toxicol 111:660–669. https://doi.org/10.1016/j.fct.2017.12.007
Cho BO, Che DN, Kim JS, Kim JH, Shin JY, Kang HJ, Jang SI (2020) *In vitro* anti-inflammatory and anti-oxidative stress activities of Kushenol C isolated from the roots of *Sophora flavescens*. Molecules. https://doi.org/10.3390/molecules25081768
Cuca-Suarez LE, Della-Monache F, Coy-Barrera E (2015) Cytotoxic constituents from bark and leaves of *Amyris pinnata* Kunth. Rec. Nat Prod 9(3):441–445
Darmawan A, Megawati, Lotulung PDN, Fajriah S, Primahana G, Meiliawati L (2015) A new flavonoid derivative as cytotoxic compound isolated from ethyl acetate extract of *Macaranga gigantifolia* Merr. Leaves. Procedia Chem 16:53–57. https://doi.org/10.1016/j.proche.2015.12.021
Daus M, Chaithada P, Phongpaichit S, Watanapokasin R, Carroll AR, Mahabusarakam W (2017) New prenylated dihydrochalcones from the leaves of *Artocarpus elasticus*. Phytochem Lett 19:226–230. https://doi.org/10.1016/j.phytol.2017.01.007
Derese S, Barasa L, Akala HM, Yusuf AO, Kamau E, Heydenreich M, Yenesew A (2014) 4′-Prenyloxyderrone from the stem bark of *Millettia oblata* ssp. teitensis and the antiplasmodial activities of isoflavones from some *Millettia* species. Phytochem Lett 8:69–72. https://doi.org/10.1016/j.phytol.2014.02.001
Desta ZY, Majinda RRT (2014) Three new isoflavonoids from *Erythrina caffra*. Nat Prod Commun 9(6):817–820. https://doi.org/10.1177/1934578x1400900622
Ding W-J, Zhang S-Q, Wang J-H, Lin Y-X, Liang Q-X, Zhao W-J, Li C-Y (2013) A new di-*O*-prenylated flavone from an actinomycete *Streptomyces* sp. MA-12. J Asian Nat Prod Res 15(2):209–214. https://doi.org/10.1080/10286020.2012.751979
Dizamatova A, Zhumanova K, Zhusupova GE, Zhussupova AI, Srivedavyasasri R, Ibrahim MA, Ross SA (2019) A new prenylated isoflavonoid from *Limonium leptophyllum*. Nat Prod Commun. https://doi.org/10.1177/1934578x19844137
Domínguez-Villegas V, Domínguez-Villegas V, García ML, Calpena A, Clares-Naveros B, Garduño-Ramírez ML (2013) Anti-inflammatory, antioxidant and cytotoxicity activities of methanolic extract and prenylated flavanones isolated from leaves of *Eysehardtia platycarpa*. Nat Prod Commun 8(2):177–180. https://doi.org/10.1007/s12272-015-0612-9
Dorn C, Bataille F, Gaebele E, Heilmann J, Hellerbrand C (2010) Xanthohumol feeding does not impair organ function and homoeostasis in mice. Food Chem Toxicol 48(7):1890–1897. https://doi.org/10.1016/j.fct.2010.04.030
Dzoyem JP, Nkuete AHL, Ngameni B, Eloff JN (2017) Anti-inflammatory and anticholinesterase activity of six flavonoids isolated from *Polygonum* and *Dorstenia* species. Arch Pharm Res 40(10):1129–1134. https://doi.org/10.1007/s12272-015-0612-9
El-Gamal AA, Al-Massarani SM, Abdel-Mageed WM, El-Shaibany A, Al-Mahbashi HM, Basudan OA, Badria FA, Al-Said MS,

Abdel-Kader MS (2017) Prenylated flavonoids from *Commiphora opobalsamum* stem bark. Phytochemistry 141:80–85. https://doi.org/10.1016/j.phytochem.2017.05.014

Etti IC, Rasedee A, Hashim NM, Abdul AB, Kadir A, Yeap SK, Waziri P, Malami I, Lim KL, Etti CJ (2017b) Artonin E induces p53-independent G1 cell cycle arrest and apoptosis through ROS-mediated mitochondrial pathway and livin suppression in MCF-7 cells. Drug Des Devel Ther 11:865–879. https://doi.org/10.2147/DDDT.S124324

Fan Y-H, Ye R, Xu H-Y, Feng X-H, Ma C-M (2019) Structures and *in vitro* antihepatic fibrosis activities of prenylated dihydrostilbenes and flavonoids from *Glycyrrhiza uralensis* Leaves. J Food Sci 84(5):1224–1230. https://doi.org/10.1111/1750-3841.14592

Fareza MS, Syah YM, Mujahidin D, Juliawaty LD, Kurniasih I (2014) Antibacterial flavanones and dihydrochalcones from *Macaranga trichocarpa*. Z Naturforsch C: J Biosci 69(9/10):375–380. https://doi.org/10.5560/znc.2014-0066

Fei W-T, Zhang J-J, Tang R-Y, Yue N, Zhou X, Wang L-Y (2020) Two new prenylated flavonoids from the seeds of *Psoralea corylifolia* with their inhibitory activity on α-glucosidase. Phytochem Lett 39:64–67. https://doi.org/10.1016/j.phytol.2020.07.005

Feng K-P, Chen R-D, Li J-H, Tao X-Y, Liu J-M, Zhang M, Dai J-G (2016) Flavonoids from the cultured cells of *Glycyrrhiza uralensis*. J Asian Nat Prod Res 18(3):253–259. https://doi.org/10.1080/10286020.2015.1074573

Festa M, Capasso A, D′Acunto CW, Masullo M, Rossi AG, Pizza C, Piacente S (2011) Xanthohumol induces apoptosis in human malignant glioblastoma cells by increasing reactive oxygen species and activating MAPK pathways. J Nat Prod 74(12):2505–2513. https://doi.org/10.1021/np200390x

Fongang YSF, Bankeu JJK, Ali MS, Awantu AF, Zeeshan A, Assob CN, Mehreen L, Lenta BN, Ngouela SA, Tsamo E (2015) Flavonoids and other bioactive constituents from *Ficus thonningii* Blume (Moraceae). Phytochem Lett 11:139–145. https://doi.org/10.1016/j.phytol.2014.11.012

Fu M, Feng S, Zhang N, Zhou X, Huang R, Huang H, Xu Z, Li X, Qiu SX (2012) A new prenylated isoflavone and a new flavonol glycoside from *Flemingia philippinensis*. Helv Chim Acta 95(4):598–605. https://doi.org/10.1002/hlca.201100360

Gao S, Sun D, Wang G, Zhang J, Jiang Y, Li G, Zhang K, Wang L, Huang J, Chen L (2016) Growth inhibitory effect of paratocarpin E, a prenylated chalcone isolated from *Euphorbia humifusa* Wild., by induction of autophagy and apoptosis in human breast cancer cells. Bioorg Chem 69:121–128. https://doi.org/10.1016/j.bioorg.2016.10.005

Gbaweng AJY, Daïrou H, Zingué S, Emmanuel T, Tchinda AT, Frédérich M, Mbafor JT (2020) Excelsanone, a new isoflavonoid from *Erythrina excelsa* (Fabaceae), with *in vitro* antioxidant and *in vitro* cytotoxic effects on prostate cancer cells lines. Nat Prod Res 34(5):659–667

George S, Ajikumaran Nair S, Johnson AJ, Venkataraman R, Baby S (2015) *O*-prenylated flavonoid, an antidiabetes constituent in *Melicope lunu-ankenda*. J Ethnopharmacol 168:158–163. https://doi.org/10.1016/j.jep.2015.03.060

Grienke U, Richter M, Walther E, Hoffmann A, Kirchmair J, Makarov V, Nietzsche S, Schmidtke M, Rollinger JM (2016) Discovery of prenylated flavonoids with dual activity against influenza virus and Streptococcus pneumoniae. Sci Rep 6:27156. https://doi.org/10.1038/srep27156

Gumula I, Heydenreich M, Derese S, Ndiege IO, Yenesew A (2012) Four isoflavanones from the stem bark of *Platycelphium voense*. Phytochem Lett 5(1):150–154. https://doi.org/10.1016/j.phytol.2011.11.012

Guo C, Yang L, Luo J, Zhang C, Xia Y, Ma T, Kong L (2016a) Sophoraflavanone G from *Sophora alopecuroides* inhibits lipopolysaccharide-induced inflammation in RAW264.7 cells by targeting PI3K/Akt, JAK/STAT and Nrf2/HO-1 pathways. Int Immunopharmacol 38:349–356. https://doi.org/10.1016/j.intimp.2016.06.021

Guo Z, Li X, Li J, Yang X, Zhou Y, Lu C, Shen Y (2016b) Licoflavonol is an inhibitor of the type three secretion system of Salmonella enterica serovar Typhimurium. Biochem Biophys Res Commun 477(4):998–1004. https://doi.org/10.1016/j.bbrc.2016.07.018

Han F, Lee I-S (2017) A new flavonol glycoside from the aerial parts of *Epimedium koreanum*. Nakai Nat Prod Res 31(3):320–325. https://doi.org/10.1080/14786419.2016.1239092

Han Y, Zhang X, Kang Y, Gao Y, Li X, Qi R, Cai R, Qi Y (2021) Sophoraflavanone M, a prenylated flavonoid from *Sophora flavescens* Ait., suppresses pro-inflammatory mediators through both NF-kappaB and JNK/AP-1 signaling pathways in LPS-primed macrophages. Eur J Pharmacol 907:174246. https://doi.org/10.1016/j.ejphar.2021.174246

Hanáková Z, Hošek J, Babula P, Dall′Acqua S, Václavík J, Šmejkal K (2015) *C*-Geranylated flavanones from *Paulownia tomentosa* fruits as potential anti-inflammatory compounds acting via inhibition of TNF-α production. J Nat Prod 78(4):850–863. https://doi.org/10.1021/acs.jnatprod.5b00005

Hanáková Z, Hošek J, Kutil Z, Temml V, Landa P, Vaněk T, Schuster D, Dall'Acqua S, Cvačka J, Polanský O, Šmejkal K (2017) Anti-inflammatory activity of natural geranylated flavonoids: cyclooxygenase and lipoxygenase inhibitory properties and proteomic analysis. J Nat Prod 80(4):999–1006. https://doi.org/10.1021/acs.jnatprod.6b01011

Harish V, Haque E, Smiech M, Taniguchi H, Jamieson S, Tewari D, Bishayee A (2021) Xanthohumol for human malignancies: Chemistry, pharmacokinetics and molecular targets. Int J Mol Sci 22(9):4478. https://doi.org/10.3390/ijms22094478

He Q-F, Wu Z-L, Huang X-J, Zhong Y-L, Li M-M, Jiang R-W, Li Y-L, Ye W-C, Wang Y (2018) Cajanusflavanols A – C, three pairs of flavonostilbene enantiomers from *Cajanus cajan*. Org Lett 20:876–879. https://doi.org/10.1021/acs.orglett.8b00010

Herlina T, Aloanis AA, Kurnia D, Harneti D, Maharani R, Supratman U (2017) Prenylated isoflavanones from the stem bark of *Erythrina poeppigiana* (Leguminosae) and its Antimalarial Properties. Nat Prod Commun 12(8):1934578X1701200825. https://doi.org/10.1177/1934578x1701200825

Hiep NT, Kwon J, Kim D-W, Hwang BY, Lee H-J, Mar W, Lee D (2015) Isoflavones with neuroprotective activities from fruits of *Cudrania tricuspidata*. Phytochemistry 111:141–148. https://doi.org/10.1016/j.phytochem.2014.10.021

Higa M, Imamura M, Shimoji K, Ogihara K, Suzuka T (2012) Isolation of six new flavonoids from *Melicope triphylla*. Chem Pharm Bull 60(9):1112–1117. https://doi.org/10.1248/cpb.c12-00213

Hikita K, Yamada S, Shibata R, Katoh M, Murata T, Kato K, Tanaka H, Kaneda N (2015) Inhibitory effect of isoflavones from *Erythrina poeppigiana* on the growth of HL-60 human leukemia cells through inhibition of glyoxalase I. Nat Prod Commun 10(9):1934578X1501000924. https://doi.org/10.1177/1934578x1501000924

Hirata H, Takazumi K, Segawa S, Okada Y, Kobayashi N, Shigyo T, Chiba H (2012) Xanthohumol, a prenylated chalcone from *Humulus lupulus* L. inhibits cholesteryl ester transfer protein. Food Chem 134(3):1432–1437. https://doi.org/10.1016/j.foodchem.2012.03.043

Ho K-H, Kuo T-C, Lee Y-T, Chen P-H, Shih C-M, Cheng C-H, Liu A-J, Lee C-C, Chen K-C (2020) Xanthohumol regulates miR-4749-5p-inhibited RFC2 signaling in enhancing temozolomide cytotoxicity to glioblastoma. Life Sci 254:117807. https://doi.org/10.1016/j.lfs.2020.117807

Hošek J, Bartos M, Chudík S, Dall′Acqua S, Innocenti G, Kartal M, Kokoška L, Kollár P, Kutil Z, Landa P, Marek R, Závalová V, Žemlička M, Šmejkal K (2011) Natural compound

cudraflavone B shows promising anti-inflammatory properties *in vitro*. J Nat Prod 74(4):614–619. https://doi.org/10.1021/np100638h

Hossain MA, Mizanur Rahman SM (2015) Isolation and characterisation of flavonoids from the leaves of medicinal plant *Orthosiphon stamineus*. Arab J Chem 8(2):218–221. https://doi.org/10.1016/j.arabjc.2011.06.016

Hsieh T-P, Sheu S-Y, Sun J-S, Chen M-H (2011) Icariin inhibits osteoclast differentiation and bone resorption by suppression of MAPKs/NF-κB regulated HIF-1α and PGE_2 synthesis. Phytomedicine 18(2–3):176–185. https://doi.org/10.1016/j.phymed.2010.04.003

Hsieh M-J, Lin C-W, Yang S-F, Chen M-K, Chiou H-L (2014) Glabridin inhibits migration and invasion by transcriptional inhibition of matrix metalloproteinase 9 through modulation of NF-κB and AP-1 activity in human liver cancer cells. Br J Pharmacol 171(12):3037–3050. https://doi.org/10.1111/bph.12626

Hu X, Wu J-W, Wang M, Yu M-H, Zhao Q-S, Wang H-Y, Hou A-J (2012) 2-Arylbenzofuran, flavonoid, and tyrosinase inhibitory constituents of *Morus yunnanensis*. J Nat Prod 75(1):82–87. https://doi.org/10.1021/np2007318

Huang Y-L, Shen C-C, Shen Y-C, Chiou W-F, Chen C-C (2017) Anti-inflammatory and antiosteoporosis flavonoids from the rhizomes of *Helminthostachys zeylanica*. J Nat Prod 80(2):246–253. https://doi.org/10.1021/acs.jnatprod.5b01164

Hudcová T, Bryndová J, Fialová K, Fiala J, Karabín M, Jelínek L, Dostálek P (2014) Antiproliferative effects of prenylflavonoids from hops on human colon cancer cell lines. J Inst Brew 120(3):225–230. https://doi.org/10.1002/jib.139

Huong TT, Nguyen XC, Tram LH, Quang TT, Duong LV, Nguyen HN, Nguyen TD, Huong PTT, Diep CN, Kiem PV, Minh CV (2012) A new prenylated aurone from *Artocarpus altilis*. J Asian Nat Prod Res 14(9):923–928. https://doi.org/10.1080/10286020.2012.702758

Huonga DTM, Vu LTN, The Anh L, Cuc NT, Nhiem NX, Tai BH, Van Kiem P, Litaudon M, Dang Thach T, Van Minh C, Pham VC (2019) Cytotoxic prenylated flavonoids from the leaves of *Macaranga indica*. Phytochem Lett 34:39–42. https://doi.org/10.1016/j.phytol.2019.09.001

Hussain N, Adhikari A, Ahmad MS, Wahab AT, Ali M, Choudhary MI (2017) Two new prenylated flavonoids from the roots of *Berberis thunbergii* DC. Nat Prod Res 31(7):785–790. https://doi.org/10.1080/14786419.2016.1244195

Hussong R, Frank N, Knauft J, Ittrich C, Owen R, Becker H, Gerhäuser H (2005) A safety study of oral xanthohumol administration and its influence on fertility in Sprague Dawley rats Molecular Nutrition &. Food Res 49:861–867. https://doi.org/10.1002/mnfr.200500089

IC Etti, R Abdullah, A Kadir, NM Hashim, SK Yeap, MU Imam, F Ramli, I Malami, KL Lam, U Etti, P Waziri, M Rahman (2017) The molecular mechanism of the anticancer effect of artonin E in MDA-MB 231 triple negative breast cancer cells. PLoS ONE 12(8):e0182357

Indran IR, Liang RL, Min TE, Yong EL (2016) Preclinical studies and clinical evaluation of compounds from the genus Epimedium for osteoporosis and bone health. Pharmacol Ther 162:188–205

Inoue M, Hitora Y, Kato H, Losung F, Mangindaan REP, Tsukamoto S (2018) New geranyl flavonoids from the leaves of *Artocarpus communis*. J Nat Med 72(3):632–640. https://doi.org/10.1007/s11418-018-1192-z

Jakimiuk K, Gesek J, Atanasov AG, Tomczyk M (2021) Flavonoids as inhibitors of human neutrophil elastase. J Enzyme Inhib Med Chem 36(1):1016–1028. https://doi.org/10.1080/14756366.2021.1927006

Jeong HM, Han EH, Jin YH, Choi YH, Lee KY, Jeong HG (2011) Xanthohumol from the hop plant stimulates osteoblast differentiation by RUNX2 activation. Biochem Biophys Res Commun 409(1):82–89. https://doi.org/10.1016/j.bbrc.2011.04.113

Ji S, Liang W-F, Li Z-W, Feng J, Wang Q, Qiao X, Ye M (2016) Efficient and selective glucosylation of prenylated phenolic compounds by *Mucor hiemalis*. RSC Adv 6(25):20791–20799. https://doi.org/10.1039/c6ra00072j

Jiang C, Liu S, He W, Luo X, Zhang S, Xiao Z, Qiu X, Yin H (2012) A new prenylated flavanone from *Derris trifoliata* Lour. Molecules 17:657–663. https://doi.org/10.3390/molecules17010657

Jiang C, Xie N, Sun T, Ma W, Zhang B, Li W (2020) Xanthohumol inhibits TGF-β1-induced cardiac fibroblasts activation via mediating PTEN/Akt/mTOR signaling pathway. Drug Des Devel Ther 14:5431–5439. https://doi.org/10.2147/DDDT.S282206

Jo YH, Kim SB, Liu Q, Lee JW, Hwang BY, Lee MK (2015) Benzylated and prenylated flavonoids from the root barks of *Cudrania tricuspidata* with pancreatic lipase inhibitory activity. Bioorg Med Chem Lett 25(17):3455–3457. https://doi.org/10.1016/j.bmcl.2015.07.017

Jo YH, Lee S, Yeon SW, Turk A, Lee JH, Hong S-M, Han YK, Lee KY, Hwang BY, Kim SY, Lee MK (2021) Anti-diabetic potential of *Masclura tricuspidata* leaves: Prenylated isoflavonoids with α-glucosidase inhibitory and anti-glycation activity. Bioorg Chem 114:105098. https://doi.org/10.1016/j.bioorg.2021.105098

Jung J-W, Ko W-M, Park J-H, Seo K-H, Oh E-J, Lee D-Y, Lee D-S, Kim Y-C, Lim D-W, Han D, Baek N-I (2015) Isoprenylated flavonoids from the root bark of *Morus alba* and their hepatoprotective and neuroprotective activities. Arch Pharmacal Res 38(11):2066–2075. https://doi.org/10.1007/s12272-015-0613-8

Kalli S, Araya-Cloutier C, Chapman J, Sanders J-W, Vincken J-P (2022) Prenylated (iso)flavonoids as antifungal agents against the food spoiler *Zygosaccharomyces parabailii*. Food Control 132:108434. https://doi.org/10.1016/j.foodcont.2021.108434

Kamel EM, Mahmoud AM, Ahmed SA, Lamsabhi AM (2016) A phytochemical and computational study on flavonoids isolated from *Trifolium resupinatum* L. and their novel hepatoprotective activity. Food Funct 7(4):2094–2106. https://doi.org/10.1039/c6fo00194g

Kang W-J, Li D-H, Han T, Sun L, Fu Y-B, Sai C-M, Li Z-L, Hua H-M (2016) New chalcone and pterocarpoid derivatives from the roots of *Flemingia philippinensis* with antiproliferative activity and apoptosis-inducing property. Fitoterapia 112:222–228. https://doi.org/10.1016/j.fitote.2016.06.003

Khamthong N, Hutadilok-Towatana N (2017) Phytoconstituents and biological activities of *Garcinia Dulcis* (Clusiaceae): a review. Nat Prod Commun 12(3):1934578X1701200337. https://doi.org/10.1177/1934578x1701200337

Kim D-C, Yoon C-S, Quang TH, Ko W, Kim J-S, Oh H, Kim Y-C (2016) Prenylated flavonoids from *Cudrania tricuspidata* suppress lipopolysaccharide-induced neuroinflammatory activities in BV2 microglial cells. Int J Mol Sci 17(2):255. https://doi.org/10.3390/ijms17020255

Kim JH, Cho CW, Kim HY, Kim KT, Choi G-S, Kim H-H, Cho IS, Kwon SJ, Choi S-K, Yoon J-Y, Yang SY, Kang JS, Kim YH (2017) α-Glucosidase inhibition by prenylated and lavandulyl compounds from *Sophora flavescens* roots and *in silico* analysis. Int J Biol Macromol 102:960–969. https://doi.org/10.1016/j.ijbiomac.2017.04.092

Kim B, Lee KY, Park B (2018a) Icariin abrogates osteoclast formation through the regulation of the RANKL-mediated TRAF6/NF-κB/ERK signaling pathway in Raw264.7 cells. Phytomedicine 51:181–190. https://doi.org/10.1016/j.phymed.2018.06.020

Kim JY, Wang Y, Uddin Z, Song YH, Li ZP, Jenis J, Park KH (2018b) Competitive neutrophil elastase inhibitory isoflavones from the

roots of *Flemingia philippinensis*. Bioorg Chem 78:249–257. https://doi.org/10.1016/j.bioorg.2018.03.024

Kim E, Kim Y-M, Ahn J, Chae H-S, Chin Y-W, Kim J (2021) Prenylated flavonoid glycosides with PCSK9 mRNA expression inhibitory activity from the aerial parts of *Epimedium koreanum*. Molecules 26(12):3590. https://doi.org/10.3390/molecules26123590

Kirkwood JS, Legette LL, Miranda CL, Jiang Y, Stevens JF (2013) A metabolomics-driven elucidation of the anti-obesity mechanisms of xanthohumol. J Biol Chem 288(26):19000–19013. https://doi.org/10.1074/jbc.M112.445452

Kırmızıbekmez H, Uysal GB, Masullo M, Demirci F, Bağcı Y, Kan Y, Piacente S (2015) Prenylated polyphenolic compounds from *Glycyrrhiza iconica* and their antimicrobial and antioxidant activities. Fitoterapia 103:289–293. https://doi.org/10.1016/j.fitote.2015.05.003

Ko W, Kim K-W, Quang T-H, Yoon C-S, Kim N, Lee H, Kim S-C, Woo E-R, Kim Y-C, Oh H, Lee D-S (2021) Cudraflavanone B isolated from the root bark of *Cudrania tricuspidata* alleviates lipopolysaccharide-induced inflammatory responses by downregulating NF-κB and ERK MAPK signaling pathways in RAW264.7 macrophages and BV2 microglia. Inflammation 44(1):104–115. https://doi.org/10.1007/s10753-020-01312-y

Koch K, Schulz G, Doring W, Bučhter C, Havermann S, Mutiso PC, Passreiter C, Watjen W (2019) Abyssinone V, a prenylated flavonoid isolated from the stem bark of *Erythrina melanacantha* increases oxidative stress and decreases stress resistance in *Caenorhabditis elegans*. J Pharm Pharmacol 71(6):1007–1016. https://doi.org/10.1111/jphp.13074

Kollar P, Bárta T, Hošek J, Souček K, Závalová VM, Artinian S, Talhouk R, Šmejkal K, Suchý P Jr, Hampl A (2013) Prenylated flavonoids from *Morus alba* L. cause inhibition of G1/S transition in THP-1 human leukemia cells and prevent the lipopolysaccharide-induced inflammatory response. Evid Based Complement Alternat Med 2013

Krajnović T, Drača D, Kaluđerović GN, Dunđerović D, Mirkov I, Wessjohann LA, Maksimović-Ivanić D, Mijatović S (2019) The hop-derived prenylflavonoid isoxanthohumol inhibits the formation of lung metastasis in B16-F10 murine melanoma model. Food Chem Toxicol 129:257–268. https://doi.org/10.1016/j.fct.2019.04.046

Kuete V, Sandjo LP, Djeussi DE, Zeino M, Kwamou GMN, Ngadjui B, Efferth T (2014) Cytotoxic flavonoids and isoflavonoids from *Erythrina sigmoidea* towards multi-factorial drug resistant cancer cells. Invest New Drugs 32(6):1053–1062. https://doi.org/10.1007/s10637-014-0137-y

Kumano T, Richard S-B, Noel J-P, Nishiyama M, Kuzuyama T (2008) Chemoenzymatic syntheses of prenylated aromatic small molecules using streptomyces prenyltransferases with relaxed substrate specificities. Bioorg Med Chem 16:8117–8126. https://doi.org/10.1016/j.bmc.2008.07.052

Kwon M, Jang M, Kim G-H, Oh T, Ryoo I-J, Ryu HW, Oh S-R, Kim BY, Jang J-H, Ko S-K, Ahn JS (2020) Kushenol E inhibits autophagy and impairs lysosomal positioning via VCP/p97 inhibition. Biochem Pharmacol 175:113861. https://doi.org/10.1016/j.bcp.2020.113861

Kyekyeku JO, Kusari S, Adosraku RK, Zühlke S, Spiteller M (2016) Prenylated 2-arylbenzofuran derivatives with potent antioxidant properties from *Chlorophora regia* (Moraceae). Fitoterapia 108:41–47. https://doi.org/10.1016/j.fitote.2015.11.013

Lai W-C, Tsui Y-T, Singab ANB, El-Shazly M, Du Y-C, Hwang T-L, Wu C-C, Yen M-H, Lee C-K, Hou M-F, Wu Y-C, Chang F-R (2013) Phyto-SERM constitutes from *Flemingia macrophylla*. Int J Mol Sci 14(8):15578–15594. https://doi.org/10.3390/ijms140815578

Lan W-C, Tzeng C-W, Lin C-C, Yen F-L, Ko H-H (2013) Prenylated flavonoids from *Artocarpus altilis*: antioxidant activities and inhibitory effects on melanin production. Phytochemistry 89:78–88. https://doi.org/10.1016/j.phytochem.2013.01.011

Lee C-W, Ko H-H, Lin C-C, Chai C-Y, Chen W-T, Yen F-L (2013) Artocarpin attenuates ultraviolet B-induced skin damage in hairless mice by antioxidant and anti-inflammatory effect. Food Chem Toxicol 60:123–129. https://doi.org/10.1016/j.fct.2013.07.029

Lee SM, Song YH, Uddin Z, Ban YJ, Park KH (2017) Prenylated flavonoids from *Epimedium koreanum* Nakai and their human neutrophil elastase inhibitory effects. Rec Nat Prod 11(6):514–520. https://doi.org/10.25135/rnp.66.17.05.090

Lee C-W, Hsu L-F, Lee M-H, Lee I-T, Liu J-F, Chiang Y-C, Tsai M-H (2018) Extracts of *Artocarpus communis* induce mitochondria-associated apoptosis via pro-oxidative activity in human glioblastoma cells. Front Pharmacol 9:411. https://doi.org/10.3389/fphar.2018.00411

Legette LL, Luna AYM, Reed RL, Miranda CL, Bobe G, Proteau RR, Stevens JF (2013) Xanthohumol lowers body weight and fasting plasma glucose in obese male Zucker fa/fa rats. Phytochemistry 91:236–241. https://doi.org/10.1016/j.phytochem.2012.04.018

Lemes BB, da Silva Miguez L, Santos RL, da Rocha Bastos Serafim JC, Figueiredo JMR, Tavares IF, de Godoi Pereira M, de Jesus Marques E, da Silva Ramos F, El-Bacha RS, Ribeiro AI, das Gracas Fernandes da Silva MF, de Souza Neta LC, (2019) Two new prenylated isoflavones from *Deguelia costata*. Phytochem Lett 30:181–185. https://doi.org/10.1016/j.phytol.2019.02.018

Li H, Zhai F, Yang M, Li X, Wang P, Ma X (2012) A new benzofuran derivative from *Flemingia philippinensis* Merr. et Rolfe Molecules 17(7):7637–7644. https://doi.org/10.3390/molecules17077637

Li J, Chen R, Wang R, Liu X, Xie D, Zou J, Dai J (2014) Gua6dt, a regiospecific prenyltransferase from *glycyrrhiza uralensis*, catalyzes the 6-prenylation of flavones. Chembiochem: A Eu J Chem Biol 15:1673–1681. https://doi.org/10.1002/cbic.201402160

Li Y-P, Yang Y-C, Li Y-K, Jiang Z-Y, Huang X-Z, Wang W-G, Gao X-M, Hu Q-F (2014a) Five new prenylated chalcones from *Desmodium renifolium*. Fitoterapia 95:214–219. https://doi.org/10.1016/j.fitote.2014.03.026

Li Y-P, Yang Y-C, Li Y-K, Jiang Z-Y, Huang X-Z, Wang W-G, Gao X-M, Hu Q-F (2014b) Prenylated chalcones from *Desmodium renifolium*. Phytochem Lett 9:41–45. https://doi.org/10.1016/j.phytol.2014.04.003

Li F-F, Sun Q, Wang D, Liu S, Lin B, Liu C-T, Li L-Z, Huang X-X, Song S-J (2016) Chiral separation of cytotoxic flavan derivatives from *Daphne giraldii*. J Nat Prod 79(9):2236–2242. https://doi.org/10.1021/acs.jnatprod.6b00305

Li Y, Wu ZH, Zeng KW, Zhao MB, Jiang Y, Li J, Tu PF (2017) A new prenylated flavone from *Pleione bulbocodioides*. J Asian Nat Prod Res 19(7):738–743. https://doi.org/10.1080/10286020.2017.1311871

Li M, Wu X, Wang X, Shen T, Ren D (2018) Two novel compounds from the root bark of *Morus alba* L. Nat Prod Res 32(1):36–42. https://doi.org/10.1080/14786419.2017.1327862

Lima NM, Cursino LMC, Lima AM, Souza JVB, de Oliveira AC, Marinho JVN, Nunez CV (2018) Antifungal activity of extracts and phenolic compounds from *Deguelia duckeana*. Rev Bras Farmacogn 28(6):697–702. https://doi.org/10.1016/j.bjp.2018.08.004

Liu B, Zhang H, Xu C, Yang G, Tao J, Huang J, Wu J, Duan X, Cao Y, Dong J (2011) Neuroprotective effects of icariin on corticosterone-induced apoptosis in primary cultured rat hippocampal neurons. Brain Res 1375:59–67. https://doi.org/10.1016/j.brainres.2010.12.053

Liu M, Yin H, Qian X, Dong J, Qian Z, Miao J (2016) Xanthohumol, a prenylated chalcone from hops, inhibits the viability and stemness of doxorubicin-resistant MCF-7/ADR cells. Molecules. https://doi.org/10.3390/molecules22010036

Liu F, Hoag H, Wu C, Liu H, Yin H, Dong J, Qian Z, Miao F, Liu M, Miao J (2018a) Experimental and simulation identification of xanthohumol as an inhibitor and substrate of ABCB1. Appl Sci 8(5):681. https://doi.org/10.3390/app8050681. /1-861-11

Liu X, Kuang X-D, He X-R, Ren G, Wang Y, Xu L-Y, Feng L-H, Wang B, Zhou Z-W (2018b) Prenylflavonoids from the twigs of *Artocarpus nigrifolius*. Chem Pharm Bull 66(4):434–438. https://doi.org/10.1248/cpb.c17-00958

Liu Y, Zhang J, Wen R, Tu G-Z, Chen H-B, Liang H, Zhao Y-Y (2018c) Anti-inflammatory and antiproliferative prenylated chalcones from *Hedysarum gmelinii*. J Asian Nat Prod Res 20(11):1009–1018. https://doi.org/10.1080/10286020.2018.1450390

Liu J, Zhao Y, Huang C, Li Y, Guo F (2019a) Prenylated flavonoid-standardized extract from seeds of *Psoralea corylifolia* L. activated fat browning in high-fat diet-induced obese mice. Phytother Res 33(7):1851–1864. https://doi.org/10.1002/ptr.6374

Liu X, Song Z, Bai J, Nauwynck H, Zhao Y, Jiang P (2019b) Xanthohumol inhibits PRRSV proliferation, alleviates oxidative stress induced by PRRSV via the Nrf2-HMOX1 axis. Vet Res 50(1):61. https://doi.org/10.1186/s13567-019-0679-2

Liu Y-P, Guo J-M, Yan G, Zhang M-M, Zhang W-H, Qiang L, Fu Y-H (2019c) Anti-inflammatory and antiproliferative prenylated isoflavone derivatives from the fruits of *Ficus carica*. J Agric Food Chem 67(17):4817–4823. https://doi.org/10.1021/acs.jafc.9b00865

Liu Y-P, Yu X-M, Zhang W, Wang T, Jiang B, Tang H-X, Su Q-T, Fu Y-H (2020) Prenylated chromones and flavonoids from *Artocarpus heterophyllus* with their potential antiproliferative and anti-inflammatory activities. Bioorg Chem 101:104030. https://doi.org/10.1016/j.bioorg.2020.104030

Long G-Q, Hu G-S, Gao X-X, Jia J-M, Wang A-H (2022) Sophoranone A and B: two new cytotoxic prenylated metabolites and their analogs from the root bark of *Sophora flavescens*. Nat Prod Res 36(6):1515–1521. https://doi.org/10.1080/14786419.2021.1894562

Lu W-J, Chang C-C, Lien L-M, Yen T-L, Chiu H-C, Huang S-Y, Sheu J-R, Lin K-H (2015) Xanthohumol from *Humulus lupulus* L. induces glioma cell autophagy via inhibiting Akt/mTOR/S6K pathway. J Funct Foods 18:538–549. https://doi.org/10.1016/j.jff.2015.08.020

Lu X, Geng J, Zhang J, Miao J, Liu M (2019) Xanthohumol, a prenylated flavonoid from hops, induces caspase-dependent degradation of oncoprotein BCR-ABL in K562 cells. Antioxidants 8(9):402. https://doi.org/10.3390/antiox8090402

Lu X, Liu M, Dong H, Miao J, Stagos D, Liu M (2022) Dietary prenylated flavonoid xanthohumol alleviates oxidative damage and accelerates diabetic wound healing via Nrf2 activation. Food Chem Toxicol 160:112813. https://doi.org/10.1016/j.fct.2022.112813

Luo Y, Li X, He J, Su J, Peng L, Wu X, Du R, Zhao Q (2014) Isolation, characterisation, and antioxidant activities of flavonoids from chufa (*Eleocharis tuberosa*) peels. Food Chem 164:30–35. https://doi.org/10.1016/j.foodchem.2014.04.103

Ma S, Huang Y, Zhao Y, Du G, Feng L, Huang C, Li Y, Guo F (2016) Prenylflavone derivatives from the seeds of *Psoralea corylifolia* exhibited PPAR-γ agonist activity. Phytochem Lett 16:213–218. https://doi.org/10.1016/j.phytol.2016.04.016

Mai HDT, Toan TP, Huu GT, Le TN, Oanh VTK, Hang NTM, Thu HT, Chau VM, Litaudon M, Pham VC (2020) New flavonoid and stilbene derivatives from the fruits of *Macaranga balansae*. Nat Prod Res 34(19):2772–2778. https://doi.org/10.1080/14786419.2019.1587425

Maués LAL, Alves GM, Couto NMG, da Silva BJM, Arruda MSP, Macchi BM, Sena CBC, Prado AF, Crespo-Lopez ME, Silva EO, do Nascimento JLM (2019) Flavonoids from the Amazon plant *Brosimum acutifolium* induce C6 glioma cell line apoptosis by disrupting mitochondrial membrane potential and reducing AKT phosphorylation. Biomed Pharmacother 113:108728. https://doi.org/10.1016/j.biopha.2019.108728

Milella L, Milazzo S, De Leo M, Vera Saltos MB, Faraone I, Tuccinardi T, Lapillo M, De Tommasi N, Braca A (2016) α-Glucosidase and α-amylase inhibitors from *Arcytophyllum thymifolium*. J Nat Prod 79(8):2104–2112. https://doi.org/10.1021/acs.jnatprod.6b00484

Minakawa T, Toume K, Arai MA, Koyano T, Kowithayakorn T, Ishibashi M (2013) Prenylflavonoids isolated from *Artocarpus champeden* with TRAIL-resistance overcoming activity. Phytochemistry 96:299–304. https://doi.org/10.1016/j.phytochem.2013.08.015

Molčanová L, Kauerová T, Dall′Acqua S, Maršík P, Kollár P, Šmejkal K (2021) Antiproliferative and cytotoxic activities of *C*-Geranylated flavonoids from *Paulownia tomentosa* Steud. Fruit. Bioorg Chem 111:104797. https://doi.org/10.1016/j.bioorg.2021.104797

Morel S, Helesbeux J-J, Séraphin D, Derbré S, Gatto J, Aumond M-C, Abatuci Y, Grellier P, Beniddir MA, Le Pape P, Pagniez F, Litaudon M, Landreau A, Richomme P (2013) Anti-AGEs and antiparasitic activity of an original prenylated isoflavonoid and flavanones isolated from *Derris ferruginea*. Phytochem Lett 6(3):498–503. https://doi.org/10.1016/j.phytol.2013.06.002

Mouffouk S, Marcourt L, Benkhaled M, Boudiaf K, Wolfender J-L, Haba H (2017) Two new prenylated isoflavonoids from *Erinacea anthyllis* with antioxidant and antibacterial activities. Nat Prod Commun 12(7):1934578X1701200716. https://doi.org/10.1177/1934578x1701200716

Muiva-Mutisya LM, Atilaw Y, Heydenreich M, Koch A, Akala HM, Cheruiyot AC, Brown ML, Irungu B, Okalebo FA, Derese S, Mutai C, Yenesew A (2018) Antiplasmodial prenylated flavanonols from *Tephrosia subtriflora*. Nat Prod Res 32(12):1407–1414. https://doi.org/10.1080/14786419.2017.1353510

Munikishore R, Rammohan A, Padmaja A, Gunasekar D, Deville A, Bodo B (2013) A new *O*-prenylated flavonol from the roots of *Sophora interrupta*. Nat Prod Res 27(20):1823–1826. https://doi.org/10.1080/14786419.2012.761622

Na Z, Fan Q-F, Song Q-S, Hu H-B (2017) Three new flavonoids from *Millettia pachyloba*. Phytochem Lett 19:215–219. https://doi.org/10.1016/j.phytol.2017.02.002

Nago RDT, Nayim P, Mbaveng AT, Mpetga JDS, Bitchagno GTM, Garandi B, Tane P, Lenta BN, Sewald N, Tene M, Kuete V, Ngouela AS (2021) Prenylated flavonoids and C-15 isoprenoid analogues with antibacterial properties from the whole plant of *Imperata cylindrica* (L.) Raeusch (Gramineae). Molecules. https://doi.org/10.3390/molecules26164717

Navrátilová A, Schneiderová K, Veselá D, Hanáková Z, Fontana A, Dall′Acqua S, Cvacka J, Innocenti G, Novotná J, Urbanová M, Pelletier J, Čížek A, Žemličková H, Šmejkal K (2013) Minor *C*-geranylated flavanones from *Paulownia tomentosa* fruits with MRSA antibacterial activity. Phytochemistry 89:104–113. https://doi.org/10.1016/j.phytochem.2013.01.002

Nenaah GE (2014) Toxic and antifeedant activities of prenylated flavonoids isolated from *Tephrosia apollinea* L. against three major coleopteran pests of stored grains with reference to their structure-activity relationship. Nat Prod Res 28(24):2245–2252. https://doi.org/10.1080/14786419.2014.932788

Nguyen MTT, Le TH, Nguyen HX, Dang PH, Do TNV, Abe M, Takagi R, Nguyen NT (2017) Artocarmins G-M, prenylated 4-chromenones from the stems of *Artocarpus rigida* and their tyrosinase inhibitory activities. J Nat Prod 80(12):3172–3178. https://doi.org/10.1021/acs.jnatprod.7b00453

Nur-e-Alam M, Yousaf M, Parveen I, Hafizur RM, Ghani U, Ahmed S, Hameed A, Threadgill MD, Al-Rehaily AJ (2019) New flavonoids from the saudi arabian plant *Retama raetam* which stimulates secretion of insulin and inhibits α-glucosidase. Org Biomol Chem 17(5):1266–1276. https://doi.org/10.1039/c8ob02755b

Nyandoro SS, Munissi JJE, Kombo M, Mgina CA, Pan F, Gruhonjic A, Fitzpatrick P, Lu Y, Wang B, Rissanen K, Erdélyi M (2017) Flavonoids from *Erythrina schliebenii*. J Nat Prod 80(2):377–383. https://doi.org/10.1021/acs.jnatprod.6b00839

Ohara K, Muroya A, Fukushima N, Yazaki K (2009) Functional characterization of LePGT1, a membrane-bound prenyltransferase involved in the geranylation of *p*-hydroxybenzoic acid. Biochem J 421:231–241. https://doi.org/10.1042/BJ20081968

Okoth DA, Chenia HY, Koorbanally NA (2013) Antibacterial and antioxidant activities of flavonoids from *Lannea alata* (Engl) Engl (Anacardiaceae). Phytochem Lett 6(3):476–481. https://doi.org/10.1016/j.phytol.2013.06.003

Ombito JO, Majinda RRT, Masesane IB, Bojase G, Schuffler A, Opatz T (2018) Prenylated isoflavones from the stem bark of *Erythrina sacleuxii*. Phytochem Lett 26:110–114. https://doi.org/10.1016/j.phytol.2018.05.026

Orazbekov Y, Ibrahim MA, Srivedavyasasri R, Chaurasiya ND, Tekwani BL, Ross SA, Orazbekov Y, Makhatov B, Ibrahim MA, Mombekov S, Datkhayev U, Tekwani BL, Ross SA (2018) Isolation and biological evaluation of prenylated flavonoids from *Maclura pomifera*. Evid Based Complement Alternat Med 2018:1370368. https://doi.org/10.1155/2018/1370368

Oyama M, Nakashima K-I, Kamiya T, Haba M, Ito T, Murata H, Tanaka T, Adachi T, Iinuma M, Kinoshita T (2013a) Flavonoids isolated from the leaves of *Melicope triphylla* and their extracellular-superoxide dismutase-inducing activity. Phytochem Lett 6(2):215–218. https://doi.org/10.1016/j.phytol.2013.01.007

Oyama SdO, de Souza LA, Baldoqui DC, Sarragiotto MH, Silva AA (2013b) Prenylated flavonoids from *Maclura tinctoria* fruits. Quim Nova 36(6):800–802. https://doi.org/10.1590/S0100-40422013000600010

Ozaki T, Mishima S, Nishiyama M, Kuzuyama T (2009) NovQ is a prenyltransferase capable of catalyzing the addition of a dimethylallyl group to both phenylpropanoids and flavonoids. J Antibiot 62(7):385–392. https://doi.org/10.1038/ja.2009.48

Pang X, Yin S-S, Yu H-Y, Zhang Y, Wang T, Hu L-M, Han L-F (2018) Prenylated flavonoids and dihydrophenanthrenes from the leaves of *Epimedium brevicornu* and their cytotoxicity against HepG2 cell. Nat Prod Res 32(19):2253–2259. https://doi.org/10.1080/14786419.2017.1405410

Pang D, Liao S, Wang W, Mu L, Li E, Shen W, Liu F, Zou Y (2019) Destruction of the cell membrane and inhibition of cell phosphatidic acid biosynthesis in *Staphylococcus aureus*: an explanation for the antibacterial mechanism of morusin. Food Funct 10(10):6438–6446. https://doi.org/10.1039/c9fo01233h

Paraiso IL, Mattio LM, Alcazar Magana A, Choi J, Plagmann LS, Redick MA, Miranda CL, Maier CS, Dallavalle S, Kioussi C, Blakemore PR, Stevens JF (2021) Xanthohumol pyrazole derivative improves diet-induced obesity and induces energy expenditure in high-fat diet-fed mice. ACS Pharmacol Transl Sci 4(6):1782–1793. https://doi.org/10.1021/acsptsci.1c00161

Park S-J, Kim T-H, Lee K, Kang M-A, Jang H-J, Ryu H-W, Oh S-R, Lee H-J (2021) Kurarinone attenuates BLM-induced pulmonary fibrosis via inhibiting TGF-β signaling pathways. Int J Mol Sci. https://doi.org/10.3390/ijms22168388

Passreiter CM, Suckow-Schnitker A-K, Kulawik A, Addae-Kyereme J, Wright CW, Waetjen W (2015) Prenylated flavanone derivatives isolated from *Erythrina addisoniae* are potent inducers of apoptotic cell death. Phytochemistry 117:237–244. https://doi.org/10.1016/j.phytochem.2015.04.002

Peng J, Hartley RM, Fest GA, Mooberry SL (2012) Amyrisins A-C, *O*-Prenylated flavonoids from *Amyris madrensis*. J Nat Prod 75(3):494–496. https://doi.org/10.1021/np200796e

Peralta MA, Santi MD, Agnese AM, Cabrera JL, Ortega MG (2014) Flavanoids from *Dalea elegans*: Chemical reassignment and determination of kinetics parameters related to their anti-tyrosinase activity. Phytochem Lett 10:260–267. https://doi.org/10.1016/j.phytol.2014.10.012

Peralta MA, Ortega MG, Cabrera JL, Paraje MG (2018) The antioxidant activity of a prenyl flavonoid alters its antifungal toxicity on Candida *albicans biofilms*. Food Chem Toxicol 114:285–291. https://doi.org/10.1016/j.fct.2018.02.042

Polbuppha I, Suthiphasilp V, Maneerat T, Charoensup R, Limtharakul T, Cheenpracha S, Pyne SG, Laphookhieo S (2021) Macluracochinones A-E, antimicrobial flavonoids from *Maclura cochinchinensis*. (Lour) Corner Phytochemistry 187:112773. https://doi.org/10.1016/j.phytochem.2021.112773

Popoola OK, Marnewick JL, Rautenbach F, Ameer F, Iwuoha EI, Hussein AA (2015) Inhibition of oxidative stress and skin aging-related enzymes by prenylated chalcones and other flavonoids from *Helichrysum teretifolium*. Molecules 20(4):7143–7155. https://doi.org/10.3390/molecules20047143

Prajapati R, Seong SH, Paudel P, Park SE, Jung HA, Choi JS (2021) *In vitro* and *In Silico* characterization of kurarinone as a dopamine D1A Receptor Antagonist and D2L and D4 receptor agonist. ACS Omega 6(49):33443–33453. https://doi.org/10.1021/acsomega.1c04109

Qin J, Fan M, He J, Wu X-D, Peng L-Y, Su J, Cheng X, Li Y, Kong L-M, Li R-T, Zhao Q-S (2015a) New cytotoxic and anti-inflammatory compounds isolated from *Morus alba* L. Nat Prod Res 29(18):1711–1718. https://doi.org/10.1080/14786419.2014.999333

Qin Y, Yang Y-C, Meng Y-L, Xia C-F, Gao X-M, Hu Q-F (2015b) Chalcones from *Desmodium podocarpum* and their cytotoxicity. Chem Nat Compd 51(6):1062–1066. https://doi.org/10.1007/s10600-015-1492-4

Qu K-J, Wang B, Jiang C-S, Xie B-G, Liu A-H, Li S-W, Guo Y-W, Li J, Mao S-C (2021) Rearranged diels-alder adducts and prenylated flavonoids as potential PTP1B inhibitors from *Morus nigra*. J Nat Prod 84(8):2303–2311. https://doi.org/10.1021/acs.jnatprod.1c00403

Quang TH, Ngan NTT, Yoon C-S, Cho K-H, Kang DG, Lee HS, Kim Y-C, Oh H (2015) Protein tyrosine phosphatase 1B inhibitors from the roots of *Cudrania tricuspidata*. Molecules 20(6):11173–11183. https://doi.org/10.3390/molecules200611173

Rahman SU, Ali T, Hao Q, He K, Li W, Ullah N, Zhang Z, Jiang Y, Li S (2021) Xanthohumol attenuates lipopolysaccharide-induced depressive like behavior in mice: involvement of NF-κB/Nrf2 signaling pathways. Neurochem Res 46(12):3135–3148. https://doi.org/10.1007/s11064-021-03396-w

Raksat A, Maneerat W, Andersen RJ, Pyne SG, Laphookhieo S (2018) Antibacterial prenylated isoflavonoids from the stems of *Millettia extensa*. J Nat Prod 81(8):1835–1840. https://doi.org/10.1021/acs.jnatprod.8b00321

Ramli F, Rahmani M, Ismail IS, Sukari MA, Abd Rahman M, Zajmi A, Akim AM, Hashim NM, Go R (2016) A new bioactive secondary metabolite from *Artocarpus elasticus*. Nat Prod Commun 11(8):1934578X1601100818. https://doi.org/10.1177/1934578x1601100818

Rea K-A, Casaretto J-A, Al-Abdul-Wahid M-S, Sukumaran A, Geddes-Mcalister J, Rothstein S-J, Akhtar T-A (2019) Biosynthesis of cannflavins a and B from *Cannabis sativa* L. Phytochemistry 164:162–171. https://doi.org/10.1016/j.phytochem.2019.05.009

Rees KA, Bermudez C, Edwards DJ, Elliott AG, Ripen JE, Seta C, Huang JX, Cooper MA, Fraser JA, Yeo TC, Butler MS (2015) Flemingin-type prenylated chalcones from the Sarawak Rainforest Plant *Desmodium congestum*. J Nat Prod 78(8):2141–2144. https://doi.org/10.1021/acs.jnatprod.5b00410

Rueda DC, De Mieri M, Hering S, Hamburger M (2014) HPLC-based activity profiling for GABAA receptor modulators in *Adenocarpus cincinnatus*. J Nat Prod 77(3):640–649. https://doi.org/10.1021/np500016z

Ryu HW, Park YJ, Lee SU, Lee S, Yuk HJ, Seo K-H, Kim Y-U, Hwang BY, Oh S-R (2017) Potential anti-inflammatory effects of the fruits of *Paulownia tomentosa*. J Nat Prod 80(10):2659–2665. https://doi.org/10.1021/acs.jnatprod.7b00325

S Maneechai, W De-Eknamkul, K Umehara, H Noguchi, K Likhitwitayawuid (2012) Flavonoid and stilbenoid production in callus cultures of *Artocarpus lakoocha*. Phytochemistry 81:42–49

Saelee A, Phongpaichit S, Mahabusarakam W (2015) A new prenylated biflavonoid from the leaves of *Garcinia dulcis*. Nat Prod Res 29(20):1884–1888. https://doi.org/10.1080/14786419.2015.1010087

Sasaki K, Mito K, Ohara K, Yamamoto H, Yazaki K (2008) Cloning and characterization of naringenin 8-prenyltransferase, a flavonoid-specific prenyltransferase of *Sophora flavescens*. Plant Physiol 146(3):1075–1084. https://doi.org/10.1104/pp.107.110544

Sasaki K, Tsurumaru Y, Yamamoto H, Yazaki K (2011) Molecular characterization of a membrane-bound prenyltransferase specific for isoflavone from *Sophora flavescens*. J Biol Chem 286(27):24125–24134. https://doi.org/10.1074/jbc.M111.244426

Sasaki H, Kashiwada Y, Shibata H, Takaishi Y (2012) Prenylated flavonoids from *Desmodium caudatum* and evaluation of their anti-MRSA activity. Phytochemistry 82:136–142. https://doi.org/10.1016/j.phytochem.2012.06.007

Sasaki T, Li W, Higai K, Quang TH, Kim YH, Koike K (2014) Protein tyrosine phosphatase 1B inhibitory activity of lavandulyl flavonoids from roots of *Sophora flavescens*. Planta Med 80(7):557–560. https://doi.org/10.1055/s-0034-1368400

Sawada K, Yamashita Y, Zhang T, Nakagawa K, Ashida H (2014) Glabridin induces glucose uptake via the AMP-activated protein kinase pathway in muscle cells. Mol Cell Endocrinol 393(1–2):99–108. https://doi.org/10.1016/j.mce.2014.06.009

Schneiderova K, Slapetova T, Hrabal R, Dvorakova H, Prochazkova P, Novotna J, Urbanova M, Cvacka J, Smejkal K (2013) Tomentomimulol and mimulone B: two new *C*-geranylated flavonoids from *Paulownia tomentosa* fruits. Nat Prod Res 27(7):613–618. https://doi.org/10.1080/14786419.2012.683002

Segun PA, Ogbole OO, Ismail FMD, Nahar L, Evans AR, Ajaiyeoba EO, Sarker SD (2019) Bioassay-guided isolation and structure elucidation of cytotoxic stilbenes and flavonols from the leaves of *Macaranga barteri*. Fitoterapia 134:151–157. https://doi.org/10.1016/j.fitote.2019.02.019

Seliger JM, Misuri L, Maser E, Hintzpeter J (2018) The hop-derived compounds xanthohumol, isoxanthohumol and 8-prenylnaringenin are tight-binding inhibitors of human aldo-keto reductases 1B1 and 1B10. J Enzyme Inhib Med Chem 33(1):607–614. https://doi.org/10.1080/14756366.2018.1437728

Selim Y, El-Sharkawy E, Abd El-Azim MHM (2020) New cytotoxic flavonoids from aerial parts of *Platycladus orientalis* L. Nat Prod Res 34(12):1763–1771. https://doi.org/10.1080/14786419.2018.1530234

Shaffer CV, Cai S, Peng J, Robles AJ, Hartley RM, Powell DR, Du L, Cichewicz RH, Mooberry SL (2016) Texas native plants yield compounds with cytotoxic activities against prostate cancer cells. J Nat Prod 79(3):531–540. https://doi.org/10.1021/acs.jnatprod.5b00908

Shah MKK, Sirat HM, Jamil S, Jalil J (2016) Flavonoids from the bark of *Artocarpus integer* var. *Silvestris* and their anti-inflammatory properties. Nat Prod Commun 11(9):1934578X1601100921. https://doi.org/10.1177/1934578x1601100921

Shahinozzaman M, Taira N, Ishii T, Halim MA, Hossain MA, Tawata S (2018) Anti-inflammatory, anti-diabetic, and anti-alzheimer′s effects of prenylated flavonoids from *okinawa propolis*: an investigation by experimental and computational studies. Molecules 23(10):24792471–24792418. https://doi.org/10.3390/molecules23102479

Shang X-Y, Chen J-J, Song X-Y, Wang W, Chen Y, Yao G-D, Song S-J (2018) Daphnegiravone D from *Daphne giraldii* nitsche induces p38-dependent apoptosis via oxidative and nitrosative stress in hepatocellular carcinoma cells. Biomed Pharmacother 107:1426–1433. https://doi.org/10.1016/j.biopha.2018.08.141

Sheliya MA, Rayhana B, Ali A, Pillai KK, Aeri V, Sharma M, Mir SR (2015) Inhibition of α-glucosidase by new prenylated flavonoids from *euphorbia hirta* L. herb. J Ethnopharmacol 176:1–8. https://doi.org/10.1016/j.jep.2015.10.018

Shen G, Huhman D, Lei Z, Snyder J, Sumner L-W, Dixon R-A (2012) Characterization of an isoflavonoid-specific prenyltransferase from *Lupinus albus*. Plant Physiol 159(1):70–80. https://doi.org/10.1104/pp.112.195271

Shen G, Huhman D, Lei Z, Snyder J, Sumner L-W, Dixon R-A (2017) Characterization of an isoflavonoid-specific prenyltransferase from *Lupinus albus*[1[w]]. Plant Physiol 159:70–80. https://doi.org/10.1104/pp.112.195271

Shi S, Li J, Zhao X, Liu Q, Song S (2021) A comprehensive review: biological activity, modification and synthetic methodologies of prenylated flavonoids. Phytochemistry 191:112895. https://doi.org/10.1016/j.phytochem.2021.112895

Shim S-H, Kim Y, Lee J-Y, Song D-G, Pan C-H, Jung S-H (2009) Aldose reductase inhibitory activity of the compounds from the seed of *Psoralea corylifolia*. J Korean Soc Appl Biol Chem 52:568–572. https://doi.org/10.3839/jksabc.2009.096

Shimomura K, Sugiyama Y, Nakamura J, Ahn M-R, Kumazawa S (2013) Component analysis of propolis collected on Jeju Island, Korea. Phytochemistry 93:222–229. https://doi.org/10.1016/j.phytochem.2012.02.018

Shindo K, Tachibana A, Tanaka A, Toba S, Yuki E, Ozaki T, Kumano T, Nishiyama M, Misawa N, Kuzuyama T (2011) Production of novel antioxidative prenyl naphthalen-ols by combinational bioconversion with dioxygenase phnA1A2A3A4 and prenyltransferase NphB or SCO7190. Biosci Biotechnol Biochem 75:505–510. https://doi.org/10.1271/bbb.100731

Shour S, Iranshahy M, Pham N, Quinn RJ, Iranshahi M (2017) Dereplication of cytotoxic compounds from different parts of *Sophora pachycarpa* using an integrated method of HPLC, LC-MS and ^{1}H-NMR techniques. Nat Prod Res 31(11):1270–1276. https://doi.org/10.1080/14786419.2016.1239095

Sianglum W, Muangngam K, Joycharat N, Voravuthikunchai SP (2019) Mechanism of action and biofilm inhibitory activity of lupinifolin against multidrug-resistant enterococcal cinical isolates. Microb Drug Resist 25(10):1391–1400. https://doi.org/10.1089/mdr.2018.0391

Slawinska-Brych A, Mizerska-Kowalska M, Krol SK, Stepulak A, Zdzisinska B (2021) Xanthohumol impairs the PMA-Driven invasive behaviour of lung cancer cell line A549 and exerts anti-EMT action. Cells 10(6):1484. https://doi.org/10.3390/cells10061484

Smadi A, Ciavatta ML, Bitam F, Carbone M, Villani G, Gavagnin M (2018) Prenylated flavonoids and phenolic compounds from the rhizomes of marine phanerogam *Cymodocea nodosa*. Planta Med 84(9/10):704–709. https://doi.org/10.1055/s-0043-122747

Soltani S, Boozari M, Nejad Ebrahimi S, Amin GR, Iranshahi M (2020) Histone deacetylase inhibitory and cytotoxic activities of the constituents from the roots of *Sophora Pachycarpa*. Iran J Pharm Res 19(4):51–58. https://doi.org/10.22037/ijpr.2020.112442.13760

Song Y-H, Cai H, Gu N, Qian C-F, Cao S-P, Zhao Z-M (2011) Icariin attenuates cardiac remodelling through down-regulating myocardial apoptosis and matrix metalloproteinase activity in rats with congestive heart failure. J Pharm Pharmacol 63(4):541–549. https://doi.org/10.1111/j.2042-7158.2010.01241.x

Song S-S, Sun C-P, Zhou J-J, Chu L (2019) Flavonoids as human carboxylesterase 2 inhibitors: inhibition potentials and molecular docking simulations. Int J Biol Macromol 131:201–208. https://doi.org/10.1016/j.ijbiomac.2019.03.060

Song M, Liu Y, Li T, Liu X, Hao Z, Ding S, Panichayupakaranant P, Zhu K, Shen J (2021) Plant natural flavonoids against multidrug resistant pathogens. Adv Sci 8(15):e2100749. https://doi.org/10.1002/advs.202100749

Sritularak B, Tantrakarnsakul K, Lipipun V, Likhiwitayawuid K (2013) Flavonoids with anti-HSV activity from the root bark of *Artocarpus Lakoocha*. Nat Prod Commun 8(8):1079–1080. https://doi.org/10.1177/1934578x1300800811

Stec E, Li S-M (2012) Mutagenesis and biochemical studies on AuaA confirmed the importance of the two conserved aspartate-rich motifs and suggested difference in the amino acids for substrate binding in membrane-bound prenyltransferases. Arch Microbiol 194(7):589–595. https://doi.org/10.1007/s00203-012-0795-0

Štern A, Furlan V, Novak M, Štampar M, Kolenc Z, Kores K, Filipič M, Bren U, Žegura B (2021) Chemoprotective effects of xanthohumol against the carcinogenic mycotoxin aflatoxin B1. Foods 10(6):1331. https://doi.org/10.3390/foods10061331

Su X-H, Li C-Y, Zhong Y-J, Yuan Z-P, Li Y-F, Liang B (2012) A new prenylated chalcone from the seeds of *Millettia pachycarpa*. Chin J Nat Medicines 10(3):222–225. https://doi.org/10.3724/SP.J.1009.2012.00222

Suh KS, Rhee SY, Kim YS, Lee YS, Choi EM (2013) Xanthohumol modulates the expression of osteoclast-specific genes during osteoclastogenesis in RAW264.7 cells. Food Chem Toxicol 62:99–106. https://doi.org/10.1016/j.fct.2013.08.047

Sukumaran A, McDowell T, Chen L, Renaud J, Dhaubhade S (2018) Isoflavonoid-specific prenyltransferase gene family in soybean: GmPT01, a pterocarpan 2-dimethylallyltransferase involved in glyceollin biosynthesis. Plant J 96:966–981. https://doi.org/10.1111/tpj.14083

Sun Y-J, Hao Z-Y, Si J-G, Wang Y, Zhang Y-L, Wang J-M, Gao M-L, Chen H (2015) Prenylated flavonoids from the fruits of *Sinopodophyllum emodi* and their cytotoxic activities. RSC Adv 5(101):82736–82742. https://doi.org/10.1039/c5ra16136c

Sun Q, Li F-F, Wang D, Wu J, Yao G-D, Li X, Li L-Z, Liu Q-B, Huang X-X, Song S-J (2016a) Flavans with cytotoxic activity from the stem and root bark of *Daphne giraldii*. RSC Adv 6(61):55919–55929. https://doi.org/10.1039/C6RA08537G

Sun Y-J, Pei L-X, Wang K-B, Sun Y-S, Wang J-M, Zhang Y-L, Gao M-L, Ji B-Y (2016b) Preparative isolation of two prenylated biflavonoids from the roots and rhizomes of *Sinopodophyllum emodi* by sephadex LH-20 column and high-speed counter-current chromatography. Molecules 21(1):101–1013. https://doi.org/10.3390/molecules21010010

Sun F, Li Q, Xu J (2017) Chemical composition of roots *Flemingia philippinensis* and their inhibitory kinetics on aromatase. Chem Biodivers. https://doi.org/10.1002/cbdv.201600193

Sun Y, Shi B, Gao M, Fu L, Chen H, Hao Z, Zhang Y, Feng W (2018a) Two new biflavonoids from the roots and rhizomes of *Sinopodophyllum emodi*. Chem Nat Compd 54(4):649–653. https://doi.org/10.1007/s10600-018-2438-4

Sun Z, Zhou C, Liu F, Zhang W, Chen J, Pan Y, Ma L, Liu Q, Du Y, Yang J, Wang Q (2018b) Inhibition of breast cancer cell survival by xanthohumol via modulation of the notch signaling pathway *in vivo* and *in vitro*. Oncol Lett 15(1):908–916. https://doi.org/10.3892/ol.2017.7434

Sun Y, Chen H, Wang J, Gao M, Zhao C, Han R, Chen H, Li M, Xue G, Feng W (2019) Sixteen new prenylated flavonoids from the fruit of *Sinopodophyllum hexandrum*. Molecules. https://doi.org/10.3390/molecules24173196

Sun T-L, Li W-Q, Tong X-L, Liu X-Y, Zhou W-H (2021) Xanthohumol attenuates isoprenaline-induced cardiac hypertrophy and fibrosis through regulating PTEN/AKT/mTOR pathway. Eur J Pharmacol 891:173690. https://doi.org/10.1016/j.ejphar.2020.173690

Tang S, Huang W, Ji S, Wang Y, Pei D, Ye M, Yu S (2016) Prenylated flavonoids from *Glycyrrhiza uralensis* as promising anti-cancer agents: a preliminary structure-activity study. J Chin Pharm Sci 25(1):23–29. https://doi.org/10.5246/jcps.2016.01.003

Tang S, Cai S, Ji S, Yan X, Zhang W, Qiao X, Zhang H, Ye M, Yu S (2021) Isoangustone a induces autophagic cell death in colorectal cancer cells by activating AMPK signaling. Fitoterapia 152:104935. https://doi.org/10.1016/j.fitote.2021.104935

Tchamgoue J, Hafizur RM, Tchouankeu JC, Kouam SF, Adhikari A, Hameed A, Green IR, Choudhary MI (2016) Flavonoids and other constituents with insulin secretion activity from *Pseudarthria hookeri*. Phytochem Lett 17:181–186. https://doi.org/10.1016/j.phytol.2016.07.015

Teisseyre A, Palko-Labuz A, Uryga A, Michalak K (2018) The influence of 6-prenylnaringenin and selected non-prenylated flavonoids on the activity of Kv1.3 channels in human jurkat T cells. J Membrane Biol 251(5–6):695–704. https://doi.org/10.1007/s00232-018-0046-7

Thai QD, Tchoumtchoua J, Makropoulou M, Boulaka A, Meligova AK, Mitsiou DJ, Mitakou S, Michel S, Halabalaki M, Alexis MN, Skaltsounis LA (2016) Phytochemical study and biological evaluation of chemical constituents of *Platanus orientalis* and *Platanus* x *acerifolia* buds. Phytochemistry 130:170–181. https://doi.org/10.1016/j.phytochem.2016.04.006

Thongnest S, Lhinhatrakool T, Wetprasit N, Sutthivaiyakit P, Sutthivaiyakit S (2013) *Eriosema chinense*: a rich source of antimicrobial and antioxidant flavonoids. Phytochemistry 96:353–359. https://doi.org/10.1016/j.phytochem.2013.06.004

Toume K, Habu T, Arai MA, Koyano T, Kowithayakorn T, Ishibashi M (2015) Prenylated flavonoids and resveratrol derivatives isolated from *Artocarpus communis* with the ability to overcome TRAIL resistance. J Nat Prod 78(1):103–110. https://doi.org/10.1021/np500734t

Tran HNK, Nguyen VT, Kim JA, Rho SS, Woo MH, Choi JS, Lee JH, Min BS (2017) Anti-inflammatory activities of compounds from twigs of *Morus alba*. Fitoterapia 120:17–24. https://doi.org/10.1016/j.fitote.2017.05.004

Tran PL, Tran PT, Tran HNK, Lee S, Kim O, Min BS, Lee JH (2018) A prenylated flavonoid, 10-oxomornigrol F, exhibits anti-inflammatory effects by activating the Nrf2/heme oxygenase-1 pathway in macrophage cells. Int Immunopharmacol 55:165–173. https://doi.org/10.1016/j.intimp.2017.12.015

Tsurumaru Y, Sasaki K, Miyawaki T, Uto Y, Momma T, Umemoto N, Momose M, Yazaki K (2012) HlPT-1, a membrane-bound prenyltransferase responsible for the biosynthesis of bitter acids in hops. Biochem Biophys Res Commun 417(1):393–398. https://doi.org/10.1016/j.bbrc.2011.11.125

Tu Y, Xiao T, Gong G, Bian Y, Li Y (2020) A new isoflavone with anti-inflammatory effect from the seeds of *Millettia pachycarpa*. Nat Prod Res 34(7):981–987. https://doi.org/10.1080/14786419.2018.1547294

Tuenter E, Zarev Y, Matheeussen A, Elgorashi E, Pieters L, Foubert K (2019) Antiplasmodial prenylated flavonoids from stem bark of *Erythrina latissima*. Phytochem Lett 30:169–172. https://doi.org/10.1016/j.phytol.2019.02.001

Umereweneza D, Atilaw Y, Rudenko A, Gutlin Y, Bourgard C, Gupta AK, Orthaber A, Muhizi T, Sunnerhagen P, Erdelyi M, Gogoll A (2021) Antibacterial and cytotoxic prenylated dihydrochalcones from *Eriosema montanum*. Fitoterapia 149:104809. https://doi.org/10.1016/j.fitote.2020.104809

van de Schans MGM, Bovee TFH, Stoopen GM, Lorist M, Gruppen H, Vincken J-P (2015a) Prenylation and backbone structure of flavonoids and isoflavonoids from licorice and hop influence their phase I and II metabolism. J Agric Food Chem 63(49):10628–10640. https://doi.org/10.1021/acs.jafc.5b04703

van de Schans MGM, Ritschel T, Bovee TFH, Sanders MG, de Waard P, Gruppen H, Vincken J-P (2015b) Involvement of a hydrophobic pocket and helix 11 in determining the modes of action of prenylated flavonoids and isoflavonoids in the human estrogen receptor. ChemBioChem 16(18):2668–2677. https://doi.org/10.1002/cbic.201500343

Venturelli S, Burkard M, Biendl M, Lauer UM, Frank J, Busch C (2016) Prenylated chalcones and flavonoids for the prevention and treatment of cancer. Nutrition 32(11–12):1171–1178. https://doi.org/10.1016/j.nut.2016.03.020

Veselova MV, Fedoreyev SA, Tarbeeva DV, Kulesh NI, Kalinovskiy AI, Kuzmich AS, Kim NY, Grigorchuk VP (2017) Cytotoxic prenylated polyphenolic compounds from *Maackia amurensis* root bark. Nat Prod Commun 12(7):1934578X1701200709. https://doi.org/10.1177/1934578x1701200709

Villinski JR, Bergeron C, Cannistra JC, Gloer JB, Coleman CM, Ferreira D, Azelmat J, Grenier D, Gafner S (2014) Pyrano-isoflavans from *Glycyrrhiza uralensis* with antibacterial activity against *Streptococcus mutans*, *Porphyromonas gingivalis*. J Nat Prod 77(3):521–526. https://doi.org/10.1021/np400788r

Vu LTN, Anh LT, Cuc NT, Nhiem NX, Tai BH, Van Kiem P, Litaudon M, Thach TD, Van Minh C, Mai HDT, Van Cuong P (2021a) Prenylated flavonoids and other constituents from *Macaranga indica*. Nat Prod Res 35(13):2123–2130. https://doi.org/10.1080/14786419.2019.1662007

Vu NK, Ha MT, Kim CS, Gal M, Kim JA, Woo MH, Lee J-H, Min BS (2021b) Structural characterization of prenylated compounds from *Broussonetia kazinoki* and their antiosteoclastogenic activity. Phytochemistry 188:112791. https://doi.org/10.1016/j.phytochem.2021.112791

Wang X, Li J, Qian L, Zang X-F, Zhang S-Y, Wang X-Y, Jin J-L, Zhu X-L, Zhang X-B, Wang Z-Y, Xu Y (2013) Icariin promotes histone acetylation and attenuates post-stroke cognitive impairment in the central cholinergic circuits of mice. Neuroscience 236:281–288. https://doi.org/10.1016/j.neuroscience.2012.12.074

Wang R, Chen R, Li J, Liu X, Xie K, Chen D, Yin Y, Tao X, Xie D, Zou J, Yang L, Dai J (2014) Molecular characterization and phylogenetic analysis of two novel regio-specific flavonoid prenyltransferases from *Morus alba* and *Cudrania tricuspidata*. J Biol Chem 289(52):35815–35825. http://www.jbc.org/cgi/doi/https://doi.org/10.1074/jbc.M114.608265

Wang D, Sun Q, Wu J, Wang W, Yao G, Li T, Li X, Li L, Zhang Y, Cui W, Song S (2017a) A new prenylated flavonoid induces G0/G1 arrest and apoptosis through p38/JNK MAPK pathways in human hepatocellular carcinoma cells. Sci Rep 7(1):5736. https://doi.org/10.1038/s41598-017-05955-0

Wang L-X, Zheng H-R, Ren F-C, Chen T-G, Li X-M, Jiang X-J, Wang F (2017b) Polysubstituted Isoflavonoids from *Spatholobus suberectus*, *Flemingia macrophylla*, and *Cudrania cochinchinensis*. Nat Prod Bioprospect 7(2):201–206. https://doi.org/10.1007/s13659-017-0121-2

Wang Q-H, Guo S, Yang X-Y, Zhang Y-F, Shang M-Y, Shang Y-H, Xiao J-J, Cai S-Q (2017c) Flavonoids isolated from *sinopodophylli fructus* and their bioactivities against human breast cancer cells. Chin J Nat Med 15(3):225–233. https://doi.org/10.3724/sp.j.1009.2017.00225

Wang W, Nakashima K-I, Hirai T, Inoue M (2019) Anti-inflammatory effects of naturally occurring retinoid X receptor agonists isolated from Sophora tonkinensis Gagnep. Via retinoid X receptor/liver X receptor heterodimers. J Nat Med 73(2):419–430. https://doi.org/10.1007/s11418-018-01277-1

Wang C-Y, Ai G-F, Zhang Y-F (2020a) Two new isoflavones from the seeds of *Psoralea corylifolia* with diacylglycerol acyltransferase inhibitory activity. J Asian Nat Prod Res 22(4):346–352. https://doi.org/10.1080/10286020.2019.1570159

Wang H, Tong Y, Xiao D, Xia B (2020b) Involvement of mTOR-related signaling in antidepressant effects of sophoraflavanone G on chronically stressed mice. Phytother Res 34(9):2246–2257. https://doi.org/10.1002/ptr.6675

Wang J, Liu X, Zheng H, Liu Q, Zhang H, Wang X, Shen T, Wang S, Ren D (2020c) Morusin induces apoptosis and autophagy via JNK, ERK and PI3K/Akt signaling in human lung carcinoma cells. Chem Biol Interact 331:109279. https://doi.org/10.1016/j.cbi.2020.109279

Wang L, Zhang Y, Johnpaul IA, Hong K, Song Y, Yang X, Lv C, Ma C (2022) Exploring two types of prenylated bitter compounds from hop plant (*Humulus lupulus* L.) against α-glucosidase *in vitro* and *in silico*. Food Chem 370:130979. https://doi.org/10.1016/j.foodchem.2021.130979

Wen L, Shi D, Zhou T, Tu J, He M, Jiang Y, Yang B (2020) Identification of two novel prenylated flavonoids in mulberry leaf and their bioactivities. Food Chem 315:126236. https://doi.org/10.1016/j.foodchem.2020.126236

Wen L, Zhou T, Jiang Y, Chang SK, Yang B (2021) Prenylated flavonoids in foods and their applications on cancer prevention. Crit Rev Food Sci 62(18):5067–5080

Win T, Htwe TT, Shwe HH, Heilmann J (2012) Lavandulyl flavanones from the stems of *Hypericum calycinum* L. Chem Biodivers 9(6):1198–1204. https://doi.org/10.1002/cbdv.201100310

Won TH, Song I-H, Kim K-H, Yang W-Y, Lee SK, Oh D-C, Oh W-K, Oh K-B, Shin J (2015) Bioactive metabolites from the fruits of *Psoralea corylifolia*. J Nat Prod 78(4):666–673. https://doi.org/10.1021/np500834d

Xiao Y, Lee I-S (2018) Microbial transformation of quercetin and its prenylated derivatives. Nat Prod Res 32(8):902–908. https://doi.org/10.1080/14786419.2017.1367780

Xiao C-Y, Li W-Y, Zhai X-X, Zhu L-Z, Zhou Y-F, Yao P-C, Shu Q-X, Gang R (2018) Prenylated flavonoids from the roots of *Artocarpus heterophyllus*. Acta Pharmacol Sin 53(4):592–597. https://doi.org/10.16438/j.0513-4870.2017-1305

Xie G, Lin B, Qin X, Wang G, Wang Q, Yuan J, Li C, Qin M (2015) New flavonoids with cytotoxicity from the roots of *Flemingia latifolia*. Fitoterapia 104:97–101. https://doi.org/10.1016/j.fitote.2015.05.015

Xu Y-L, He J-L, Jiang S-P, Wang Y-J, Zhu W-P (2020) A new prenylated flavonoid glycoside from *Sinopodophyllum hexandrum*. Chin Tradit Herbal Drugs 51(17):4388–4392

Xue J, Li R, Zhao X, Ma C, Lv X, Liu L, Liu P (2018) Morusin induces paraptosis-like cell death through mitochondrial calcium overload, dysfunction in epithelial ovarian cancer. Chem Biol Interact 283:59–74. https://doi.org/10.1016/j.cbi.2018.02.003

Yan H-W, Zhu H, Yuan X, Yang Y-N, Feng Z-M, Jiang J-S, Zhang P-C (2019) Eight new biflavonoids with lavandulyl units from the roots of *Sophora flavescens* and their inhibitory effect on PTP1B. Bioorg Chem 86:679–685. https://doi.org/10.1016/j.bioorg.2019.01.058

Yang Z, Wang Y, Wang Y, Zhang Y (2012) Bioassay-guided screening and isolation of α-glucosidase and tyrosinase inhibitors from leaves of *Morus alba*. Food Chem 131(2):617–625. https://doi.org/10.1016/j.foodchem.2011.09.040

Yang D-S, Wei J-G, Peng W-B, Wang S-M, Sun C, Yang Y-P, Liu K-C, Li X-L (2014) Cytotoxic prenylated bibenzyls and flavonoids from *Macaranga kurzii*. Fitoterapia 99:261–266. https://doi.org/10.1016/j.fitote.2014.10.003

Yang D-S, Li Z-L, Peng W-B, Yang Y-P, Wang X, Liu K-C, Li X-L, Xiao W-L (2015a) Three new prenylated flavonoids from *Macaranga denticulata* and their anticancer effects. Fitoterapia 103:165–170. https://doi.org/10.1016/j.fitote.2015.04.001

Yang D-S, Wang S-M, Peng W-B, Yang Y-P, Liu K-C, Li X-L, Xiao W-L (2015b) Minor prenylated flavonoids from the twigs of *Macaranga adenantha* and their cytotoxic activity. Nat Prod Bioprospect 5(2):105–109. https://doi.org/10.1007/s13659-015-0059-1

Yang D-S, Peng W-B, Yang Y-P, Liu K-C, Li X-L, Xiao W-L (2015c) Cytotoxic prenylated flavonoids from *Macaranga indica*. Fitoterapia 103:187–191. https://doi.org/10.1016/j.fitote.2015.04.002

Yang X, Jiang Y, Yang J, He J, Sun J, Chen F, Zhang M, Yang B (2015) Prenylated flavonoids, promising nutraceuticals with impressive biological activities. Trends Food Sci Technol 44(44):93–104. https://doi.org/10.1016/j.tifs.2015.03.007

Yang Z, Ma X, Tan W, Zhou L, Zhuang X, Yang S, Qian Z, Zhou Z (2015d) Two new chalcones from *Shuteria sinensis*. Nat Prod Res 29(20):1909–1913. https://doi.org/10.1080/14786419.2015.1012718

Yang X, Yang J, Jiang Y, Yang H, Yun Z, Rong W, Yang B (2016) Regiospecific synthesis of prenylated flavonoids by a prenyltransferase cloned from *Fusarium oxysporum*. Sci Rep 6:24819. https://doi.org/10.1038/srep24819

Yang W-J, He J-X, Zhou M-X, Huang M, Wang S-Q, Wang X-N, Lou H-X, Ren D-M, Shen T (2019) An isopentenyl-substituted flavonoid norartocarpin activates Nrf2 signalling pathway and prevents oxidative insults in human lung epithelial cells. Free Radic Res 53(3):348–358. https://doi.org/10.1080/10715762.2019.1582769

Yang J, Zhou T, Jiang Y, Yang B (2020) Substrate specificity change of a flavonoid prenyltransferase AhPT1 induced by metal ion. Int J Biol Macromol 153:264–275. https://doi.org/10.1016/j.ijbiomac.2020.03.005

Yang Y-N, Zhu H, Yuan X, Zhang X, Feng Z-M, Jiang J-S, Zhang P-C (2021) Seven new prenylated flavanones from the roots of *Sophora flavescens* and their anti-proliferative activities. Bioorg Chem 109:104716. https://doi.org/10.1016/j.bioorg.2021.104716

Yao J, Wang Z, Wang R, Wang Y, Xu J, He X (2021) Anti-proliferative and anti-inflammatory prenylated isoflavones and coumaronochromones from the fruits of *Ficus altissima*. Bioorg Chem 113:104996. https://doi.org/10.1016/j.bioorg.2021.104996

Ye X-S, Tian W-J, Zhou M, Zeng D-Q, Lin T, Wang G-H, Yao X-S, Chen H-F (2021) Prenylated flavonoids from *Ficus hirta* induces HeLa cells apoptosis via MAPK and AKT signaling pathways. Bioorg Med Chem Lett 38:127859. https://doi.org/10.1016/j.bmcl.2021.127859

Yeh C-J, Chen C-C, Leu Y-L, Lin M-W, Chui M-M, Wang H-W (2017) The effects of artocarpin on wound healing: *in vitro* and *in vivo* studies. Sci Rep 7:1–13. https://doi.org/10.1038/s41598-017-15876-7

Yen T-L, Hsu C-K, Lu W-J, Hsieh C-Y, Hsiao G, Chou D-S, Wu G-J, Sheu J-R (2012) Neuroprotective effects of xanthohumol, a prenylated flavonoid from hops (*Humulus lupulus*), in ischemic stroke of rats. J Agric Food Chem 60(8):1937–1944. https://doi.org/10.1021/jf204909p

Yim D, Kim MJ, Shin Y, Lee S-J, Shin JG, Kim DH (2019) Inhibition of cytochrome P450 activities by *Sophora flavescens* extract and its prenylated flavonoids in human liver microsomes. Evid Based Complement Alternat Med 2019:2673769

Yin H, Zhang S, Wu J, Nan H, Long L, Yang J, Li Q (2006) Pongaflavanol: a prenylated flavonoid from *Pongamia pinnata* with a modified ring A. Molecules 11(10):786–791. https://doi.org/10.3390/11100786

Yin S, Song M, Zhao R, Liu X, Kang W-K, Lee J-M, Kim Y-E, Zhang C, Shim J-H, Liu K, Dong Z, Lee M-H (2020) Xanthohumol inhibits the growth of keratin 18-overexpressed esophageal squamous cell carcinoma *in vitro* and *in vivo*. Front Cell Dev Biol 8:366. https://doi.org/10.3389/fcell.2020.00366

Yoneyama K, Akashi T, Aoki T (2016) Molecular characterization of soybean pterocarpan 2-dimethylallyltransferase in glyceollin biosynthesis: local gene and whole-genome duplications of prenyltransferase genes led to the structural diversity of soybean prenylated isoflavonoids. Plant Cell Physiol 57(12):2497–2509. https://doi.org/10.1093/pcp/pcw178

Yoshioka Y, Kubota Y, Samukawa Y, Yamashita Y, Ashida H (2019) Glabridin inhibits dexamethasone-induced muscle atrophy. Arch Biochem Biophys 664:157–166. https://doi.org/10.1016/j.abb.2019.02.006

Yu X, Li S-M (2011) Prenylation of flavonoids by using a dimethylallyltryptophan synthase, 7-DMATS, from *Aspergillus fumigatus*. ChemBioChem 12:2280–2283. https://doi.org/10.1002/cbic.201100413

Yu Q, Cheng N, Ni X (2013) Identifying 2 prenylflavanones as potential hepatotoxic compounds in the ethanol extract of *Sophora flavescens*. J Food Sci 78(11):T1830–T1834. https://doi.org/10.1111/1750-3841.12275

Yusook K, Weeranantanapan O, Hua Y, Kumkrai P, Chudapongse N (2017) Lupinifolin from *Derris reticulata* possesses bactericidal activity on *Staphylococcus aureus* by disrupting bacterial cell membrane. J Nat Med 71(2):357–366. https://doi.org/10.1007/s11418-016-1065-2

Zakaria I, Ahmat N, Jaafar FM, Widyawaruyanti A (2012) Flavonoids with antiplasmodial and cytotoxic activities of *Macaranga triloba*. Fitoterapia 83(5):968–972. https://doi.org/10.1016/j.fitote.2012.04.020

Zarev Y, Foubert K, Lucia de Almeida V, Anthonissen R, Elgorashi E, Apers S, Ionkova I, Verschaeve L, Pieters L (2017) Antigenotoxic prenylated flavonoids from stem bark of *Erythrina latissima*. Phytochemistry 141:140–146. https://doi.org/10.1016/j.phytochem.2017.06.003

Zelová H, Hanáková Z, Čermáková Z, Šmejkal K, Dall Acqua S, Babula P, Cvačka J, Hošek J (2014) Evaluation of anti-inflammatory activity of prenylated substances isolated from *Morus alba* and *Morus nigra*. J Nat Prod 77(6):1297–1303. https://doi.org/10.1021/np401025f

Zeutsop JF, Nono RN, Frese M, Chouna JR, Lenta BN, Nkeng-Efouet-Alango P, Sewald N (2021) Phytochemical, antibacterial, antioxidant and cytoxicity investigation of Tarenna grandiflora. Z Naturforsch C J Biosci 76(7–8):285–290. https://doi.org/10.1515/znc-2020-0187

Zhang N-L, Zhu Y-H, Huang R-M, Fu M-Q, Su Z-W, Cai J-Z, Hu Y-J, Qiu S-X (2012) Two new stilbenoids from *Cajanus cajan*. Z Naturforsch B 67:1314–1318. https://doi.org/10.5560/znb.2012-0184

Zhang L-B, Lei C, Gao L-X, Li J-Y, Li J, Hou A-J (2016) Isoprenylated flavonoids with PTP1B inhibition from *Macaranga denticulata*. Nat Prod Bioprospect 6(1):25–30. https://doi.org/10.1007/s13659-015-0082-2

Zhang N, Tian B, Zhao S, Zhang X, Pan D, Shen X, Zhang Y (2017) A new formylated chalcone from *Humulus lupulus* with protective

effect on HUVECs injury by angiotensin II. Nat Prod Res 33(5):617–621. https://doi.org/10.1080/14786419.2017.1402318

Zhang H, Wu X, Wang J, Wang M, Wang X, Shen T, Wang S, Ren D (2020) Flavonoids from the leaves of *Epimedium Koreanum* Nakai and their potential cytotoxic activities. Nat Prod Res 34(9):1256–1263. https://doi.org/10.1080/14786419.2018.1560283

Zheng Z-P, Tan H-Y, Chen J, Wang M (2013) Characterization of tyrosinase inhibitors in the twigs of *Cudrania tricuspidata* and their structure-activity relationship study. Fitoterapia 84:242–247. https://doi.org/10.1016/j.fitote.2012.12.006

Zheng Y, Xie Y-G, Zhang Y, Li T, Li H-L, Yan S-K, Jin H-Z, Zhang W-D (2016) New norlignans and flavonoids of *Dysosma versipellis*. Phytochem Lett 16:75–81. https://doi.org/10.1016/j.phytol.2016.03.001

Zheng Y, Wang H, Yang M, Peng G, Dong TTX, Xu ML, Tsim KWK (2018) Prenylated flavonoids from roots of *Glycyrrhiza uralensis* induce differentiation of B16–F10 melanoma cells. Int J Mol Sci. https://doi.org/10.3390/ijms19082422

Zhou H, Yuan Y, Liu Y, Deng W, Zong J, Bian Z-Y, Dai J, Tang Q-Z (2014) Icariin attenuates angiotensin II-induced hypertrophy and apoptosis in H9c2 cardiomyocytes by inhibiting reactive oxygen species-dependent JNK and p38 pathways. Exp Ther Med 7(5):1116–1122. https://doi.org/10.3892/etm.2014.1598

Zhou K, Xia Y, Xie X, Li S-M (2015) Complementary flavonoid prenylations by fungal indole prenyltransferases. J Nat Prod 78(9):2229–2235. https://doi.org/10.1021/acs.jnatprod.5b00422

Zhu H-R, Wang Z-Y, Zhu X-L, Er-guang Li, Xu Y (2010) Icariin protects against brain injury by enhancing SIRT1-dependent PGC-1α expression in experimental stroke. Neuropharmacol 59:70–76. https://doi.org/10.1016/j.neuropharm.2010.03.017

Zhu H, Yang Y-N, Feng Z-M, Jiang J-S, Zhang P-C (2018) Sophoflavanones A and B, two novel prenylated flavanones from the roots of *Sophora flavescens*. Bioorg Chem 79:122–125. https://doi.org/10.1016/j.bioorg.2018.04.019

Zoofishan Z, Kúsz N, Csorba A, Tóth G, Hajagos-Tóth J, Kothencz A, Gáspár R, Hunyadi A (2019) Antispasmodic activity of prenylated phenolic compounds from the root bark of *Morus nigra*. Molecules 24(13):2497. https://doi.org/10.3390/molecules24132497

Zulfiqar F, Khan SI, Ross SA, Ali Z, Khan IA (2017) Prenylated flavonol glycosides from *Epimedium grandiflorum*: cytotoxicity and evaluation against inflammation and metabolic disorder. Phytochem Lett 20:160–167. https://doi.org/10.1016/j.phytol.2017.04.027

Zuo B, Liao Z-X, Xu C, Liu C (2016) Two novel prenylated kaempferol derivatives from fresh bud's fur of *Platanus acerifolia* and their anti-proliferative activities. Nat Prod Res 30(22):2523–2528. https://doi.org/10.1080/14786419.2015.1118632